Characterization of RISUG® (Reversible Inhibition of Sperm Under Guidance) based polymeric formulations having selective anti-microbial activity, bio-compatibility and anti-HIV activity for the application as non-hormonal female contraceptive implant

Thesis submitted by

Bhuvaneshwaran Subramanian

for award of the degree

Doctor of Philosophy (Engineering)

School of Bioscience and Engineering
Faculty Counsil of Engineering & Technology
Jadavpur University
Kolkata, India

2019

RESEARCH PUBLICATIONS

1. **BhuvaneshwaranSubramanian**, Tarun Agarwal, Sanjoy Kumar Ghorai, Pijush Mandal, Santanu Chattopadhyay, Piyali Basak, Tapas Kumar Maiti, Sujoy K Guha. Biocompatible polyvinyl alcohol and RISUG® blend polymeric films with spermicidal potential. Journal of Biomedical Materials 14:1-12 **Impact factor 2.89**

2. **BhuvaneshwaranSubramanian**, Tarun Agarwal, Piyali Basak, Tapas Kumar Maiti, Sujoy K. Guha. RISUG® based improved intrauterine contraceptive device (IIUCD) could impart protective effects against development of endometrial cancer. Journal of Medical Hypothesis 124:64-71 **Impact factor 1.15**

3. **BhuvaneshwaranSubramanian**, Arun Prabhu Rameshbabu, Kuntal Ghosh, Pradeep K. Jha, Rakhi Jha, Selvakumar Murugesan, Santanu Chattopadhyay, Santanu Dhara, Keshab C. Mondal, Piyali Basak, Sujoy K. Guha. Impact of styrene maleic anhydride (SMA) based hydrogel on rat fallopian tube as contraceptive implant with selective antimicrobial property. Journal of Materials Science and Engineering: C 94:94-107 **Impact factor 5.08**

4. Sanjoy Kumar Ghorai, Somnath Maji, **Bhuvaneshwaran Subramanian**, Tapas Kumar Maiti, Santanu Chattopadhyay. Coining attributes of ultra-low concentration graphene oxide and spermine: An approach for high strength, anti-microbial and osteoconductive nanohybrid scaffold for bone tissue regeneration. Carbon 141:370-389 **Impact factor 7.08**

5. Paulomi Ghosh, ArunPrabhu Rameshbabu, Dipankar Das, **Bhuvaneshwaran Subramanian**, Sintu Kumar Samanta, Sabyasachi Roy, Sagar Pal, Sudip Kumar Ghosh, Santanu Dhara. Single-Pot Biofabrication of Living Fibers for Tissue Engineering Applications. Journal of Materials Research: Cambridge core 33:2019-2028 **Impact factor 1.49**

6. Elavarasan Subramani, Arun Prabhu Rameshbabu, Manivannan Jothiramajayam, **Bhuvaneshwaran Subramanian**, Debangana Chakravorty, Gunja Bose, Mamata joshi, Chaitali Datta Ray, Indrani Lodh, Ratna Chattopadhyay, Sudipto Saha, Anita Mukherjee, Santanu Dhara, Baidyanath Chakravarty and Koel Chaudhury. Mycobacterial heat shock protein 65 mediated metabolic shift in decidualization of human endometrial stromal cells. Nature Scientific reports 7:3942 **Impact factor 4.2**

RESEARCH PUBLICATIONS

7. Arun Prabhu Rameshbabu, Paulomi Ghosh, Elavarasan Subramani, Kamakshi Bankoti, Kausik Kapat, Sayanti Datta, Priti Prasana Maity, **Bhuvaneshwaran Subramanian**, Sabyasachi Roy, Koel Chaudhury and Santanu Dhara. Investigating the potential of human placenta-derived extracellular matrix sponges coupled with amniotic membrane-derived stem cells for osteochondral tissue engineering. Journal of Material Chemistry B 4:613-625 **Impact factor 4.7**

8. Paulomi Ghosh, Arun Prabhu Rameshbabu, Dipankar Das, Nimmy K. Francis, Harpreet Singh Pawar, **Bhuvaneshwaran Subramanian**, Sagar Pal, Santanu Dhara. 2014. Covalent Cross-links in Polyampholytic Chitosan Fibers Enhances Bone Regeneration in a Rabbit Model. Colloids and Surfaces B: Biointerphases 125:160-169 **Impact factor 4.4**

9. B.Dineshkumar, **SP.Bhuvaneshwaran**, P.Vigneshkumar, Analava Mitra, Manjunatha Mahadevappa. 2010. A brief description of diabetes in India. Journal of Pharmacy Research Solutions 3(8): 1719-1723 **Impact factor** 2

CONFERENCE PUBLICATIONS

1. Bhuvaneshwaran Subramanian, Arun Prabhu Rameshbabu, Kuntal Gosh, M Selvakumar, Piyali: 30 Mar 2016. **Cite Score 4.36**

2. Satarupa Sarkar, Amrita Chaudhary, Swarnendu Basak, Santanu Dhara, Sujoy K Guha. Styrene Maleic Anhydride formulated polyelectrolyte hydrogel with selective antimicrobial property, potentially favorable for the application as female contraceptive implant. Frontiers in Bioengineering and Biotechnology. Published OnlineBag, **Bhuvaneshwaran Subramanian**, Amit K. Das, Provas Banerjee, Jyotirmoy Chatterjee. Regenerative potential of characterised honey in wound healing. Published Online: 30 Mar 2016. **Cite Score 4.36**
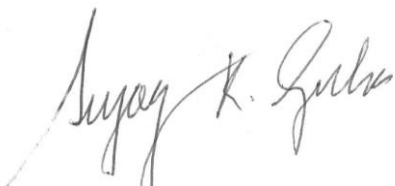
/   /

This is to certify that the thesis entitled "**Characterization of RISUG® (Reversible Inhibition of Sperm Under Guidance) based polymeric formulations having selective anti-microbial activity, bio-compatibility and anti-HIV activity for the application as non-hormonal female contraceptive implant**" submitted by Shri **Bhuvaneshwaran Subramanian** who got his name registered on 04/09/2013 for fthe award og Ph.D (Engineering) degree of Jadavpur University is absolutely based upon his own work under the supervision of **Dr. Piyali Basak, Assistant professor, Schoo lof Bioscience and Engineering, Faculty Counsil of Engineering & Technology, Jadavpur University, Kolkata** and **Dr. Sujoy K. Guha, Professor of Biomedical Engineering, Centre for Biomedical Engineering, Indian Institute of Technology & All India Institute of Medical Sciences, New Delhi** and that neither his thesis nor any part of the thesis has been submitted for any degree/diploma or any other academic award anywhere before.

1._____   2._____

     Dr. Sujoy K. Guha   **Dr. Piyali Basak,**
Professor of Biomedical Engineering   Assistant Professor,
Centre for Biomedical Engineering   School of Bioscience and Engineering,
Indian Institute of Technology &   Jadavpur University, Kolkata
All India Institute of Medical Sciences,
New Delhi

Dedicated to Shri Narthamalai Muthumaari Amman

TABLE OF CONTENTS

Intentionally blank page

LIST OF FIGURES

LIST OF TABLES

LIST OF SYMBOLS AND ABBREVIATIONS

Abbreviation	Full name
RISUG®	Reversible Inhibition of Sperm Under Guidance
SMA	Styrene Maleic Anhydride
SMAc	Styrene Maleic Acid
SUF	Simulated Uterine Fluid
SVF	Simulated Vaginal Fluid
ER-α	Estrogen receptor alpha
ER-β	Estrogen receptor beta
IUCD	Intra-uterine contraceptive device
IIUCD	Improved intra-uterine contraceptive device
FDA	Food and Drug Administration
DMSO	Dimethyl sulfoxide
Gy	Gray
Gy/s	Gray/Second
Co	Cobalt
^{1}H NMR	Proton nuclear magnetic resonance
^{13}C NMR	Carbon-13 nuclear magnetic resonance
GC/MS	Gas Chromatography/Mass Spectroscopy
°C/min	Degree Celsius/minute
WXRD	Wide angle X-ray diffraction
ATR	Attenuated total reflection

Abbreviation	Full name
Zn-se	Zinc selenide
SEM	Scanning electron micrscopy
DSC	Differential scanning calorimetry
MTCC	Microbial Type Culture Collection
IMTECH	Institute of Microbial Technology
MRS	deMan, Rogosa and Sharpe
Pvt. Ltd	Private limited
H	Hour
CFU	Colony forming unit
MTT	3[4,5-dimethylthiazol-2-yl]-2,5-diphenyltetrazolium bromide
DMEM	DMEM Dulbecco`s Modified Eagle Media
FBS	Fetal Bovine Serum
HEPES	4-(2-hydroxyethyl)-1-piperazineethanesulfonic acid
PVDF	Polyvinylidene difluoride
PCR	Polymerase chain reaction
RNA	Ribonucleic acid
DNA	Deoxyribonucleic acid
ER-α	Estrogen Receptor alpha
VEGF	Vascular Endothelial Growth Factor

Abbreviation	Full name
CDK4	Cyclin-dependent Kinase 4
GAPDH	Glyceraldehyde 3-phosphate dehydrogenase
DAPI	4′,6-diamidino-2-phenylindole
M	Molar
HRP	Horseradish peroxidase
HBG	Haemoglobin
MCH	Mean Corpuscular Hemoglobin
MCHC	Mean Corpuscular Hemoglobin Concentration
MCV	Mean Corpuscular Volume
T-RBC	Total Red Blood Cell Count
TLC	Total Leucocyte Count
PCV	Packed Cell Volume
HCT	Haematocrit
GLU	Glucose
CHOL	Cholesterol
TG	Triglycerides
TP	Total proteins
ALB	Albumin
BUN	Blood Urea Nitrogen
CRTN	Creatinine
P	Phosphorus

Abbreviation	Full name
CA	Calcium
ALP	Alkaline phosphatase
ALT	Alanine aminotransferase
AST	Aspartate aminotransferase
TBL	Total Bilirubin
ANOVA	Analysis of variance
PVOH	Polyvinyl alcohol
FBS	Fetal Bovine Serum Albumin
AFM	Atomic force microscopy
HIV	Human immunodeficiency virus
NCCS	National centre for cell science
AVI	Antiviral index
EDTA	Ethylenediaminetetraacetic acid
PBS	Phosphate-buffered saline
AZT	Azidothymidine
PCL	Poly(ε-caprolactone)
PEG	Polyethylene glycol
DA	Diacrylate
AIBN	Azobisobuobutyronitrile
FWHM	Full width at half maximum
V%	Viability percentage

Abbreviation	Full name
rad	Radian
s	Second
rad/s	Radian/Second
T_g	Glass transition temperature
P_C	Crystallinity percent
X_C	Degree of crystallinity
R	Interchain distance
d	Interplanar distance
mM	Millimolar
ns	Nonsignificant
kV	Kilo volt
kg	Kilogram
mg/Kg	milligram/ Kilogram
cDNA	Complementary DNA
Cm	Centimeter
η^*	Complex viscosity
G^*	Complex modulus
G'	Storage modulus
G''	Loss modulus
θ	Theta
λ	Lambda
%	Percentage

Abbreviation	Full name
~	Approximate
℃	Degree Celsius
α	Alpha
γ	Gamma
δ	Delta
μ	Micro
μg	Microgram
μg/ mL	Microgram/ milliliter
μl	Microliter
μm	Micrometer

Abstract

It was reported in world population prospects: the 2008 revision that the world's population is increasing 80 million yearly and by 2050, it will reach 9-10 billion. Unintended pregnancy plays major role in population increase. This increased incidence of unintended pregnancy is owing to inadequate access to the presently available contraceptive methods. Non-hormonal female contraception has become more attractive method as it avoids the adverse connotations associated with the use of hormones used in hormonal contraceptives. The process of non-hormonal female contraception is accomplished through the intra-uterine contraceptive device (IUCD) over the past decades. However, IUD associated complications and side effects over presently existing form of IUDs leads to non-preference of IUDs by majority of female individuals.

RISUG® (Reversible Inhibition of Sperm Under Guidance) is a hydrogel and is useful as vas deferens injected reversible male contraceptive which is under advanced phase III clinical trial in India. The use of polymeric hydrogel RISUG® for the purpose of establishing as a non-hormonal female contraceptive implant is evaluated in this article. Different formulations of RISUG® hydrogel were developed by grafting with suitable bio-polymers was developed in order to develop non-hormonal female contraceptive implant. Physiochemical characterizations for all the polymeric formulations were evaluated in order to identify the chemical integrity and mode of interactions between the polymeric mixtures. Selective antimicrobial property and antiviral property of RISUG® polymer was evaluated.

Cytocompatibility for all the polymeric formulations were evaluated using respective cell lines. *In vivo* biocompatibility of the polymeric formulations was evaluated by histological and immunohistochemical evaluation of respective rat tissue sections. Hematology, blood biochemistry and organ toxicity for the polymeric formulations was also performed to reveal the biocompatibility of all the polymeric formulations. The results of the current study indicated that the RISUG® has excellent opportunity to be formulated as various forms of non-hormonal female contraceptive implant as respective concentrations which can be implanted at respective sites.

Chapter 1

Introduction and Literature Survey

1.1 Introduction

Health promoters and professionals in collaboration with policy makers and funding bodies are trying to establish the reasons and need for contraceptive techniques in developing countries due to the prevalence of unmet need for contraception in these countries [1]. Timely use of contraception can minimize the burden of unsafe abortion and undesired child birth that may ultimately promote well-being of both mother and child. These measures may indirectly contribute to other developmental factors like reducing poverty and reduce the burden of population explosion [2-4]. The global development program gives prime importance in empowering women to take decisions on their pregnancy desires. With the aim of adding 120 million new women aware of modern contraceptive methods by the year of 2020 among 69 poorest countries of world, a global partnership has been established in the year of 2012 [5]. It was estimated in 2014 that about 225 million women of developing countries does not want preferential use of contraceptive for their need to control child birth. Among these 225 million women, 160 million were not using any contraceptive methods and 65 million were practicing traditional contraceptive methods. Reason behind this lack of interest to use contraceptive methods may be due to the adverse effects of prevailing female contraceptive techniques present till date [3].

According to global trend, the use of permanent contraceptive procedures in order to prevent un-intended pregnancies show high prevalence rate than any other methods. However the trend also depicts an increase in use of long-acting reversible contraceptive techniques. Copper Intra-uterine Device (IUD), levonorgestrel Intra-uterine System (LNG-IUS), injectable contraceptives (depot medoxy progeterone (DMPA) and

norethindrone enanthate (NET-EN)) and Etonogestrel single-rod contraceptive implant are the major long acting reversible contraceptive techniques [6]. Owing to the long term associated side effects like stress, obesity, headache, nausea, breast tenderness, mood swing, missed periods, cardio vascular disease risk factors, etc caused by hormonal female contraceptive techniques, a substantial research focus is undergoing to ensure a new form of potent non-hormonal female contraceptive [7, 8]. It is reported that around 14.3% of reproductive age women worldwide use IUD for contraception purpose. It was reported that IUD post implantation inside the uterus hinder mechanically with embryo implantation and the rate of pregnancy is decreased with increased interaction of uterine surface with IUD. These IUDs also expected to exert inflammatory reaction in the endometrium that provides unfavorable environment for the survival of spermatozoa. Increase in uterine motility and increase in tubal motility also have been evidenced. Presence of prostaglandins were also identified in uterine fluid post implantation of IUD. However exact mechanism of action for IUD is not well established. These changes inside the uterus exerted by IUD depend on shape, size and flexibility of the IUD [9-12]. Although IUD is considered as an effective way for establishing long term reversible form of contraception not less than 10 years [6], it also have major complications and side effects even lethal to female users. Notable complications associated with IUDs are expulsion, bleeding, cramping pain that leads to major form of side effects like penetration of IUD inside uterine wall, exogenous and endogenous infections [12]. These complications and side effects of presently existing form of IUDs leads to non-preference of IUDs by majority of female individuals who are in need of contraception and if they use then also of early removal of implanted IUD [73].

Regardless of substantial developments in new contraceptive methodologies un-intended pregnancies remain as a considerable universal public health problem. Even though women have acquired rights over multiple contraceptive techniques in 21st century; about 222 million women in low income countries have not met their needs to access contraceptive techniques to delay or to avoid their gestation. It was identified that availability of limited contraceptive choices and family planning services, problems faced due to complications and side effects, religious and cultural hostility and inequality to female partners are major reasons for the increase in the incidence of un-intended pregnancy [6]. Thus this introduction and literature survey focuses on impact of unintended pregnancy on socio-economic point of health system and use of intra uterine contraceptive device (IUD) to prevent the rate of un-intended pregnancies worldwide.

1.2 Un-intended pregnancy

The pregnancies occurring unwanted for at least one of the couples which are inopportune and unplanned is said to be un-intended pregnancy. Un-intended pregnancy is considered as undesired to one or both of the partners which may leads to public health tribulations especially foremost reproductive health problems [13]. It was reported that about 87 million of unintended pregnancies are occurring among 210 million of total pregnancies of every year (WHO 2005). It was also reported that unsafe abortion has lead to 18% of maternal death per year (2008). The rate of unsafe abortion was accounted as 22 per 1000 women of 15 - 44 age groups worldwide. About 48% of sexually mature women (15-44 age) in America might have experienced one abortion [14-16]. This high rate of unintended pregnancies has major negative impact on pregnancy related health and social issues to mother, child and the male partner. Social issues like suicide, mental

depression, unstable family relationships, physical and psychological violence and health related issues like gestational malnutrition, psychological health issues, birth of infants with low body weight and also risk of miscarriage [17, 18]. Year wise estimation on % occurrence of unintended pregnancies worldwide is represented in Figure 1.1. Several macro level studies had reported that, population health play a significant role in economic performance and growth of a nation. Un-intended pregnancy entails noteworthy financial and social impact on nation which is considered as most critical challenges faced by the public health system of a nation [19, 20].

1.3 Economic effect of unintended pregnancy and unsafe abortion

Devoid of any race or socio economic status, unintended pregnancy is recorded as high risk involving conception which shows high occurrence in poor or low-income adult female [21]. This leads to dramatic increase in rate of illegal abortion. The global statistics reports that more than 15 million women are experiencing illegal unsafe abortion every year in Asia. The effect of pregnancy complication leads to death rate of 50,000 women for a year in developing countries. This portrays that illegal abortion accounts for main cause for mortality rate worldwide. The medicinal expenses to treat complications due to unsafe abortion exceed the expenditure for safe abortion. About 98% of illegal abortions were recorded in the year of 2008 in developing countries and about 43.8% of abortions were recorded worldwide among which 50% of abortions were illegal abortions [22-24]. The unsafe abortion may lead to irretrievable severe medical ill health to the female individual both mentally and physically. This medical complication may indirectly affect the cost of medical expenditure that acts as a heavy burden for government programs. US economic analysis had reported that more than 12 billion was

spent for a year on unsafe abortions. Avoiding these expenditures on unintended pregnancies can save three-quarters of federal government allocated budget for INICEF research assignments in 2010. Maternal mortality rate is considered as an effective indicator for a countries' development in the world. It was aimed by Millennium Development Goals that maternal mortality rate has to be reduced to 75% between 1990 to 2015. Family planning and effective contraceptive technique may reduce the incidence of un-intended pregnancies worldwide [25, 26].

1.4 Population and socioeconomic effect of unintended pregnancy

The economic status of a country is affected by factors like reproductive behavior healthcare, population welfare behavior and characteristics. The large-scale economic system outcome of a country is influenced either positively or negatively by population health. It was estimated that at every 40 years the population of the world doubles but it occurs less than 20 years in developing countries [27-29]. The increase in population in turn increases poverty and sickness in a country which also leads to dissimilar distribution of health services. Increase in population will leads to deprived access to edification and income. Population increase may show economic burden on third party payers like employer supporting insurance programs to meet the rising demands. This economic burden will directly reflect in Consumer Pay Index (CPI) that may direct to noteworthy burden on common tax payers [30-32].

1.5 Effect of population increase leads to health problems

Health indicators could able to express the effect of population of a community. Important factors like labor, physical and human capital certainly affect the economic growth [33, 34]. Economic literature defines education, training, skills, health, migration, expertise, experience and some other investments are included in human capital [35]. Effect of public health should be inspected as one among the significant factors in collecting human capital. But unintended pregnancy has a direct impact on health and wellness in so many ways.
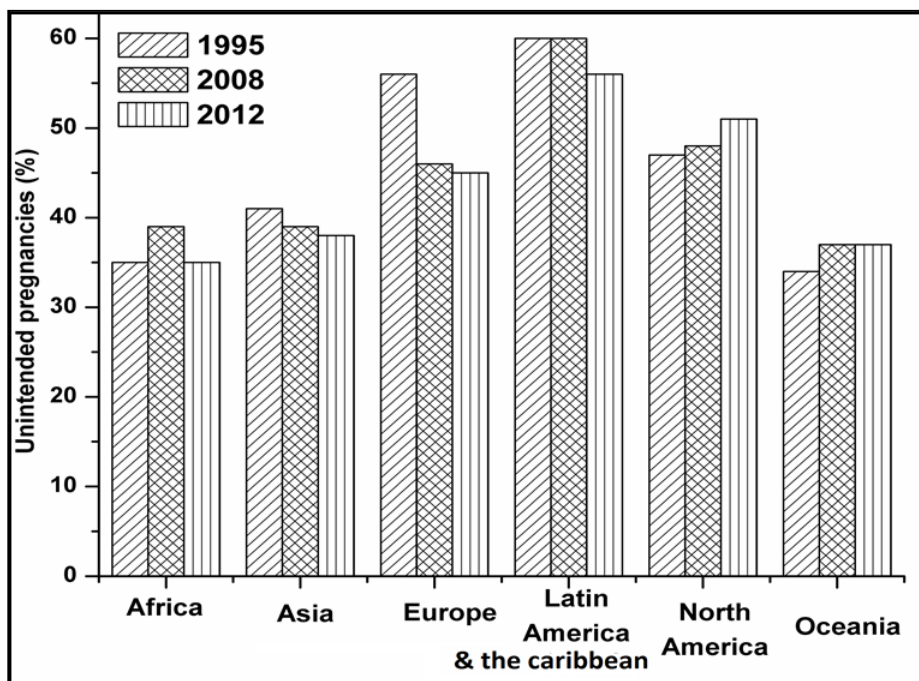
Figure 1.1. Prevalence of unintended pregnancies worldwide. (Data Source [36])

It reduces the productivity of labor by reducing the eminence of existence. The health stock of individual can be reduced by unintended pregnancies by reducing the labor productivity which ultimately reduces the living standards [37-40].

1.6 Effect of un-intended pregnancy in reproductive health

Reproductive health can be subdivided into categories like; discussion, information, andragogy and communication regarding family planning, encouraging individuals in right to independently choose marriage partner, gender equality contribution and equal rights in marriage decision making, family planning assistance, promoting reproductive decisions, provision for prenatal and health care for women, assuring sexual and reproductive health, measures to prevent infertility, suitable therapy for abortion, infertility and treating its complications as well as reproductive tract infections and sexually treated diseases therapy. Unintended pregnancy may lead to high risk in child mortality rate [41-44]. This un-intended pregnancy may also leads to mental illness like schizophrenia for infants due to malnutrition and child abuse [45]. This may leads to poor academic performance of the particular child. Child mortality within the age of 5 acts as an important marker for reproductive health which can be influenced by prevalence of unintended pregnancy influenced unsafe abortion leading to maternal deaths [46]. Among 43.8 million worldwide abortion, 86% of abortion occurred in low or middle income countries which accounts for 13% of maternal death due to unsafe abortion between the years of 2003 to 2008 [24, 47]. Lack of awareness regarding family planning is associated with these unintended pregnancy and maternal deaths. Proper use of family planning measures may reduce un-intended pregnancy that will reduce the economic burden of the society. This safe and effective use of family planning will provide significant economic savings for the government budget that will in turn be used in different government development programs leading to economic growth [26].

1.7 General prevalence of contraceptive techniques

Methods to improve reproductive health generally depend on use of contraceptive techniques and their prevailing unmet needs. From the year of 1990 to 2011 the prevalence of contraceptive techniques among women was observed to be increased from 55% to 63% globally [48]. The number of female individuals practicing any method of contraceptive technique is represented in Figure 1.2. About 36% of women were using contraceptive techniques. However the use of contraceptive techniques is high in economically high income countries. Number of female individuals using modern method of contraceptive technique at reproductive age is represented in Figure 1.3. Among many contraceptive techniques, the use of IUD and female sterilization showed high prevalence rate from the year 1990 to 2011 in global scenario. It was observed that the prevalence of female sterilization was common in Asia, Latin America, North America and Caribbean and use of IUD was observed to be common in Europe and Asia. In countries like India, female sterilization was observed to be more where gestation was observed at young age. This clearly portrays that need for new contraceptive techniques to delay gestation. About 57% of comprehensive contraceptive prevalence was observed in low-income countries for which IUD (15%) and female sterilization (21%) shows highest prevalence [49]. But the truth is this prevalence rate occurs only in low income countries. Number of female individuals with unmet need for any method contraception and modern method of contraception is represented in Figure 1.4 (A), (B) respectively.
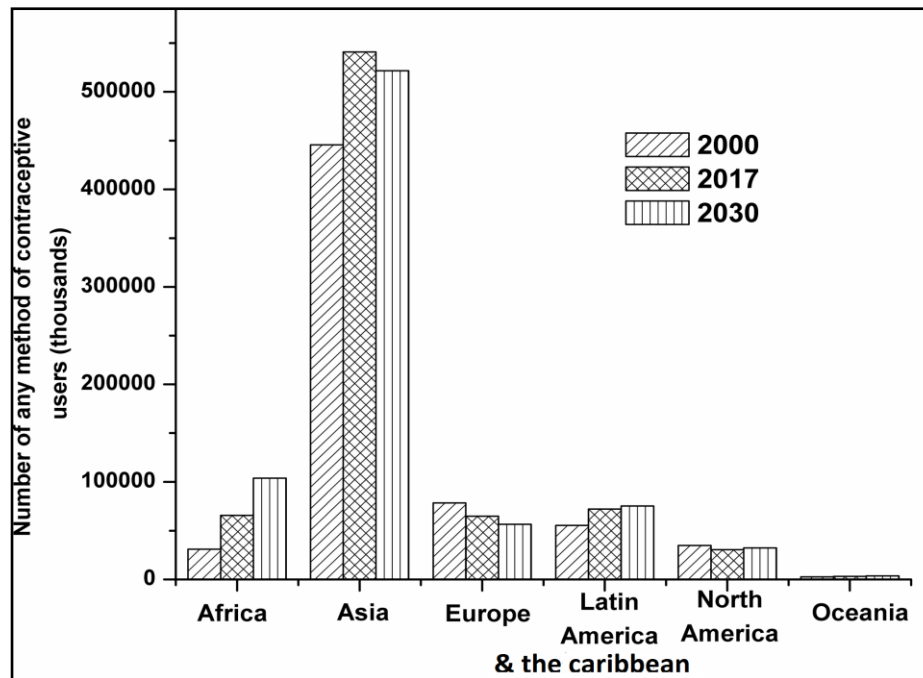
Figure 1.2. Female individuals using any method for contraception globally (Data Source

[50])

1.8 Long Acting Reversible Contraceptive (LARC) techniques

LARC is used as modern contraceptive technique that includes copper bearing Intra Uterine Devices (IUD) and levonorgestrel Intra Uterine System (IUS). Sixty-one percentage (61%) of reproductive age group (15 - 49 years) women were practicing some form of contraceptive technique. Among them 9% in high income and 18% in low income countries practice LARC in the year of 2003 [49]. The reproductive age US women use only 17% of LARC among 56% of contraception practicing women. Globally only 14% of reproductive age group women use IUD However, in Asia IUDs are used by 18% reproductive age group women and within Asia in China itself 40% IUDs are used in China by reproductive age group women [49].
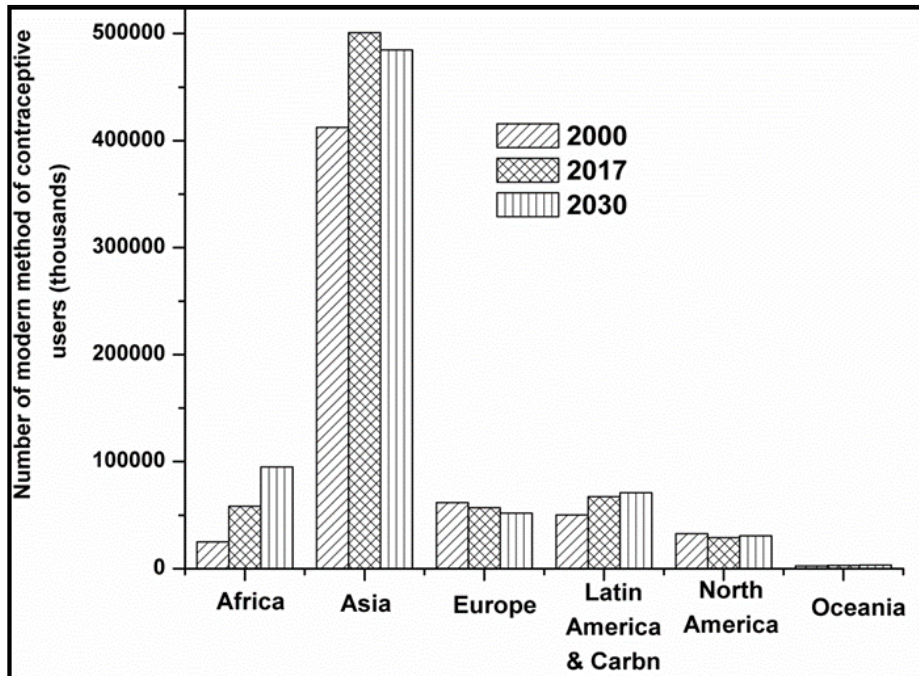
Figure 1.3. Female individuals using modern methods for contraception globally (Data

source [50])

1.9 Uterine architecture

1.9.1 Mammalian uterus and its anatomical difference

The duplex, bicornuate and simplex (Figure 1.5) are the three anatomically different types of the uterus [51]. The duplex type has two fallopian tubes joining externally together and opens independently in to the cervical canals. In some species, the fallopian tube combined inside the cervical region and opens in the vagina with single ostium.
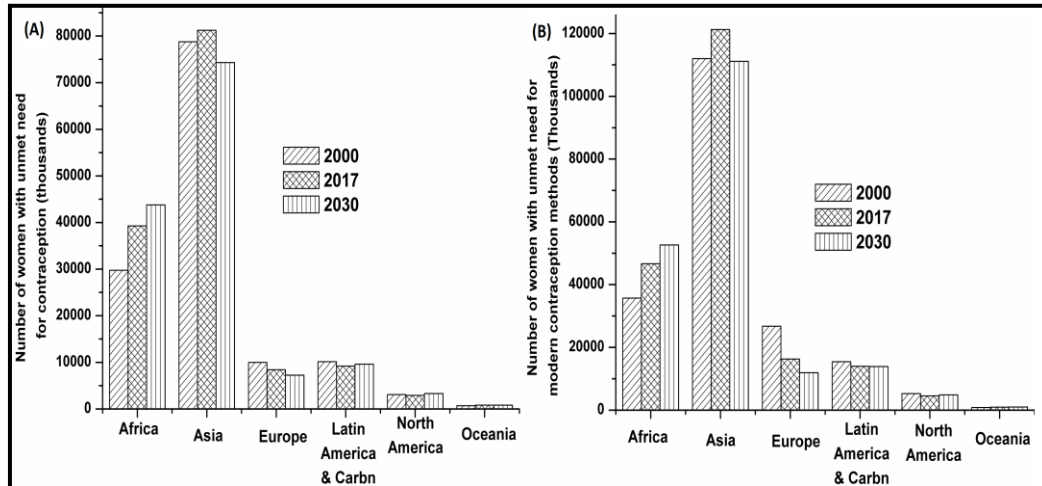
Figure 1.4. (A) Number of women with unmet need for contraception. (B) Number of women using modern contraception worldwide (Data source [50])

The bicornuate type has two fallopian tubes joining externally at cervical beginning and is internally joined to form corpus - the body that opens in the vagina by a single cervical canal. The simplex type uterus has externally unpaired single corpus that consists internal cornual lumina with small rudiments.
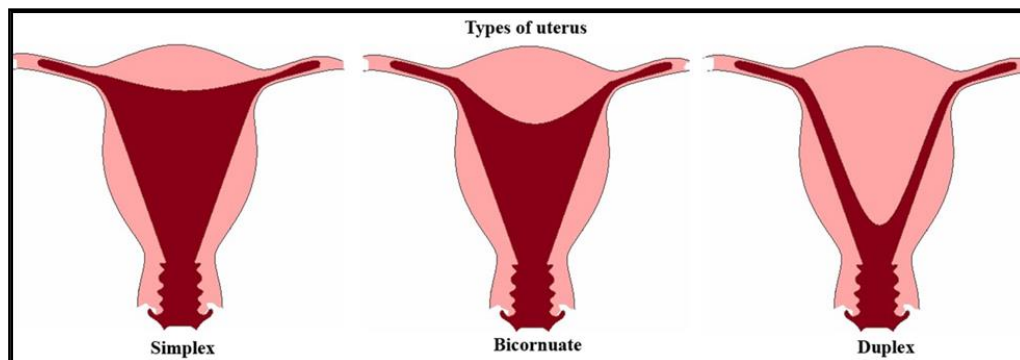
Figure 1.5. Anatomically different types of female uterus

They have single cervical canal to communicate with the vagina. The evolution of functional uterus might be originated from the region of each egg - transporting fallopian tube of primordial egg laying mammals as similar to duplex type of marsupials. Due to

the evolution of the eutherian type vagina, there arises a possibility for the external and internal fusion of the uterus to originate as united corpus and cervical canal. Followed by the fusion, the long bicornuate type might be evolved to short bicornuate and at last to simplex type. There is a vast variation inside orders and suborders of the class of uterus of a given mammalian species. Two to three different types of uterus are observed in *Megachiropeta, Microcheropeta, Rodentia* and *Artiodactyla*. Particular species of bats have double, bicornuate and simplex types of uterus [52, 53].

1.9.2 Macroscopic anatomy of human uterus

Uterus is the hollow, pear shaped fibro-muscular organ (Figure 1.6.) possess considerable variation in shape, weight and dimensions depending on both estrogenic stimulation and previous parturition. Uterus serves as incubator and nourishing chamber to the embryo and fetus with the aid of continuous contraction attributed by its thick muscular wall that expels the fetus to external parturition. This complex phenomenon of the uterus is said to occur during child birth. Uterus measures 8 cm long, 5 cm wide and 2.5 cm thick and approximately weights 30 - 40 g in nulliporpus women.
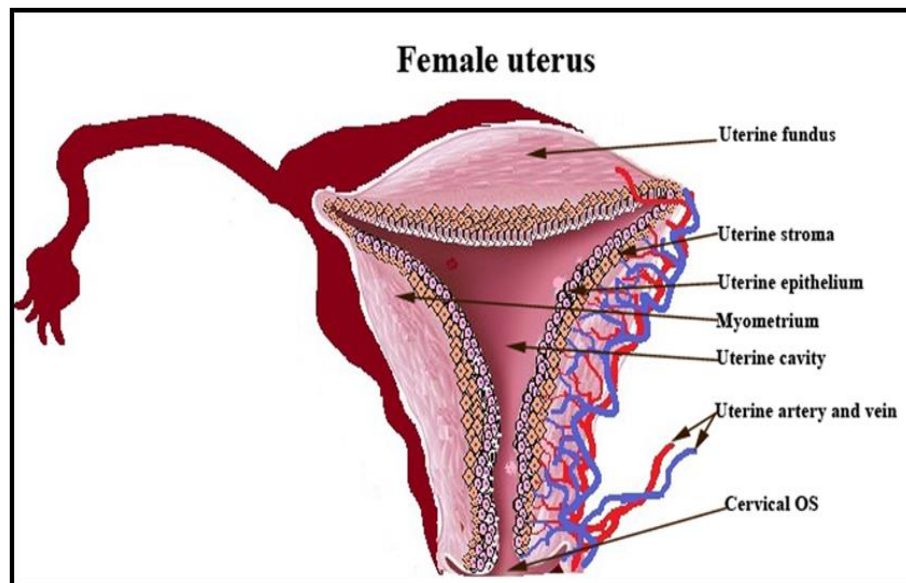
Figure 1.6. Female uterus anatomy

Uterus consists of two portions; corpus and cervix. Corpus lies in the upper portion of the uterus having muscular in nature and cervix lies in the lower portion of the uterus having fibrous in nature. Uterus narrows down to the cervix after a small constriction slightly below the midpoint of the uterus. The region of the uterus extending its portion above the beginning point of origin of the fallopian tube is called as fundus. Uterine body lies below the initial opening of the uterine tubes. The size of the uterus corpus is similar (larger in size in reproductive women) before menarche and after menopause. Due to thick uterine wall, the cavity of uterus is comparatively small that appears similar to cleft in sagittal plane having the anterior and posterior walls appears to be in contact. The coronal section of uterus seems to be triangular in shape [54].

1.9.3 Microscopic anatomy of uterus

Uterus consists of two muscular coats and serous coat. The endometrium which is inner and mucous membrane coat; the highly vascular middle myometrium poised of smooth muscular fibers having interspersed fibrous and elastic connective tissue; the outer perimetrium is extended from peritoneal membrane which engulf maximum of uterine surface but not the cervix [54].

1.9.4 Uterine Myometrium

Uterine myometrium is composed of several muscular layer composed of smooth muscle fibers. The uterine myometrium contains vascularized thin connective tissue septa separating the layers of flat bundles of smooth muscle fibers. The myometrial muscular pattern originates from paramesonephric primordial pair. These muscular fibers are arranged as criss-cross diagonal pattern originating from opposite side of each half. The second statum submucosal layer consists of longitudinal muscular fibers with some circular and oblique muscular bundles. The muscular layer of stratum submucosal layer have sphincter like pattern in the inner walls of uterine tubes. The spongy intermediate layer of myometrium is called as stratum vasculare which is rich in blood vessels especially with large channels of vein [54].

1.9.5 Uterine endometrium

Endometrium is the mucous membrane which lines the uterine body and also extends as lining of uterine tubes. The epithelium and lamina propria of endometrium consists of simple tubular glands. Endometrial epithelial cells are composed of simple columnar cells along with secretory and rare ciliated cells. Cellular rich connective tissue

lamina propria is composed of cells containing amorphous intercellular components as abundant material. Endometrium is nourished by specialized coiled arteries. Endometrium can be divided in to two portions. First portion is the proliferative, secretary and degenerating functional layer that prepare endometrium a suitable place for implantation of blastocyst. This functional layer occupies two third portion of endometrium. The lower basis layer nourishes endometrium for its regeneration post menstrual cycle [54].

1.9.6 Cervix uteri

The extreme lower segment of the uterus which forms a small conversion region between the corpus uteri and the vagina is called the cervix. Cervix can be divided in to supra-vaginal cervix that lies superior to the vaginal vault and the portio vaginalis that lies inferior and get exposed along with vagina. About 90% of the cervix is made up of dense fibrous connective tissue and remaining 10% is made up of smooth muscle. The columnar epithelial cells line the cervical canal and are secretary in nature. These epithelial cells are arranged as V-shaped leaves folded as palm tree and so is called as, plicae palmatae. The superficial portion of the cervical canal widens from narrow cervical channel which consists of change over to columnar epithelium from squamous epithelium. The secretions of cervical cavity originates from both uterus and cervix and run towards vagina. This secretary nature of the uterine cavity has significant consideration in administering any drug inside uterine cavity since it dilutes the drug post administration. Secretions of uterus play a significant role in oocyte fertilization. The secretions are watery during ovulation which facilitates the sperm to fertilize oocyte

through penetrating the uterus. During pregnancy the viscosity of the secretions becomes viscous that prevents microbial invasion and sperm penetration inside the uterus [54].

1.10 Methods of LARC

These methods of contraceptives are considered as cost effective and can be used during intercourse which do not rely on user adherence furthermore this mode of contraceptives do not demand daily observation [55].

1.10.1 Etonogestrel single-rod contraceptive implant

This cost effective form of contraceptive implant can provide three years of contraception that shows high efficacy, low failure due to which high rate of continuation were observed. They show lighter or less frequent bleeding which resumes normal ovulation immediately post removal. Furthermore it shows less failure rate than IUDs, LNG - IUS and ectopic pregnancies [6, 56-59].

1.10.2 Injectable mode of contraceptive

Norethindrone enanthate (NET-EN) and depot medoroxy progesterone acetate (DMPA) is the most commonly prevailing injectable mode of contraceptive. The average time to conceive after administration of DMPA is 8 - 10 months of duration [60].

1.10.3 Levorgesterel Intrauterine System (IUS)

The kind of implant is used not only for contraception but also to treat menorrhagia and its contraceptive efficacy last minimum of five years and maximum of seven years in parous women [61]. About 80% of women get their gestation within 12

months of removal of IUS. The hormone reduces the proliferative efficacy of endometrium which reduces menstrual bleeding and also prevents anemia [62]. Side effects like oligomenorrhea and amenorrhea was observed maximum of 24 months post implantation. However the prevalence of IUS among women preferring contraception is only 1% of rate [6].

1.10.4 Copper IUD

Copper IUD effectively provides contraception for not less than 10 years. It can also acts as an effective emergency contraceptive if implanted with in the interval of five days post unprotected sex. The mode of action is still not clear. However, it was assumed that IUD directly disturbs the implantation of embryo. Furthermore copper containing IUDs exert spermicidal actions by influencing local inflammatory response inside the uterus. These induced inflammatory responses exert deleterious effect to developing embryo. It is expected that inert metal like copper enhances the inflammatory response inside the uterus that could conduct through lysosomal activation [6, 54].

1.11 IUD exerted biological changes in endometrium

IUD is always recognized as a foreign material by the uterine cavity that enhances cellular biological and secretary changes inside uterine cavity. Changes like enhanced vascular permeability, stromal leukocytic infiltration that includes mononuclear cells, macrophages and neutrophils were observed [63]. A rise in leukocytic population was observed post implantation of IUDs. Similar kind of leukocytic infiltration could be observed 24 - 48 h prior to beginning of menstruation [64]. The adjacent area around IUD inside the uterus cavity shows biological changes similar to endometriosis. The increased

rate of leukocytes and macrophages was expected to exert unfavorable environment that promotes fertility inside uterine cavity. IUD users have reported increased levels of proteins from intrauterine cavity that was considered as a marker for cellular damage of neutrophils and macrophages that in turn promotes unfavorable environment for fertility. Furthermore copper IUDs affect cellular DNA of endometrium, glycogen metabolism and estrogen response by mucosa of uterine cavity. These cellular and biological changes may leads to normal enzymatic activity of endometrial cavity. Experimental observation in non-primate animals has reported increased prostaglandin (PGF_2) synthesis inside uterus which includes luteolysis [65-68]. Endometrial cells that are adjacent to IUDs have the ability to synthesize PGF_2 and PGE_2. Certain amount of copper from copper bearing IUDs are released from inside the uterine cavity which enhances systemic copper absorption via endometrium. However certain studies had reported no significant increase of copper in serum post implantation of IUD. These studies suggest that copper released from IUD reacts only with uterine fluid [54].

1.12 IUD exerted complication

The reason for less prevalence of IUDs are the IUD associated complications like expulsion, perforation, pelvic inflammatory disease (PID), pregnancy with IUD, carcinogenicity and abnormal bleeding. These complications can be explained in detail as follows.

1.12.1 Uterine perforation of IUD

Uterine perforation is considered as serious complications associated with IUD use. About 0.6 to 1.2 for 1000 IUD insertions has reported uterine perforations. There was no significant difference in the rate of uterine perforations were observed during push and withdrawal techniques of IUD implantation. IUDs are usually implanted during menstruation in order to prevent fear of patients from bleeding. The cervical orifice also observed to be wide open which facilitates the implantation of IUD during menstruation. Serious medical consequences like bowel perforation or bowel obstruction could be resulted due to intra-abdominal IUD. Immediate removal of IUD through laproscopy is advised to remove IUD located in abdomen. Some times laprotomy is advised to remove IUD which is observed showing peritoneal cavity adhesions [54].

1.12.2 Pregnancy with IUD

Pregnancy with IUD may result to septic abortion during second trimester. About 3 - 9% of pregnancies with IUDs are observed to be ectopic pregnancies. About 10 fold of fetal loss was estimated in patients showing pregnancies with IUDs during second trimester and about 26 fold of fetal loss was observed by septic abortion. The fetal loss was observed to be minimized by removing IUDs during first trimester. Septic fetal loss may result in both fetal and maternal mortality [54, 69, 70].

1.12.3 IUD expulsion

The rate of expulsion of IUD varies depending up on the devices from 11 to 13 per 100 women. The expulsion rate is higher in non medicated IUD and in nulliparous women. Expulsion occurs during menstruation and especially 3 months of post IUD

insertion. The absence of IUD investigation thread in vagina may leads to expulsion of IUD [54].

1.12.4 IUD exerted carcinogenecity

Subcutaneous implantation of foreign body in laboratory rats resulted in development of sarcoma. Furthermore uterine sarcoma or carcinoma was observed in uterus of laboratory rats implanted with plastic or stainless steel. But poor evidence for IUD associated sarcoma or carcinoma was seen in human practitioners [71, 72].

1.12.5 IUD associated improper menstrual bleeding

Copper or non-medicated IUDs leads to double the amount of blood loss during menstruation especially during first 3 months inter menstrual bleeding that may potentially leads to iron deficiency and anemia. The contraction and relaxation of uterus during menstruation has shown uterine trauma due to the presence of foreign body inside the uterus [73, 74].

1.12.6 IUD associated PID

Symptoms like uterine motion tenderness, pain felt in abdominal region, purulent cervical discharge, temperature of about 38º C and above, adnexal swelling with pain and inter-menstrual bleeding acts as positive for PID. The probability of getting PID is more if sedimentation rate of erythrocyte is more than 15 mm/h, which is generally observed greater than 10,000 WBC/mm^3 of blood. If the inflammation marker C-reactive protein is positive and cervical microbial culture shows positive for micro-organisms *Nisseria gonorrhoea* and *Clamydia trachomatis,* then there is greater chance for PID.

Predominantly in nulliparous young women antibiotic treatement is provided often due to serious PID associated consequences like pelvic adhesions and infertility. Patients who are suspected with PID are advised to remove IUD. Two different groups of micro-organisms are involved in PID: exogenous microorganisms especially *Neisseria gonorrhea*, *Mycoplasm hominis, Chlamidia trachomatis* and endogenous microorganisms includes lower female reproductive tract microbial flora [75, 76]. Although endogenous microflora were also observed in patients with sexually transmitted disease associated PID. IUD associated PID is more in initial few days usually not more than 30 days post implantation. The mode of insertion of IUD acts as a main reason for pathogenic microbial invasion to uterus. It is suggested that female individual having sexual intercourse less than five times in a week and having single sexual partner whose age is above 25 years were expected to have PID at less than 2 per 1000 IUD insertion. IUD removal is advised as early as possible after detection of PID in order to avoid further complications [77, 78].

1.13 RISUG® (Reversible Inhibition of Sperm Under Guidance)

RISUG® acronymed as Reversible Inhibition of Sperm Under Guidance is composed of styrene maleic anhydride (SMA) and styrene Maleic acid (SMAc) dissolved in dimethyl sulfoxide (DMSO) to form viscous hydrogel. This hydrogel is injected in to vas deferens of male reproductive system to establish non-hormonal long term contraceptive effect [79]. The hydrogel is injected in to vas deferens through minimally invasive technique. When RISUG® comes in contact with biological fluid inside vas deferens; the polymer tends to reduce the pH of the surrounding medium through ionic dispersions from the polymer to the surrounding medium. This pH imbalance inactivates

the male gamete sperm [80, 81] through establishing structural damages like acrosomal damage, motility damage, etc. and these damages to sperm inactivates them from fertilization. RISUG® also provides additional biological activities like anti-microbial property and it is also proposed that, the polyelectrolytic property of RISUG® gel post implantation in to vas deferens could inhibit the interaction between gp120 of HIV and host CD4 cells through which it could also establish entry inhibitory activity against HIV virus [82, 83]. Information on using RISUG® as non-hormonal female contraceptive implant is not yet explored clearly. The present thesis focuses on developing RISUG® as a non-hormonal female contraceptive implant and exploring its toxicology and anti-fertility effects. Furthermore different implantable formulations of RISUG® polymeric hydrogel by grafting with various bio-compatible polymers were developed. The toxicological and anti-fertility effect of nude RISUG® polymer and RISUG® grafted other polymeric formulations were also evaluated. Tissue specific reaction and histo-architecture of the polymer implanted tissue sites were examined. The physiochemical properties of RISUG® polymer, RISUG® grafted polymeric mixture were evaluated to understand the chemical integrity of the polymers and the mechanism of polymer-polymer interactions. Chapter wise objectives for this thesis are described as follows.

Chapter 2 describes an innovative insight about the use of hydrogel formulation consisting of Styrene Maleic Anhydride (SMA) dissolved in Dimethyl Sulfoxide (DMSO) as non-hormonal fallopian tube contraceptive implant. Firstly, *in vitro* behavior of SMA hydrogel was evaluated by *in vitro* swelling and rheological properties to comprehend the polymeric hydrogel property post implantation inside the fallopian tube. Simulated Uterine Fluid (SUF) was used to simulate female reproductive tract

environment in this study. Mechanical strength of the hydrogel when subjected to dynamic environment post implantation in the fallopian tube was estimated by the G' values demonstrated. SMA hydrogel expressed selective antimicrobial activity against opportunistic pathogens (*Escherichia coli, Pseudomonas aeruginosa* and *Staphylococcus aureus*) while having limited consequence over the growth of *Lactobacillus spp*. After confirmation of cytocompatibility against primary rat endometrial cell lines, the polymeric hydrogel was implanted inside the uterine horns of Sprague-Dawley rats. *In vivo* biocompatibility of the hydrogel was confirmed by histological and immunohistochemical evaluation of uterine tissue sections. Hematology, blood biochemistry and organ toxicity (kidney, liver, spleen, lungs and heart) also revealed biocompatibility of SMA hydrogel.

Chapter 3 delineates the use of RISUG® based non-hormonal female contraceptive films. RISUG® was blended with polyvinyl alcohol (PVOH) to formulate biodegradable intra-vaginal contraceptive films. The formulated films were characterized for their thermal, physiochemical and biological features. The results showed that both RISUG® and PVOH were miscible and interacted extensively at the intermolecular level. Variations in the concentration of RISUG® resulted in the changes in physicochemical, thermal and rheological characteristics of the formulated blends. *In vitro* toxicological assay of the polymeric formulations did not show any significant toxicity. However, the blend films retained spermicidal potential of RISUG®. Furthermore, *in vivo* toxicological evaluation of the polymeric blend in the rat model revealed their biocompatibility with no significant organ toxicity, hematological and biochemical alterations.

Chapter 4 describes about fabricating a novel biodegradable flexible block co-polymeric scaffold composed of PCL-DA: PEG-DA blend grafted with different concentrations of RISUG®. The fabricated polymeric scaffolds were further investigated for their physicochemical properties, mechanical property, anti-microbial property, sperm killing ability, *in-vitro* biodegradability, *in-vitro* and *in-vivo* toxicological property for the application of new form of implantable non-hormonal biodegradable intrauterine contraceptive device.

Chapter 5 presents and validates a hypothesis that RISUG®-based intrauterine could exert a potential anticancer effect in the earlier stages of cancer development. The mechanism of anti-cancerous activity is hypothesized that RISUG® involves its lipid membrane destabilizing activity. This activity is modulated by both, the cellular microenvironment and lipid bilayer composition. Acidic environment along with the significantly higher fluidic nature of lipid bilayer of the cancerous cells make them more prone to lipid solubilisation effect of RISUG®. We here present an in-depth insight into the factors that would favour faster solubilisation of cancer cell membrane, thereby exerting an anticancer effect. Antiviral index of the polymer was characterized using Cellosaurus cell line (CEMss) cell lines. More specific studies could further validate the hypothesis in order to establish Improved Intrauterine Contraceptive Device (IIUCD) as anti-cancerous and anti-viral female contraceptive implant.

Bibliography

[1] J.E. Darroch, S. Singh, Adding it up: the costs and benefits of investing in family planning and maternal and newborn health—estimation methodology, New York: Guttmacher Institute, DOI (2011).

[2] S. Singh, J.E. Darroch, L.S. Ashford, Adding it up: The costs and benefits of investing in sexual and reproductive health 2014, DOI (2014).

[3] S. Moreland, S. Talbird, Achieving the Millennium Development Goals: the contribution of fulfilling the unmet need for family planning, DOI (2006).

[4] D. Canning, T.P. Schultz, The economic consequences of reproductive health and family planning, The Lancet, 380 (2012) 165-171.

[5] M. Ali, A. Seuc, A. Rahimi, M. Festin, M. Temmerman, A global research agenda for family planning: results of an exercise for setting research priorities, Bulletin of the World Health Organization, 92 (2013) 93-98.

[6] R. Joshi, S. Khadilkar, M. Patel, Global trends in use of long-acting reversible and permanent methods of contraception: Seeking a balance, International Journal of Gynecology & Obstetrics, 131 (2015) S60-S63.

[7] N.G. Barr, Managing adverse effects of hormonal contraceptives, American Family Physician, 82 (2010).

[8] R. Sabatini, R. Cagiano, T. Rabe, Adverse effects of hormonal contraception, Journal für Reproduktionsmedizin und Endokrinologie-Journal of Reproductive Medicine and Endocrinology, 8 (2011) 130-156.

[9] H.J. Davis, J. Lesinski, Mechanism of action of intrauterine contraceptives in women, Obstetrics & Gynecology, 36 (1970) 350-358.

[10] N. Sagiroglu, Phagocytosis of spermatozoa in the uterine cavity of woman using intrauterine device, International journal of fertility, 16 (1971) 1-14.

[11] L.P. Bengtsson, A.H. Moawad, The effect of the Lippes loop on human myometrial activity, American Journal of Obstetrics & Gynecology, 98 (1967) 957-965.

[12] B.N. Barwin, S. Tuttle, E.E. Jolly, The intrauterine contraceptive device, Canadian Medical Association Journal, 118 (1978) 53.

[13] L.B. Finer, M.R. Zolna, Unintended pregnancy in the United States: incidence and disparities, 2006, Contraception, 84 (2011) 478-485.

[14] A. Sonfield, K. Kost, R.B. Gold, L.B. Finer, The public costs of births resulting from unintended pregnancies: National and state-level estimates, Perspectives on sexual and reproductive health, 43 (2011) 94-102.

[15] F. Amani, J. Bashiri, Y. Tabarraie, Applicdation of logistic regression model in surveying effective causes of unwanted pregnancy, Majallah-i Dānishgāh-i ʿUlūm-i Pizishkī-i Qum, 4 (2010) 32-36.

[16] S. Jahanfar, T.F. Ramezani, H.S. Sadat, The prevalence of unwanted pregnancy and it, DOI (2002).

[17] M. Pourheydari, A. Souzani, N. Shamaiian, Prevalence of unwanted pregnancies and their correlates in pregnant woman in Shahrood, Iran, DOI (2007).

[18] L. Fourn, S. Ducic, L. Séguin, Factors associated with low birth weight: a multivariate analysis, Sante (Montrouge, France), 9 (1999) 7-11.

[19] S. Singh, G. Sedgh, R. Hussain, Unintended pregnancy: worldwide levels, trends, and outcomes, Studies in family planning, 41 (2010) 241-250.

[20] Z. Karaçam, K. Önel, E. Gerçek, Effects of unplanned pregnancy on maternal health in Turkey, Midwifery, 27 (2011) 288-293.

[21] A. Thomas, E. Monea, The high cost of unintended pregnancy, CCF Brief, 45 (2011) 2-7.

[22] F. Amin Shokravi, P. Howden Chapman, A study on the effective factors of unwanted pregnancies in pregnant women of Tehran city, Journal of Reproduction & Infertility, 5 (2004) 249-258.

[23] M.-K. Moos, Unintended pregnancies: a call for nursing action, MCN: The American Journal of Maternal/Child Nursing, 28 (2003) 24-30.

[24] H. Wurtz, Indigenous women of Latin America: unintended pregnancy, unsafe abortion, and reproductive health outcomes, Pimatisiwin, 10 (2012) 271.

[25] M. Kirkman, D. Rosenthal, S. Mallett, H. Rowe, A. Hardiman, Reasons women give for contemplating or undergoing abortion: A qualitative investigation in Victoria, Australia, Sexual & Reproductive Healthcare, 1 (2010) 149-155.

[26] L.M. Morgan, E.F. Roberts, Reproductive governance in latin america, Anthropology & Medicine, 19 (2012) 241-254.

[27] F. Abazari, M. Arab, A. Abbasszadeh, Relationship of unwanted pregnancy and fertility behavior in pregnant women who visited maternity wards of Kerman hospitals, Journal of Reproduction & Infertility, 4 (2003).

[28] M.W.C. Hsiao, What should macroeconomists know about health care policy: a primer, International Monetary Fund2000.

[29] W.H. Organization, Report of the Commission on Macroeconomics and health, DOI (2002).

[30] N.A. Halpern, S.M. Pastores, H.T. Thaler, R.J. Greenstein, Changes in critical care beds and occupancy in the United States 1985–2000: Differences attributable to hospital size, Critical care medicine, 34 (2006) 2105-2112.

[31] B.G. Carr, D.K. Addyson, J.M. Kahn, Variation in critical care beds per capita in the United States: implications for pandemic and disaster planning, JAMA, Journal of the American Medical Association, 303 (2010) 1371-1372.

[32] J.D. Gipson, M.A. Koenig, M.J. Hindin, The effects of unintended pregnancy on infant, child, and parental health: a review of the literature, Studies in family planning, 39 (2008) 18-38.

[33] O.H. Kasule, Social and religious dimensions of unwanted pregnancy: an Islamic perspective, The Medical journal of Malaysia, 58 (2003) 49-60.

[34] C. Solomon-Fears, R. Ronquillo, Teenage pregnancy prevention: Statistics and programs, US Congressional Research Service, Library of Congress, 2000.

[35] E. Frankenberg, A. Buttenheim, B. Sikoki, W. Suriastini, Do women increase their use of reproductive health care when it becomes more available? Evidence from Indonesia, Studies in Family Planning, 40 (2009) 27-38.

[36] G. Sedgh, S. Singh, R. Hussain, Intended and unintended pregnancies worldwide in 2012 and recent trends, Studies in family planning, 45 (2014) 301-314.

[37] S.M. Skevington, Advancing cross-cultural research on quality of life: observations drawn from the WHOQOL development, Quality of Life research, 11 (2002) 135-144.

[38] M. Yazdkhasti, M. Keshavarz, E.M. Khoei, A. Hosseini, S. Esmaeilzadeh, M.A. Pebdani, H. Jafarzadeh, The effect of support group method on quality of life in post-menopausal women, Iranian journal of public health, 41 (2012) 78.

[39] M. Yazdkhasti, M. Keshavarz, Z. Mahmoodi, A.F. Hosseini, Self-directed learning and its impact on menopausal symptoms, Iranian Red Crescent Medical Journal, 16 (2014).

[40] J.T. King Jr, J. Tsevat, J.J. Moossy, M.S. Roberts, Preference-based quality of life measurement in patients with cervical spondylotic myelopathy, Spine, 29 (2004) 1271-1280.

[41] M. Yazdkhasti, A. Pourreza, A. Pirak, F. Abdi, Unintended pregnancy and its adverse social and economic consequences on health system: A narrative review article, Iranian journal of public health, 44 (2015) 12.

[42] H. Sadeghi, N. Aminisani, S. Arshi, S. Sezavar, Reproductive factors among migrant Tribes (Ashayer) women in Ardabil province, Journal of Ardabil University of Medical Sciences, 3 (2003) 38-43.

[43] S.S.M. Mahmood-Abad, F. Shahidi, M. Abbasi-Shavazi, F. Shahrizadeh, Evaluating knowledge, attitude and behavior of women on reproductive health subjects in seven central cities of Iran, Journal of reproduction & infertility, 7 (2007).

[44] A. Mohammadi, A.H. Eftekhar, F. Akbari-haghighi, A. Pourreza, M. Mahmoudi, Evaluation of services quality based on the patients'expectations and perceptions in zanjan hospitals, DOI (2003).

[45] J. Bongaarts, Trends in unwanted childbearing in the developing world, Studies in Family planning, DOI (1997) 267-277.

[46] S. Aghababaei, R. Bakht, R. Moien, Study of Contraceptives Used in Unwanted Pregnancies, SSU_Journals, 18 (2010) 307-314.

[47] H.H. Le, M.P. Connolly, L. Bahamondes, J.G. Cecatti, J. Yu, H.X. Hu, The burden of unintended pregnancies in Brazil: a social and public health system cost analysis, International journal of women's health, 6 (2014) 663.

[48] M.S. Fabic, Y. Choi, J. Bongaarts, J.E. Darroch, J.A. Ross, J. Stover, A.O. Tsui, J. Upadhyay, E. Starbird, Meeting demand for family planning within a generation: the post-2015 agenda, The Lancet, 385 (2015) 1928-1931.

[49] C. d'Arcangues, Worldwide use of intrauterine devices for contraception, Contraception, 75 (2007) S2-S7.

[50] G. Sedgh, L.S. Ashoford, R. Hussain, Unmet need for contraception in developing countries: examine women's reasons for not using a method, The Guttmacher Institute, 2016.

[51] R. Richter, Ein mittel zur Verhütung der Konzeption, DMW-Deutsche Medizinische Wochenschrift, 35 (1909) 1525-1527.

[52] E. Gräfenberg, An intrauterine contraceptive method, DOI (1931).

[53] J. Lippes, A study of intra-uterine contraception: development of a plastic loop, DOI (1962).

[54] U. Elchalal, Y. Abramov, Uterine biology and the intrauterine device, Advanced drug delivery reviews, 17 (1995) 151-164.

[55] W.H. Organization, Mechanism of action, safety and efficacy of intrauterine devices: report of a WHO Scientific Group [meeting held in Geneva from 1 to 4 December 1986], DOI (1987).

[56] J. Flores, M.L. Balderas, M.C. Bonilla, L. Vázquez-Estrada, Clinical experience and acceptability of the etonogestrel subdermal contraceptive implant, International Journal of Gynecology & Obstetrics, 90 (2005) 228-233.

[57] S. Funk, M.M. Miller, D.R. Mishell Jr, D.F. Archer, A. Poindexter, J. Schmidt, E. Zampaglione, I.U.S. Group, Safety and efficacy of Implanon™, a single-rod implantable contraceptive containing etonogestrel, Contraception, 71 (2005) 319-326.

[58] F. Lakha, A.F. Glasier, Continuation rates of Implanon® in the UK: data from an observational study in a clinical setting, Contraception, 74 (2006) 287-289.

[59] L. Mäkäräinen, A. van Beek, L. Tuomivaara, B. Asplund, H.C. Bennink, Ovarian Function During the Use of a Single Contraceptive Implant: Implanon Compared with Norplant 1, Fertility and sterility, 69 (1998) 714-721.

[60] P. Schwallie, J. Assenzo, The effect of depo-medroxyprogesterone acetate on pituitary and ovarian function, and the return of fertility following its discontinuation: a review, Contraception, 10 (1974) 181-202.

[61] J. Díaz, A. Faúndes, M. Díaz, N. Marchi, Evaluation of the clinical performance of a levonorgestrel-releasing IUD, up to seven years of use, in Campinas, Brazil, Contraception, 47 (1993) 169-175.

[62] P. Blumenthal, A. Voedisch, K. Gemzell-Danielsson, Strategies to prevent unintended pregnancy: increasing use of long-acting reversible contraception, Human reproduction update, 17 (2010) 121-137.

[63] S. Shaw Jr, L. Macaulay, W. Hohman, Morphologic studies on IUD-induced metrorrhagia I. Endometrial changes and clinical correlations, Contraception, 19 (1979) 47-61.

[64] G.W. Bartelmez, The human uterine mucous membrane during menstruation, American Journal of Obstetrics and Gynecology, 21 (1931) 623-643.

[65] A. Sedlis, J.V. Reyniak, Endometrial leukocytes in patients using intrauterine contraceptive devices, American Journal of Obstetrics & Gynecology, 108 (1970) 1209-1212.

[66] N. Sagiroglu, E. Sagiroglu, Biologic mode of action of the Lippes loop in intrauterine contraception, American Journal of Obstetrics & Gynecology, 106 (1970) 506-515.

[67] A.B. Kar, A.D. Engineer, R. Goel, V. Kamboj, P. Dasgupta, S. Chowdhury, Effect of an intrauterine contraceptive device on biochemical composition of uterine fluid, American Journal of Obstetrics & Gynecology, 101 (1968) 966-970.

[68] C. Spilman, R. Duby, Prostaglandin mediated luteolytic effect of an intrauterine device in sheep, Prostaglandins, 2 (1972) 159-168.

[69] D. Mishell, Pregnancy-related complications and bleeding problems with IUDs, Risks, Benefits and Controversies in Fertility Control, 428 (1978).

[70] M. Potts, J.J. Speidel, E. Kessel, Relative risks of various means of fertility control when used in less-developed countries, Risks, Benefits and Controversies in Fertility Control, DOI (1978) 28-51.

[71] P.A. Corfman, R.M. Richart, A.P. Parenthood, Uterine epidermoid carcinoma induced in rats by plastic and stainless steel intra-uterine devices, Excerpta Medica International Congress Series, 1968, pp. 89.

[72] P.C.J. Rowe, The intrauterine device: A review of recent advances and controversies, Oxford reviews of reproductive biology, 3 (1981) 49-94.

[73] G. Rybo, The IUD and endometrial bleeding, The Journal of reproductive medicine, 20 (1978) 175.

[74] G. Rybo, A. Bergqvist, Comparison of menstrual blood loss with the Progestasert® system and the Cu-T-200: preliminary results, Proceedings of a symposium on Clinical Experience with the Progesterone Uterine Therapeutic System, Excerpta Medica, Princetown, 1978, pp. 106-110.

[75] R.L. Sweet, Pelvic inflammatory disease, Sexually transmitted diseases, 13 (1986) 192-198.

[76] N.C. Lee, G.L. Rubin, H.W. Ory, R.T. Burkman, Type of intrauterine device and the risk of pelvic inflammatory disease, Obstetrics and Gynecology, 62 (1983) 1-6.

[77] R.T. Burkman, Association between intrauterine device and pelvic inflammatory disease, Obstetrics and gynecology, 57 (1981) 269-276.

[78] D.R. Mishell Jr, J.H. Bell, R.G. Good, D.L. Moyer, The intrauterine device: a bacteriologic study of the endometrial cavity, American journal of obstetrics and gynecology, 96 (1966) 119.

[79] S. Roy, D. Ghosh, S.K. Guha, Polyelectrolyte polymer properties in relation to male contraceptive RISUG® action, Colloids and Surfaces B: Biointerfaces, 69 (2009) 77-84.

[80] S. Kumar, K. Chaudhury, P. Sen, S.K. Guha, Topological alterations in human spermatozoa associated with the polyelectrolytic effect of RISUG®, Micron, 37 (2006) 526-532.

[81] K. Chaudhury, A. Bhattacharyya, S. Guha, Studies on the membrane integrity of human sperm treated with a new injectable male contraceptive, Human Reproduction, 19 (2004) 1826-1830.

[82] S.K. Guha, RISUG™(reversible inhibition of sperm under guidance)–An antimicrobial as male vas deferens implant for HIV free semen, Medical hypotheses, 65 (2005) 61-64.

[83] S. Banerjee, S.K. Guha, RISUG®: A potential candidate for the entry inhibitor group of antiretroviral drugs, Medical hypotheses, 73 (2009) 150-152.

Chapter 2

Preclinical Assessment of Styrene-Maleic Anhydride Based Hydrogel for the Application of Improved Intra-Uterine Contraceptive Implant

2.1 Introduction

It was reported in world population prospects in the 2008 revision that the world's population is increasing 80 million yearly and by 2050, it will reach 9-10 billion. Population explosion is the principal reason of environmental dilapidation and human suffering from poverty, starvation. Unintended pregnancy plays major role in population increase. This increased incidence of unintended pregnancy is owing to inadequate access to the presently available contraceptive methods. The presently available short term or long term female contraceptives and sterilization methods have their own restrictions and side effects. Non-hormonal female contraception has become more attractive method as it avoids the adverse effects of hormonal contraceptives. The process of non-hormonal female contraception is accomplished through the intra-uterine contraceptive device (IUCD) over the past decades. However, there is a need for potentially superior techniques as the known IUDs causes trauma to the lining of the internal cavity of the uterus. This mechanical trauma triggers nerves and pain sensors and bleeding, which causes uterus to become more susceptible to various endogenous or exogenous infections. In order to prevent IUCD associated bacterial infections FDA approved antibiotics are generally used. However, these antibiotics also kill beneficial *Lactobacillus* population inhabiting in the female reproductive tract. These adverse side effects limit acceptance of known IUCDs by females in the reproductive age, and if accepted then often lead to the demand for early removal thereof.

RISUG® (Reversible Inhibition of Sperm Under Guidance) is a hydrogel made up with styrene maleic anhydride (SMA) and styrene maleic acid dissolved in DMSO is useful as vas deferens injected reversible male contraceptive [1]. This drug is presently

under advanced phase III clinical trial in India [2]. The polymeric hydrogel RISUG® is not bio-inert material, but instead, the polymer has the property to reduce pH of the medium in its instantaneous vicinity. The polymeric hydrogel inactivates most of the sperm through damaging the acrosome by reducing the pH of the surrounding environment. The low pH not only damages the acrosome but also alter sperm morphology that results in poor motility due to which the fertilizing ability is lost in the sperm. The possibility of using RISUG® as a fallopian tube implant provides an opportunity to develop a novel and improved form of non-hormonal female contraceptive implant which has not been explored yet. Besides providing contraception it may also act as an antibacterial agent which is considered as vital biological property for a synthetic bio-polymer [3-8].

The shape of the fallopian tube and the character of isthmic layers could restrict the use of RISUG® as human female contraceptive implant especially for the long term application. Interestingly RISUG® after deployment in the upper female reproductive tract will be converted to semisolid mass upon exposure with the reproductive tract fluid. The converted semisolid RISUG® should have sufficient structural strength to withstand various shears which may vary from $0.1s^{-1}$ to $100.0s^{-1}$ due to gravity and capillary flow inside the female reproductive tract. These internal forces existing in the female reproductive tract and dilution of RISUG® due to the exposure with reproductive tract fluid will have significant direct effect on rheological properties of RISUG® [9-11].

Keeping these demands of rheological properties of RISUG® for application as female contraceptive gel, its rheological behavior has been evaluated. In order to mimic the fallopian tube environment, RISUG® was allowed to react with Simulated Uterine

Fluid (SUF) in three different conditions based on proportion of RISUG® and SUF; such as 1) RISUG® is higher than SUF (R_3U_1), 2) RISUG® and SUF are in equal proportion (R_1U_1), 3) RU is RISUG® only and 4) SUF is higher than RISUG® (R_1U_3) at 37°C. All the rheological study was carried out in all four conditions. The descriptions of samples were given in Table 2.1. The present study also aims to identify the selective antibacterial profile of the test hydrogel RISUG® against opportunistic pathogens of the female reproductive tract for using as fallopian tube implantable hydrogel formulation which make RISUG® as a prime candidate for the development of the novel female contraceptive hydrogel. Furthermore, RISUG®, as an implantable hydrogel, should posses' significant biocompatibility without altering the biological properties of the female reproductive tract. Given the research hypothesis, *in vitro* toxicological profile of RISUG® was characterized using rat primary uterine cell lines. Investigation of *in vivo* toxicity of any biological implant is vital for its medical application. Despite the circumstance that fallopian tube of rat is extremely long-winded and significantly smaller when compared with that of human, the uterine horns of rat owns sole characteristics making it equivalent to the isthmic portion of human fallopian tube. The *in vivo* toxicity of RISUG® was investigated in uterine horns of female rat for 29 days post implanting the RISUG® hydrogel.

Table 2.1. Samples used and their nature

Sample RISUG®: SUF	Abbreviation	Nature of samples
1:0	RU	No precipitation
3:1	R_3U_1	Less precipitation
1:1	R_1U_1	Medium precipitation
1:3	R_1U_3	Complete precipitation

2.2 Materials and Methods

2.2.1 Synthesis of RISUG®

The RISUG® used in this study was synthesized in our laboratory according to the method patented [12]. Styrene Maleic Anhydride (SMA) is prepared through gamma radiation polymerization. Styrene and maleic anhydride were taken in the ratio of 1:1 and dissolved in ethyl acetate ≥99% (monomer conc. 50% by wt.). The polymerization was carried after purging the nitrogen gas in to polymerization vessel in order to remove the dissolved oxygen. Samples were subjected to gamma irradiation (0.3 Gy/s at 37 ºC with a total dosage of 2.4 Gy) in a Co-60 gamma radiation chamber. The co-polymers were precipitated and vacuum dried. The homopolymer of styrene was removed from precipitated SMA co-polymer by soxhlation using 1, 2-Dichloroethane. Furthermore the homopolymers of polymaleic anhydride was removed from SMA co-polymer by washing in distilled water. Finally the SMA precipitate is dried, powdered and stored in stoppered sterile glass tubes inside vacuum desiccators. To obtain the final product RISUG®, SMA was dissolved in dimethyl sulfoxide in the ratio 1:2 under controlled atmosphere. Schematic representation for the synthesis of SMA polymer and RISUG® is provided in Figure. 2.1a.

2.2.2 Preparation of Simulated uterine fluid (SUF)

SUF was prepared according to the standard procedure [13]. The composition used for SUF preparation is given in Table 2.2. The pH of SUF was adjusted to 7.3 using 1M hydrochloric acid.

2.2.3 *In vitro* characterization of RISUG®

^{1}H NMR spectrum for the synthesized polymer was recorded (^{1}H NMR 400 MHz Bruker ACF200 spectrometer) with deuterated DMSO as solvent to validate the chemical structure of synthesized SMA co-polymer and the residual DMSO protons are used as reference. Elemental analysis (C, H, N) for SMA polymer and RISUG® were done using 2400 series II Perkin Elmer, CHN analyzer. Static headspace - Gas Chromatography/Mass Spectroscopy (GC/MS, Perkin Elmer Turbomatrix 650) having 30 meter XTI-5, 5% phenyl dimethylpolysiloxane column was used to determine the aggregate of free DMSO in the RISUG®. The oven was held at 100º C for 0 minutes and increased to 300º C at a rate of 12º C/min and held for 4 minutes. Mass Spectroscopy (MS) temperature was 280º C. The temperature of front inlet was 210º C with 200:1 split ratio (0.5% on-column). The flow rate inside the column was 1 ml/min.

The MS ion scan range was 25 - 100 amu. RISUG® gel (233.5 mg) was placed in to tared 20 mL head space vial. The vial was then sealed and placed in to oven (for 15 min). Following the fifteen minutes out gas, the gasses within the vial was analyzed using GC/MS. Two DMSO standards with known aggregate of 0.05 mg and 5.5 mg were analyzed along with the samples in order to determine the amount of free or unreacted DMSO after formation of RISUG® gel.
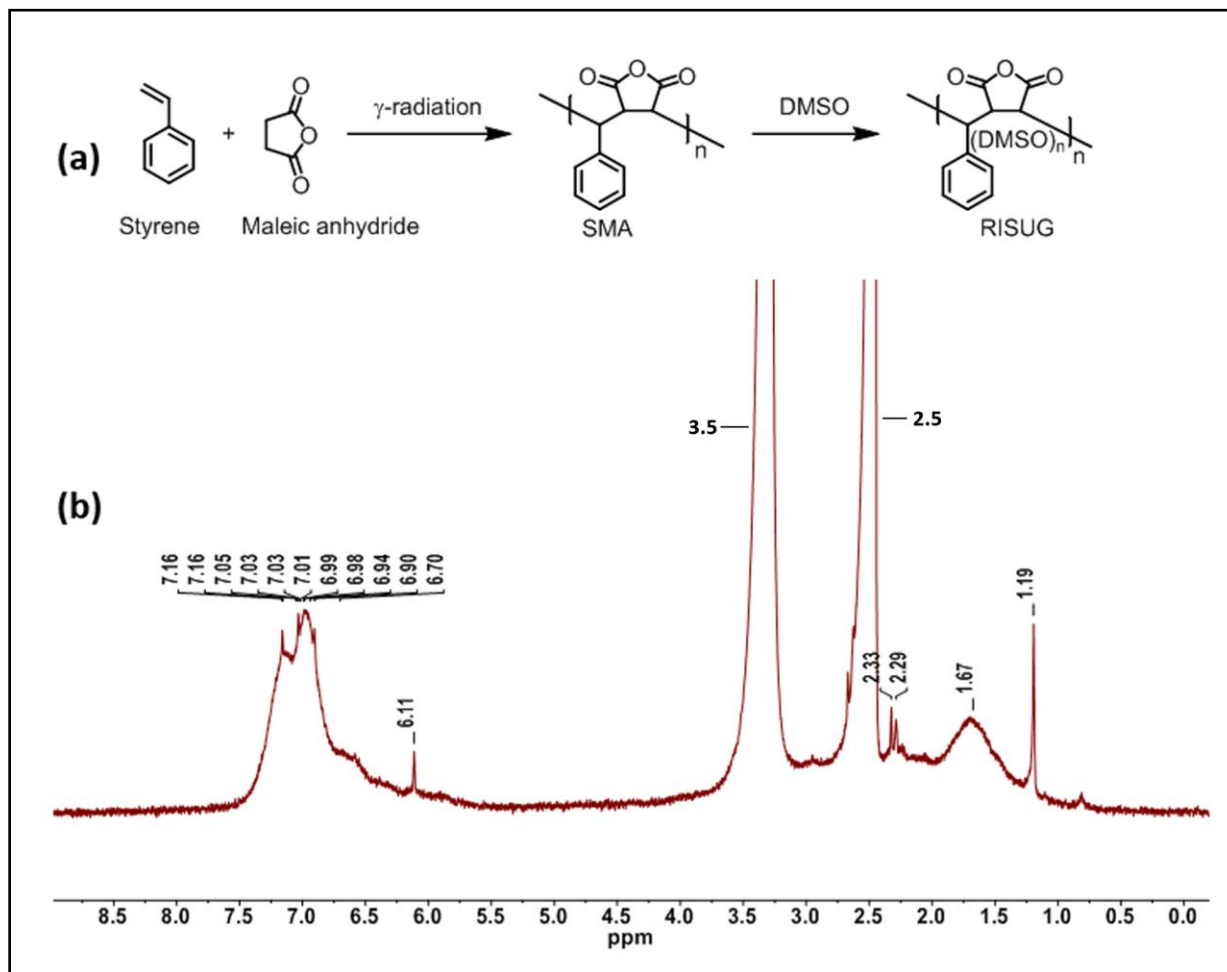
Figure 2.1. (a) Schematic representation for the synthesis of SMA polymer. **(b)** ^{1}H NMR spectra of SMA polymer in deuterated DMSO

Wide angle X-ray diffraction (WXRD) was performed to examine the crystal structure of Styrene maleic anhydride powder, RISUG® and RISUG® precipitated in SUF. The Philips PW-1710 X-ray diffractometer (Eindhoven, The Netherlands), with crystal monochromator CuKα radiation (λ=1.540598 Å) with an accelerating voltage of 40 kV and a beam current of 20 mA for the angular range of 10–80° (2θ), was used for performing WXRD of samples. The crystallite sizes were measured using the principle of Scherrer's equation. For SEM (EVO ZEISS, Carl Zeiss SMT AG, Oberkochen, Germany) analysis, the contraceptive gel RISUG® and RISUG® precipitated in SUF were

spread on aluminum foil and allowed to dry in desiccators for 60 h. Images of the samples were obtained after gold-coating using plasma coater under high vacuum. FTIR spectroscopy results of the RISUG®, RISUG® precipitated in SUF were obtained from Nexus-870 FTIR spectrometer with Attenuated total reflection (ATR) mode to reveal the intermolecular interaction between RISUG® and SUF. For every spectrum, 36 scans were accumulated and the measurements were collected and co-added with a spectral resolution of 1 cm^{-1}. Zinc selenide (Zn-se) ATR crystal was used in the spectrometer.

2.2.4 Rheological characterization

Rheological studies were performed using Bohlin CVO rheometer (Malvern Instrument, Malvern, United Kingdom) using parallel plate (20 mm diameter spindle) geometry maintaining a constant gap of 100 μm for different samples of hydrogel RISUG® as indicated in (Table 2.1).

Table 2.2 Composition of SUF in Distilled water

Composition Name	Amount (mg/L)
Sodium bicarbonate	250
Sodium dihydrogen phosphate	72
Calcium chloride	167
Potassium chloride	224
Sodium chloride	4970
Glucose	50
Urea	48

The gelation kinetics of the contraceptive gel RISUG® was studied using time sweep complex viscosity (η*) and complex modulus (G*) within the elastic limit of the gels under oscillatory mode. Viscosities of different samples of RISUG® were measured at a shear rate ranging from 0.1 to 15000 s^{-1} and their flow behavior was characterized by

Oswalt-de Waele power law model. Oscillatory stress sweeps from 100 to 10000 were measured at a constant frequency of 1 Hz to obtain storage (G') and loss (G") modulus. The frequency sweep measurements were performed from 0.01 to 100 Hz in a constant stress of 100 Pa. The experiments were performed at 37ºC in SUF (pH:7.4) to mimic the uterine environment.

2.2.5 Swelling Kinetics

Triplicates of RISUG® hydrogel samples were weighed before immersing in SUF at 37°C. The weight of the hydrogel samples was weighed at specific time intervals after removing the excess liquid over the hydrogel through gentle tapping. Swelling kinetics of the hydrogel sample was analysed after the samples reach their equilibrium weight. Swelling percentage (%S) and nature of diffusion of fluid into the hydrogel sample was calculated using the following equations 1, 2:

$$\% \, S = \frac{M_t - M_0}{M_0} \rightarrow (1)$$

$$F_t = \frac{M_t}{M_{eq}} = Kt^n \rightarrow (2)$$

Here M_t is the mass of swollen hydrogel at respective time t and M_0 is the initial mass of hydrogel. F_t represents the amount of solvent fraction at respective time t, K is water constant that represents the structure of the polymeric network and exponent n reveals the nature of diffusion of fluid into the hydrogel. The nature of fluid diffusion can be classified in to Fickian diffusion (n = 0.5) and Non-Fickian diffusion (0.5 < n <1)

2.2.6 Agar Well Diffusion Assays

Staphylococcus aureus (MTCC96), *Pseudomonas aeruginosa* (MTCC741) and *Escherichia coli* (MTCC40) (procured from the Microbial Type Culture Collection and gene bank (MTCC), Institute of Microbial Technology (IMTECH), Chandigarh, India) were used as representative microorganisms for opportunistic pathogens. *Lactobacillus fermentum* (KKL1) and *Lactobacillus plantarum* (MTCC1407) was provided by Department of Microbiology, Vidyasagar University, West Bengal, India. A pure isolate of microbial inoculums was maintained in their respective media (Nutrient media for MTCC96, MTCC741, MTCC40 and deMan, Rogosa and Sharpe (MRS) media for *Lactobacillus* strains procured from Himedia Pvt. Ltd., Mumbai, India). All the microbial strains were maintained in their log phase by subculturing them in freshly prepared nutrient broth for 3 h. Agar well diffusion assay was performed to identify the minimal concentration of RISUG® hydrogel that could inhibit the growth of pathogens. Three different concentrations were selected for the agar well diffusion assay (25, 50 and 100 mg). Bacterial colonies (100 µL) were spread on respective agar and small well was carefully made using aseptic 1000 µL micro pipette tip. The wells were provided with hydrogel sample and gentamycin (100 µg/mL) was used as positive control. After overnight incubation in ambient environment microbial zone of incubation was measured.

2.2.7 Direct contact inhibition assay

Time-kill method of direct contact inhibition studies was performed as described elsewhere [14]. Microbial inoculums were allowed to grow in their respective broth holding 50 mg of the test sample in a total volume of 5 mL broth. This assay will mimic the direct exposure of test hydrogel to the micro-organisms and the ability of test hydrogel to control the microbial load. The test hydrogel occupies the bottom of the culture tubes over which the broth along with particular micro-organisms was inoculated. Broth culture without test hydrogel was used as control. 12 h grown cultures of bacterial strains were diluted to 10^3 colony forming unit (CFU)/mL before inoculating along with test hydrogel. *Staphylococcus aureus*, *Pseudomonas aeruginosa* and *Escherichia coli* growing along with direct contact with test hydrogel were incubated under aerobic environment and *Lactobacillus* strains were incubated under anaerobic environment. At regular time intervals of 0, 1, 3, 6 and 24 h; 100 μL of culture broth was removed for enumerating by drop plate counting method. All the assay procedure was performed in triplicates.

2.2.8 Microbial growth in pH adjusted media

Bacterial broth cultures of opportunistic pathogens and *Lactobacillus* strains were grown in ambient environment for 12 h. Respective broth media was adjusted to pH 4.5 using 30% lactic acid. 100 μL of 12 h grown microbial samples were inoculated in 5 mL of pH adjusted media. Microbial population growing in media without pH adjustment serves as a control. At regular time intervals of 0, 1, 3, 6 and 24 h turbidity of the medium

were measured at 595nm using 96 well plate reader. All the experiments were conducted in triplicates [14].

2.2.9 *In vitro* cytotoxicity studies

2.2.9.1 MTT assay

MTT (3[4,5-dimethylthiazol-2-yl]-2,5-diphenyltetrazolium bromide) assay was determined by calorimetric method. This cell proliferation assay measures the ability of metabolically active proliferating cells to cleave tetrazolium ring of MTT to blue color formazan crystals. *In-vitro* cell proliferation assay was performed using primary rat uterine cell lines isolated using standard procedure. Briefly, Uterine horns from mature female rats were aseptically resected and incubated in 0.2% of collagenase type I in DMEM and Ham's F-12 (Thermo Fisher Scientific, India) at 1:1 volume ratio at 37°C for 1 h provided with continuous shaking. Collagenase type I treated uterine horns were neutralized by adding an equal volume of DMEM/F12 cell culture media containing 10% charcoal stripped Fetal Bovine Serum (FBS), 1% penicillin-streptomycin solution, 10 mmol/L HEPES, 1 nmol/L β-estradiol and 100 nmol/L progesterone. The tissue suspension was filtered through 100 and 40 µm strainer and centrifuged at 250 g for 5 minutes at 4°C. The viable cells collected as pellet was seeded on to 6 well plates. The media was frequently changed with fresh media for removing the non-adherent uterine cells. Passage numbers between 3 to 5 were used for further experiments. Rat uterine primary cell lines were inoculated in both normal media and conditioned media separately at a density of 10,000 cells per well on to 24 well plates. For preparing conditioned media, twenty five micrograms of RISUG® suspended in five millilitres of

DMEM/F12 cell culture media and vortexed for 3 h which was then incubated for thirty days under aseptic condition. This conditioned medium was then filtered using 0.22 μm (Millex® - GV PVDF) filter unit before using for cell culture assay. The cell lines were then inoculated at 37°C in 5% CO_2 and 95% air humidified atmosphere for 24, 48 and 72 h. Absorbance at 590 nm was measured to quantify cell viability. Uterine primary cells grown in normal media was considered as control cells [15].

2.2.9.2 Real time-PCR

Seventy two hours grown uterine cell lines in normal and conditioned media were collected in RNA later (Procured from Qiagen) and stored in -80°C for RNA extraction. Total RNA extraction from uterine primary cell lines was carried by using Hipure Kit (Procured from Himedia, Mumbai, India). The purity of the RNA extracted was spectrometrically checked before synthesizing cDNA. One microgram of extracted RNA was used for the cDNA synthesis using High-Capacity cDNA Reverse Transcription kit (Applied Biosystems) by following manufacturer's protocol in GeneAmp® PCR system 2720 Thermal Cycler (Applied Biosystems). Light Cycler® 480 SYBR Green I Master from Roche Diagnostics GmbH, Mannheim, Germany was used for the reactions of Estrogen Receptor-α (ER-α), Vascular Endothelial Growth Factor (VEGF), Cyclin D1 and Cyclin-dependent Kinase 4 (CDK4) genes on Light Cycler® 480 II (Roche Diagnostics GmbH, Mannheim, Germany). Glyceraldehyde 3-phosphate dehydrogenase (GAPDH) was used as an endogenous control. In a total reaction volume of 10 μL about 1 μL of 10 X diluted cDNA template was used for amplification [16, 17]. Best reproducibility was ensured by performing Reverse Transcription reactions in triplicates.

In each set of PCR assays, negative controls without template were included. Details of the primers of each gene along with their cycling conditions are mentioned in Table 2.3.

Table 2.3 Cycling conditions along with primer sequences for real time PCR.

Gene	Forward Primer	Reverse Primer	Annealing temperature
ER-α	GGAGACATGAGAGCTGCCAAC	CCAGCAGCATGTCGAAGATC	58°C
Cyclin D1	CTGGCCATGAACTACCTGGA	GTCACACTTGATCACTCTGG	55°C
VEGF	GATCAAGTTCATGGACGTCT	GATCAAGTTCATGGACGTCT	55°C
CDK4	TGGTGTCGGTGCCTATGGGA	GGTAGCTGTAGATTCTGGCT	55°C
GAPDH	GACATCAAGGTGGTGAAGCAG	CACCCTGTTGCTGTAGCCATATTC	55°C

Cycling conditions: 95°C for 5 min (1 cycle), 95°C for 30s, annealing cycle for 30s, 72°C for 30 S (40 cycles)

2.2.9.3 Cellular morphology analysis

Rat primary uterine cell morphology was analyzed after the cells were cultivated in conditioned media for 24h, 120 h and staining via Rhodamine-Phalloidin and DAPI (Life technologies) fluorescent stains. The morphology of the cell was visualized in Zeiss ZEN Fluorescence microscope and Scanning Electron Microscopy (SEM; EVO ZEISS, Carl Zeiss SMTAG, Oberkochen, Germany). The rat uterine primary cell lines were washed three times with cold phosphate-buffered saline (pH:7.4) and fixed overnight in formaldehyde 4% (in phosphate-buffered saline) at each time point for Fluorescence Imaging. For SEM analysis, the test conditioned media treated uterine cells were washed with cold phosphate-buffered saline (pH7.4) and dehydrated through a series of ethanol dilutions (20, 40, 60, 80, and 100%, 10 min each). The uterine cell lines were sputter

coated with gold to enhance the conductivity and observed under SEM at an accelerating voltage of 5 kV.

2.2.10 *In vivo* toxicity studies

2.2.10.1 Animals Maintenance

15-16 weeks old female Sprague-Dawley rats were isolated from the breeding colony and maintained under controlled conditions having $25\pm2°C$ temperature and $50\pm15\%$ relative humidity. The animals were exposed to normal photoperiods of 12 h dark and 12 h light. All the animals were provided with sterile food pellets and water *ad libitum*. Vaginal lavage of the animals was checked periodically to identify the estrus cycle. All the experiments were performed after prior approval from the institutional animal ethical committee. Two groups (n=10 each) were randomly selected for the study.

2.2.10.2 Test hydrogel treatment

Animals were anaesthetized by intraperitoneal injection of ketamine (75 mg/Kg) and xylazine (100 mg/kg). After confirming the surgical anesthetic stage through toe withdrawal reflex, a low abdominal middle incision was made. The uterine horns were exposed with the help of blunt end sterile cotton swab. Uterine horns of the test animals were injected with 8.03 mg/Kg [18] of test hydrogel and uterine horns of the control animals were injected with saline water. Postoperative pain management and suitable antibiotic coverage was performed. From each group 5 animals were sacrificed using chloroform as inhalant on Day 29. Uterine tissues were removed and quickly washed in

0.9% (w/v) saline. At first tissue samples were aseptically excised from control, treated animals and then fixed with 4% of formalin solution. Tissue samples were further dehydrated with graded ethanol (50 - 100%), cleared with xylene and embedded in paraffin blocks. Post embedding, the 3 μm sections were sliced using microtome and placed on 3-aminopropyltriethoxysilane treated glass slides for further pathological evaluation.

2.2.10.3 Histology and Immunohistochemistry

The paraffin embedded tissues were dewaxed using xylene followed by graded dehydration using 70 to 100% alcohol subsequently. 3 μm paraffin sections were stained by hematoxylin-eosin double staining procedure following manufacturer's protocol. The double stained tissue sections were observed under microscope. The tissue sections were subjected to immunohistochemistry after the process of deparaffination, hydration and were subjected to antigen retrieval process (EZ-Retriever System V.2; BioGenex, San Ramon, California, USA) in 0.1M sodium citrate buffer (pH 6.0) for 20 min. Chromogenic methods were then used to immunostain sections. Anti-ER-α, anti-Cyclin D1, anti-VEGF and anti-CDk4 (Santa Cruz Biotechnology, CA, 1:250) were used as primary antibodies [19]. The secondary antibody used was goat anti-rabbit HRP-conjugated secondary antibody (1:1000).

2.2.10.4 Immunohistochemistry scoring

The qualitative immunohistochemistry was converted to the quantitative method by scoring the staining intensity in the areas of epithelial cells, blood vessels and the stromal area of uterine tissues. Ten different areas of tissue sections were randomly

chosen for scoring a single tissue sample by a person who did not know from which group the tissue samples originated. Score values were semi-quantitatively assigned from 0 to 10 (0 = no staining, 2.5 = staining of less than one third of total area, 5 = staining of only one third of total area, 7.5 = staining of two third of total area and 10 = staining of more than two third of total area). For every tissue samples, separately the areas of epithelial cells, blood vessels and the stromal area of uterine tissues was counted to score individually and then scores from every tissue samples were summed to calculate the mean values.

2.2.10.5 Hematology, blood biochemistry and organ pathology studies

Both control and treated animals were observed daily for any signs of behavioral changes, reaction to treatment or ill health throughout the study. Cage-side observations were made to detect any changes in skin, fur, eyes and general activity of the animals. Blood samples were collected from heart by cardiac puncture of anaesthetized animals before sacrifice. Standard hematology markers including Eosinophil, Haemoglobin (HBG), Lymphocyte, Mean Corpuscular Hemoglobin (MCH), Mean Corpuscular Hemoglobin Concentration (MCHC), Mean Corpuscular Volume (MCV), Monocyte, Neutrophil, Platelets, Total Red Blood Cell Count (T-RBC), Total Leucocyte Count (TLC) and Packed Cell Volume (PCV) or Haematocrit (HCT) were observed. Blood biochemical analysis were performed to elucidate general metabolic functions [Glucose (GLU), Cholesterol (CHOL), Triglycerides (TG), Total proteins (TP) and Albumin (ALB)], Kidney function [Blood Urea Nitrogen (BUN), Creatinine (CRTN), Phosphorus (P), Calcium (CA) and Urea] and Liver function [Alkaline phosphatase (ALP), Alanine aminotransferase (ALT), Aspartate aminotransferase (AST) and Total Bilirubin (TBL)].

Organs like heart, kidney, liver, lung and spleen were collected and representative pieces of all the isolated organs were processed for paraffin embedding and tissue sections of 3 µm thickness were made for staining with hematoxylin and eosin for histopathological examination.

2.3 Statistical analysis

The experimental data in this manuscript have been reported as average $\pm$ standard deviation. Statistical significance between the experimental groups was calculated by one-way ANOVA using Origin Pro 8.5 software under CI (Confidence Interval) of 95%. Symbol "*" in the respective images represents significantly different values with $p < 0.05$. Values which have not shown significant difference with $p > 0.05$ were mentioned as "n.s".

2.4 RESULTS

2.4.1 NMR and Elemental analysis

^{1}H NMR was used to validate the chemical structure of SMA polymer synthesized. As shown in Figure. 2.1b. ^{1}H signals at 1.7 ppm is correlated to 3H, -CH_3 of -$CH(CH_3)$ phenyl chain moiety, 2.1 - 3.3 ppm corresponds to -CH_2-CH_2- in styrene chain and -CH-CH- in maleic anhydride chain, -CH_2- and -CH- of terminal group. The resonance signals of 6.2 - 6.9 ppm may correspond to styrene molecule consisting of aryl protons of its aromatic groups. New peak around 2.3 ppm corresponds to DMSO interacted with SMA polymer. Aromatic protons of styrene appeared around 7 ppm. Broad peak around 1.7 and 3.0 ppm corresponds to aliphatic protons of SMA polymer [28]. Peaks around 2.5 and 3.5 ppm correspond to Deuterated DMSO and water

respectively. The SMA polymer and RISUG® gel are moisture sensitive due to susceptibility to hydrolysis of acid anhydride group. The best obtained CHN values are depicted in Table 2.4.

Table 2.4 Elemental analysis of SMA and RISUG® polymer

Element	% Calculated for SMA polymer	% Obtained for SMA polymer	% Calculated for RISUG®	% Obtained for RISUG®
Carbon	71.21	65.69	53.61	54.62
Hydrogen	4.98	5.57	6.19	6.32
Nitrogen	0	0.05	0	0.01

2.4.2 GC/MS analysis

GC/MS analysis was performed to calculate the amount of free DMSO present in RISUG®. The obtained aggregate of free DMSO in the RISUG® gel, based on GC/MS standard curve depicts the presence of negligible or minimal concentration (2.54%) of free DMSO in the sample. Almost all the DMSO molecules (92%) are interacting with SMA polymer to form the RISUG® gel. It can be attributed that DMSO not only act as a solvent molecule, it reacts with SMA polymer to form a pharmacological ingredient of RISUG®. The amount of free DMSO eluted after synthesis of RISUG® was presented in Table 2.5. and Figure. 2.2.

Table 2.5 Concentration of free DMSO eluted from RISUG® analysed using GC/MS

Concentration of RISUG® gel used (mg)	Concentration of DMSO present in RISUG® gel used (mg)	Concentration of free DMSO eluted from RISUG® gel (mg)	% of DMSO reacted with SMA to form RISUG® gel
233.5	160	13.07	92%

2.4.3 ATR-FTIR spectrometry studies

The ATR/FTIR spectrums of RISUG® and RISUG® precipitated in SUF were shown in Figure. 2.4a. The spectrum of RISUG® shows peaks for sulfonyl group at (d) 1015 cm^{-1} and (c) 1175 cm^{-1}. These bands can be attributed due to the symmetric vibrations of sulfonyl group, respectively.
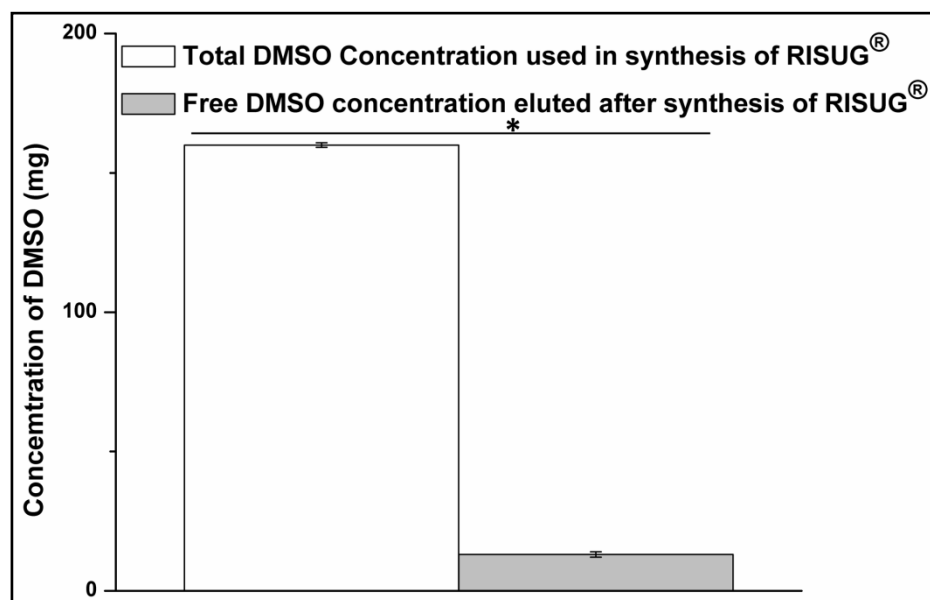
Figure 2.2. Concentration of residual DMSO concentration eluted in GC/MS. The experiment was carried out in triplicates. Symbol "*" represents significantly different values with $p < 0.05$

The appearance of broadband at around (a) 3415 cm^{-1} may be associated with the stretching mode of –OH bond of SO_3H. RISUG® precipitated in SUF due to the

intermolecular interaction between OH in SUF and C=O (carbonyl group) from maleic anhydride. This intermolecular interaction of the OH group with maleic anhydride shows peak shift about ~8 cm^{-1} toward the lower wave number side (b and e) thereby altering the electrochemistry of RISUG® [20-24].

2.4.4 Wide angle X-ray diffraction studies

The WXRD spectrum of RISUG® and RISUG® precipitated in SUF are shown in the Figure. 2.4b. All the samples exhibited major broad diffraction peaks at 23^0 (2θ value). RISUG® and RISUG® precipitated in SUF, demonstrated amorphous characteristics and there have been no structural alterations in both the spectrums. The mean crystallite size of RISUG® and RISUG® precipitated in SUF were calculated by using Scherrer's equation as follows [25-27]

$$D = \frac{k * \lambda}{\beta \cos\theta} \rightarrow (3)$$

Where D is the crystallite size; λ is the wavelength of X-ray radiation. The λ for Cu K$_\alpha$ radiation is 1.5418Å and the constant K= 0.89; β is full width half maximum by subtracting the equipment broadening (from the software X'Pert HighScore) and θ is the Bragg angle of the peak. The calculated crystallite size is shown in Table 2.6. Crystallite size of RISUG® and RISUG® precipitated in SUF has not shown the significant difference which reports that RISUG® is structurally stable even after mixing it with SUF. SUF had no impact on the polymeric structure of RISUG® instead it may act as a transport vehicle to the surface of the uterus.

Table 2.6 WXRD data of RISUG® and RISUG® in SUF

Sample	2θ (Degree)	D (Angstrom) A⁰
RISUG®	23	0.36
RISUG® in SUF	23	0.44

2.4.5 Scanning Electron Microscopy (SEM) of RISUG and RISUG in SUF

Surface morphology of RISUG® and RISUG® precipitated in SUF is shown in Figure. 2.3. RISUG® precipitated in SUF had a rough surface with flake formation (Figure. 2.3b), which was not observed in RISUG® (Figure. 2.3a). The maleic anhydride present in RISUG® has electronegative oxygen group which has high affinity towards the hydrogen molecules of SUF.
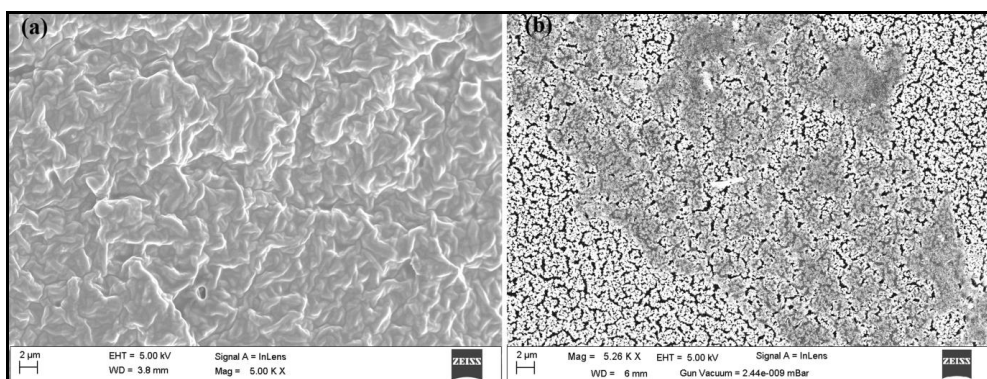
Figure 2.3. SEM images of **(a)** Vacuum dried RISUG® gel and **(b)** Vacuum dried RISUG® in SUF

Interaction of positively charged hydrogen molecules of SUF with the negatively charged oxygen molecules of maleic anhydride commences the hydration process in RISUG®. This hydration of RISUG® may be responsible for the formation of precipitate flakes that may results in the generation of the irregular rough surface in RISUG® mixed with SUF.

2.4.6 Gelation Kinetics of RISUG

The gelation kinetics was studied for RISUG® with the addition of SUF (pH 7.6) as described (Figure. 2.4c). The gel was precipitated by forming flakes [28] while mixed with SUF. In order to observe the rate of gelation in accordance with time, the gelation forming ability was studied through complex modulus in Figure. 2.4c. (G*) and phase angle in Figure. 2.4d (tan δ) against time sweep measurement in the linear viscoelastic range (at frequency 1 Hz and shear stress of 10 Pa) before and after addition of SUF (pH 7.6) at 37 °C. Addition of SUF in RISUG® resulted in instantaneous gel formation which is evidenced by the rapid rise in G* and change in tan δ demonstrating the viscoelastic nature of the gel [29]. Furthermore, the sudden drop in tan δ (stress/strain) was observed after the addition of SUF which indicates the SUF guided gelation process in RISUG® test hydrogel sample.

RISUG® being a hydrogel absorbs the water molecule. This hydrogel property may act as external media acting on RISUG® which increase the G*. A steady flow of RISUG® was observed before addition of SUF at the continuous shear stress of 10 Pa. After addition of SUF, RISUG® (along with viscous flow) tends more towards the elastic displacement thus exhibiting the viscoelastic property. This viscoelastic property may thereby provide structural strength to RIUSG® for resisting expulsion and for retaining in the upper reproductive tract for an extended duration.

2.4.7 Frequency Sweep measurements of RISUG®

Frequency sweep measurements indicate the elastic nature of RISUG® and its dilutions [(a) RU (b) R_3U_1 (c) R_1U_1 and (d) R_1U_3] in SUF (Figure. 2.5). Values of elastic modulus (G') and viscous modulus (G'') of RISUG® dilutions (R_3U_1, R_1U_1 and R_3U_3) exhibited increasing trend more than RISUG® (RU) with increase in the frequency. At any given frequency, G' is higher than G'' and they are independent to each other which demonstrates the viscoelastic nature of the samples. This independent and highest value of G' (Table 2.7) specify the rigidity of the RISUG® dilutions which is capable of application in dynamic environment [30]. This rigidity may help RISUG® to retain in the uterus and to resist the expulsion. As the rate of frequency increases G' should always be higher which describes the limit of the energy that the material could withstand. Higher the G', higher the material can withstand energy and can return to its original state after subjecting to dynamic applications.

Table 2.7 Frequency sweep values for RISUG® and its dilutions

Samples	Freuency Sweep G'/G"
RU	2.42
R_1U_3	2.28
R_1U_1	2.11
R_3U_1	1.01
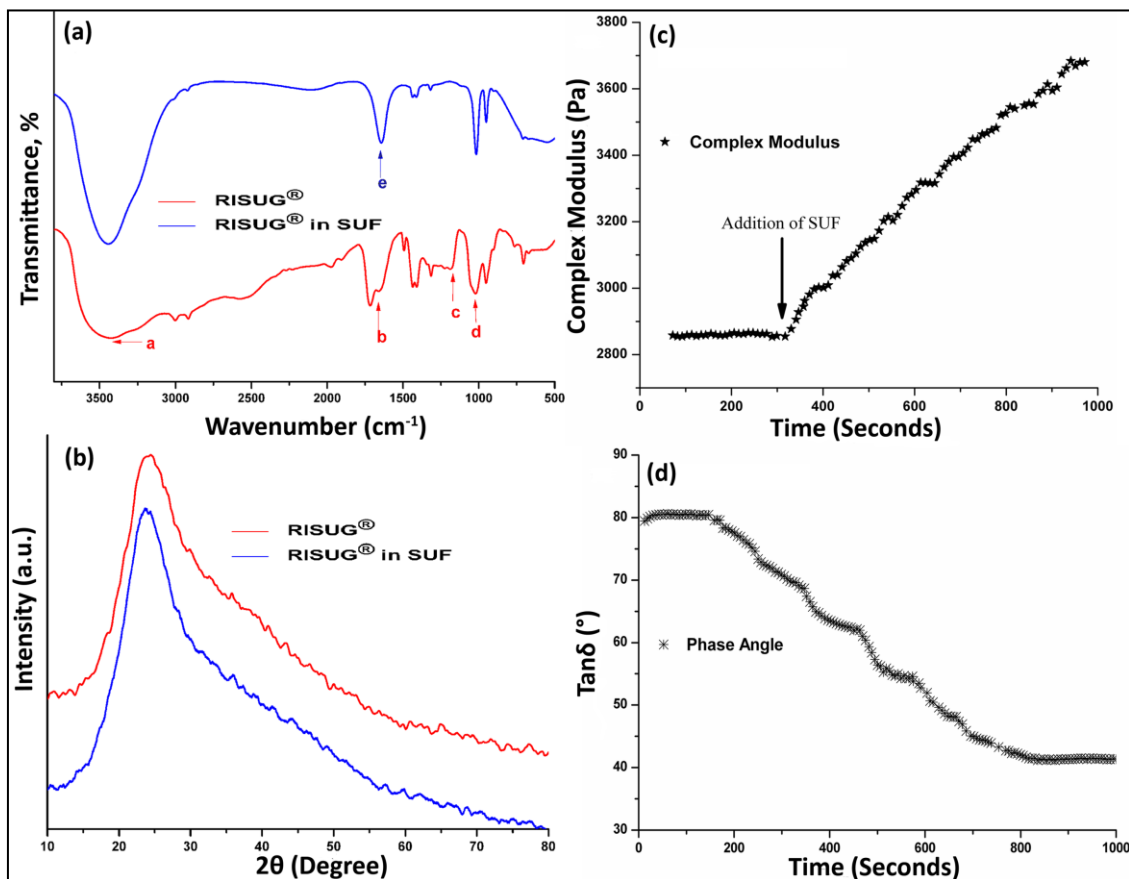
Figure 2.4. (a) ATR-FTIR results of RISUG® and RISUG® in SUF**(b)** WXRD results of RISUG and RISUG in SUF **(c)** Gelation kinetics of RISUG® before and after addition of SUF determined by complex modulus(G*) against time sweep measurement at frequency 1 and shear stress of 10 Pa (37 °C) **(d)** Gelation kinetics of RISUG® before and after addition of SUF determined by phase angle (Tan δ) against time sweep measurement at frequency 1 and shear stress of 10 Pa (at generally accepted normal body temperature 37 °C)

These results imply that at even higher frequencies RISUG® behaves as polymeric gel without any structural damage. When subjected to various frequencies RISUG® and its dilutions exhibited viscoelastic behavior which implies that RISUG® have viscous property to flow and once get precipitated after reacting with SUF, it attains better elastic property to withstand dynamic stress [31].
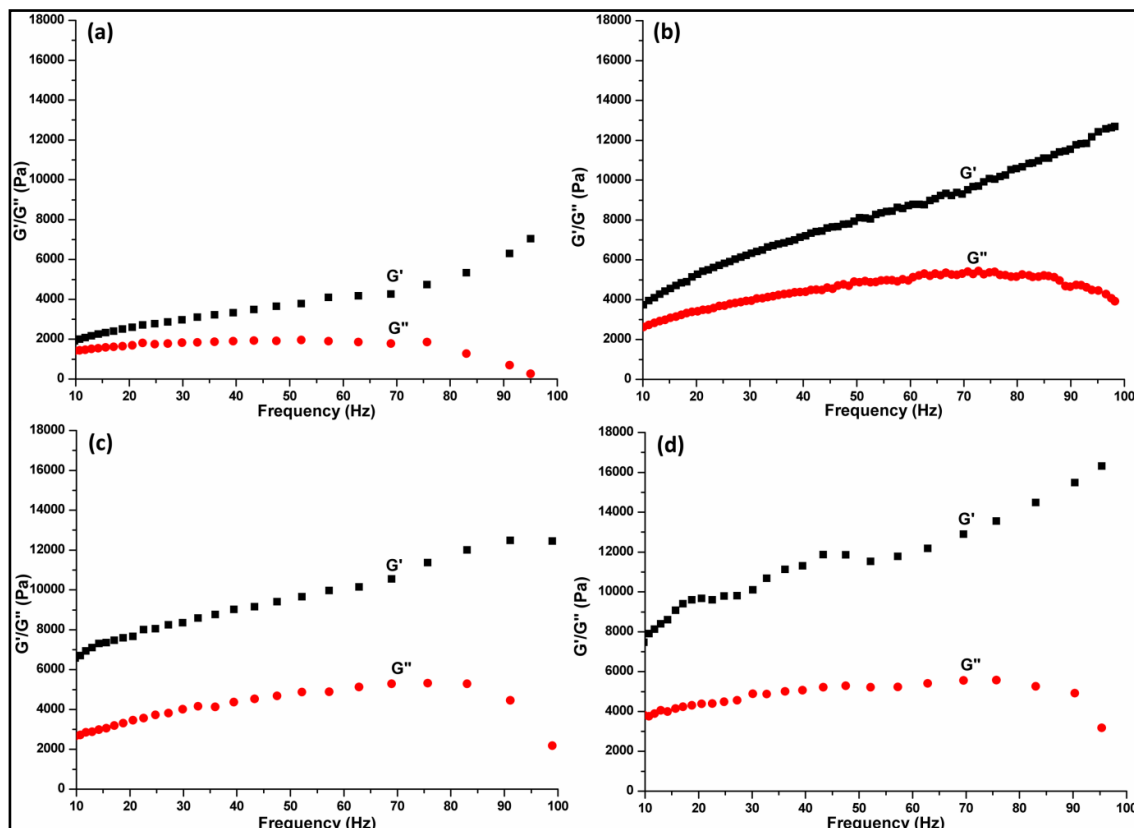
Figure 2.5. Variation in the Elastic modulus (G') and viscous modulus (G") with frequency of **(a)** RU **(b)** R_3U_1 **(c)** R_1U_1 and **(d)** R_1U_3

2.4.8 Gel Strength of RISUG®

In order to identify the critical stress value at which RISUG® starts to flow after being reacted with SUF, the *G'* and *G"* versus applied stress (σ) at a constant frequency of 1Hz was plotted for precipitated samples [R_1U_1 (b) and R_1U_3 (a)] (Figure. 2.6). At certain value above critical stress, both *G'* and *G"* rapidly falls to lower value which confirms the flow property of RISUG® after mixing with SUF. The critical stress value at which the gel starts flowing is called as yield stress (σ_y) [32]. According to the values in Table 2.8, R_1U_3 have a highest (σ_y) value. Yield stress may influence the spreadability and retention of gels. The average molecular weight between crosslinks ($\overline{M_C}$) for

RISUG® and its dilution were calculated using G' based on rubber elasticity [29, 32] as per equation 4.

$$\overline{M}_C = \rho RT / G' \rightarrow (4)$$

Where ρ is the density, R is the gas constant (8.314), T is the absolute temperature (37°C). Table 2.9 shows that, R_1U_3 shows higher $\overline{M}_C$ than R_1U_1. This change in $\overline{M}_C$ may be due to the interaction between positively charged hydrogen molecule in SUF and negatively charged oxygen molecule of maleic anhydride in RISUG®. RISUG® after implantation inside the fallopian tube should retain its mechanical strength at various dynamic environments for extended duration in order to provide contraception and antimicrobial property. Gel strength analysis shows the values of elastic and viscous modulus at different increasing rate of shear stress. The σ_y value of both the dilutions of RISUG® is quite larger (Table 9) which suggests that both the dilutions of RISUG® have high mechanical strength when subjected to dynamic environment. The σ_y exhibited by the gel may be due to the intermolecular hydrogen bonding in RISUG® when mixed with SUF. These values collectively indicates that after interacting with increasing amount of SUF, RISUG® express high mechanical strength that may help RISUG® to provide contraception and antimicrobial property at a range of dynamic environments after implantation.

Table 2.8 Average molecular weight between effective cross links and yield stress of

RISUG® dilutions

Sample	M_C (kDa)	Yield stress (σ_y)
R_1U_3	145.50	2321.32
R_1U_1	212.92	1589.51

Table 2.9 Amplitude sweep values of RISUG® dilutions

RISUG® Dilutions	Amplitude Sweep	
	Yield stress (σ_y)	G'/G"
R$_1$U$_3$	2321.32	1.088
R$_1$U$_1$	1589.51	1.018

2.4.9 Viscosity behavior of RISUG® and its dilutions

Shear rate dependent viscosity of RISUG® (RU) and its dilutions (R$_3$U$_1$, R$_1$U$_1$ and R$_1$U$_3$) are shown in the Figure. 2.6c. The RISUG® and its dilutions showed shear thinning behavior due to polymer chain entanglements. Relative constant slopes were observed by plotting the logarithmic graph. Shear thinning behavior exhibited by RISUG® and its dilutions (R$_3$U$_1$, R$_1$U$_1$ and R$_1$U$_3$) is the characteristic feature of non-Newtonian fluid. Oswalt-de Waele power law is a mathematical relationship to describe the behavior of the real non-Newtonean fluid. If the flow behavior index of power-law value is less than 1 then the material will have shear thinning behavior.

$$Y(x) = K(x)\hat{n} \rightarrow (5)$$

The flow characteristics of RISUG® and its dilutions can be quantified by power law constants n (flow behavior index) and k (consistency index) (Table 2.10). The values of n and K were determined by slope and intersection of the linear fit of the logarithmic value of viscosity-vs. logarithmic value of shear rate plot. RISUG® and its dilutions have n value less than 1 that confirms that RISUG® has shear thinning behavior as like a pseudoplastic polymeric gel [33, 34]. As a solution of large polymeric molecules,

RISUG® with large molecular chain may form clumsy at random and affect the flow of fluid by resisting against low shear rate. When high shear rate is applied the polymeric molecules in RISUG® gradually align themselves in the direction of increasing shear and produce less resistant to flow towards the shear rate which ultimately leads to the shear thinning behavior of RISUG®. The consistency index (K) increases when RISUG® get diluted more with SUF. The increase in consistency index may be due to the intermolecular hydrogen bond in RISUG® when mixed with SUF.

Table 2.10 Flow behavior index (n) and consistency index (k) of RISUG® and its dilutions

RISUG® Dilutions	Power law constants		Regression coefficient r^2
	Flow behavior index	Consistency index	
	(n)	(k) (kPa s)	
RU	0.53	109.0	0.944
R_1U_3	0.49	120.1	0.965
R_1U_1	0.46	149.3	0.985
R_3U_1	0.44	151.4	0.921

2.4.10 Swelling kinetics

Figure. 2.6d explains the swelling kinetics of RISUG® hydrogel in the simulated uterine fluid. The test hydrogel attains equilibrium swelling after 110 h, which is evidenced by the plateau region of % swelling in the graph. The diffusion behavior of SUF into test hydrogel was determined as non-Fickian diffusion by the value of n (n = 0.85). The formation of intermolecular hydrogen bonding between strong electronegative oxygen group of maleic anhydride and hydrogen molecule in SUF plays an essential role in the swelling behavior of RISUG®. The hydrogen molecule of SUF attaches on the surface of RISUG® which may enhances the precipitation of the hydrogel. This property of affinity towards hydrogen molecules in SUF leads to the increase in weight of

RISUG® hydrogel. The precipitation of hydrogel RISUG® provides the property of viscoelasticity that may help in expressing high mechanical strength under dynamic environment.

2.4.11 Effect of RISUG® hydrogel on bacterial cultured agar plate.

Figure. 2.7 a, b and c. portrays the agar plates with a zone of inhibition against *Escherichia coli, Pseudomonas aeruginosa* and *Staphylococcus aureus* respectively. Three different concentrations of test hydrogel RISUG® (25, 50 and 100 mg in what mL of which solvent) were used to determine the minimum concentration of test hydrogel to inhibit microbial growth in well diffusion assay. Microbial zone of inhibition was observed in all three concentrations. The zone of inhibition provided by the positive control (+) was significantly greater (Table 2.11) than the 25 mg (A), 50 mg (B) and 100 mg (C) of test hydrogel [4].
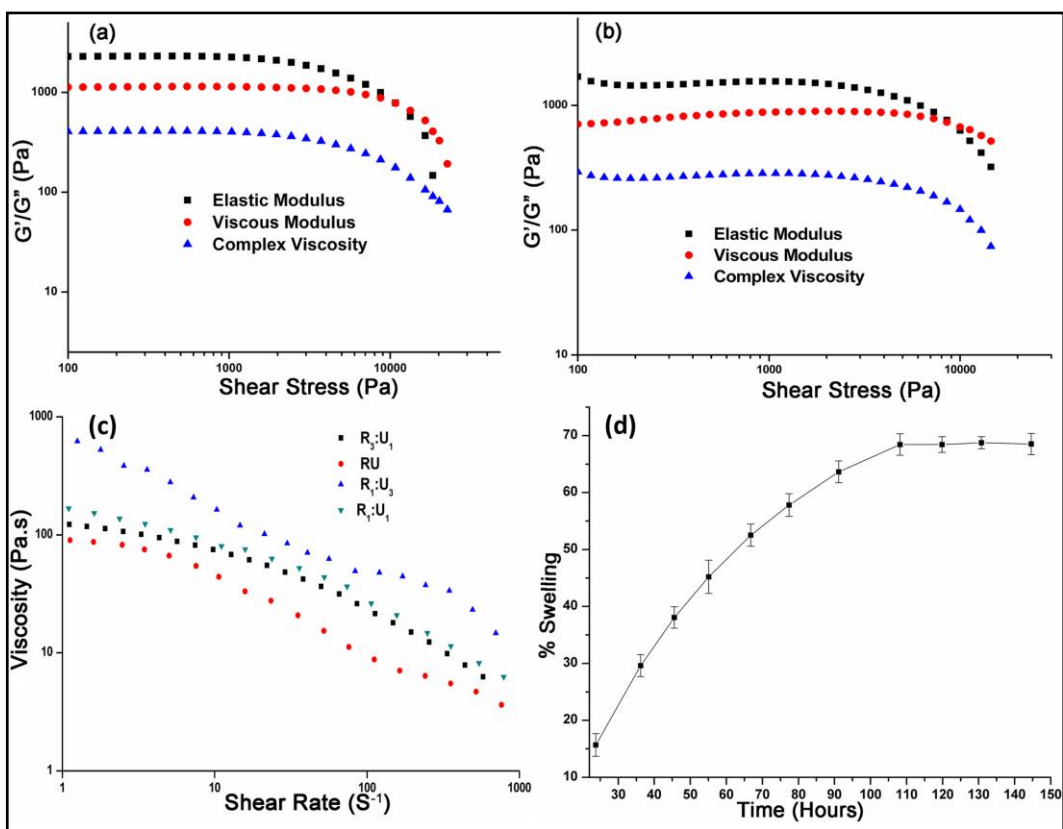
Figure 2.6. Gel Strength analysis for **(a)** R_1U_3 and **(b)** R_1U_1. **(c)** Viscosity vs. Shear rate for RISUG and its dilutions. **(d)** Swelling kinetics of RISUG in SUF

It is assumed that the dispersion of hydrogel into the agar was less that resulted in a reduced a zone of inhibition compared to the positive control. It is due to the test hydrogel byproducts that diffuse into the agar medium to show antimicrobial activity against *Escherichia coli, Pseudomonas aeruginosa* and *Staphylococcus aureus*. From FTIR result it was observed that test hydrogel in contact with biological fluid, results in the alteration in electrochemistry of RISUG® which may exert anti-microbial activity against *Staphylococcus aureus*, *Pseudomonas aeruginosa* and *Escherichia coli* in the agar well diffusion assay. The test hydrogel has not exerted any evidences of zone of

inhibition in *Lactobacillus fermentum* and *Lactobacillus plantarum* growing agar plates (Figure. 2.7d and e respectively).
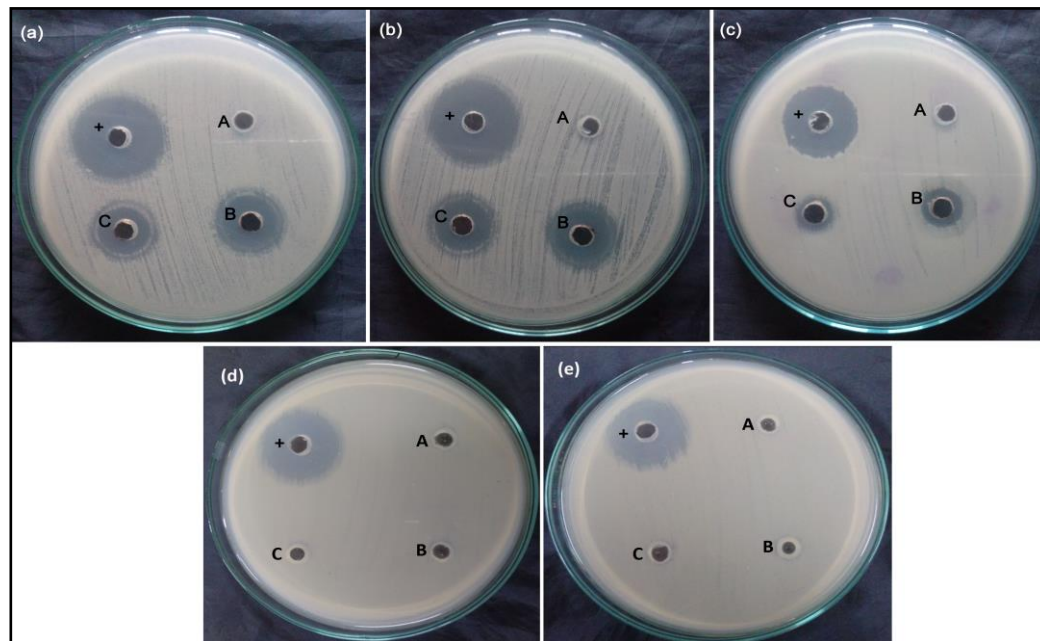
Figure 2.7. Microbial zone of inhibition **(a)** *Escherichia coli,***(b)** *Pseudomonas aeruginosa* **and (c)** *Staphylococcus aureus*, **(d)** *Lactobacillus fermentum and* **(e)** *Lactobacillus plantarum*

2.4.12 Selective anti-microbial activity of test hydrogel RISUG® towards opportunistic pathogen

The effect of test hydrogel on *Staphylococcus aureus*, *Pseudomonas aeruginosa* and *Escherichia coli* in well diffusion assay was inferred through the zone of inhibition against microbial growth. To identify the effect of test hydrogel directly on the microbial growth, direct contact assay was performed. Fifty (50) mg test hydrogel sample was selected for the assay since the concentration of 50 and 100 mg hydrogel produced a similar zone of inhibition. The viability of bacterial cells was monitored at frequent time

intervals. Direct exposure of test hydrogel (Figure. 2.8a) provided significant growth reduction ($p < 0.05$) of the microbial population. The p values were obtained by statistically estimating (ANOVA) the values of CFU/mL between control and test group of micro-organisms. About 99% of growth inhibition to *E. coli* and *P. aeruginosa*, 98% of growth inhibition to *S. aureus* was observed after 24 h. However, there is no significant reduction ($p > 0.05$) in the growth of *Lactobacillus spp* (Figure. 2.8b). *Lactobacillus planatarum* expressed minimal growth reduction at 6 h exposure with test hydrogel. However, the microbial population increased during 12 and 24 h of test hydrogel exposure. Thus the test hydrogel could able to reduce the growth of opportunistic pathogens but has not shown any harmful effect on *Lactobacillus spp* which maintains the healthy ecology in the vagina. The test hydrogel may have the potency to establish selective toxicity towards harmful bacteria associated with reproductive tract infections without disturbing the beneficial flora of female reproductive tract.
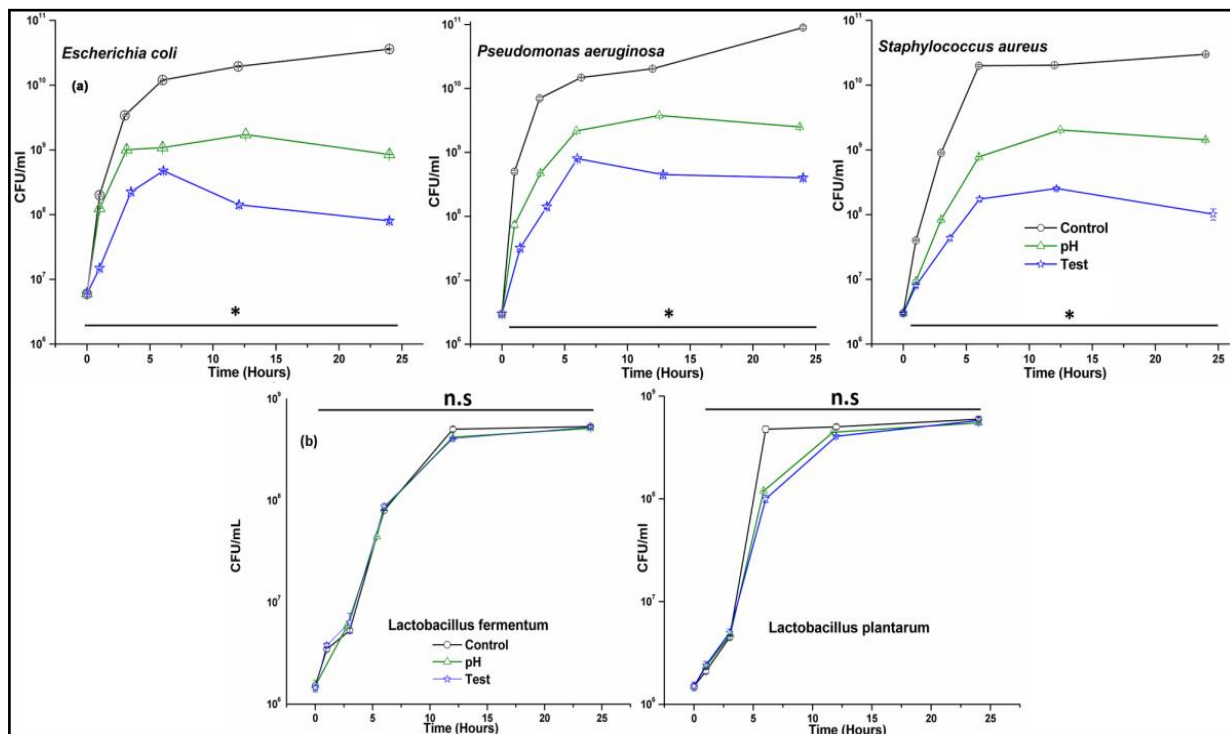
Figure 2.8. Antimicrobial activity against (a) *Escherichia coli, Pseudomonas aeruginosa, Staphylococcus aureus,* (b) *Lactobacillus fermentum* and *Lactobacillus plantarum*. All the experiment was carried out in triplicates. Symbol "*" represents significantly different values with p < 0.05. Values which has not shown significant difference with p > 0.05 were mentioned as "n.s"

2.4.13 Microbial growth on pH adjusted media

The test hydrogel when comes in contact with biological media have the property of reducing the pH of surrounding media through ionization due to the formation of intermolecular hydrogen bonds with the polymeric network. The micro-organisms were grown on pH adjusted media to know the effect of pH on the viability of micro-organisms. The viability of the micro-organisms got reduced (P < 0.05) not only to the opportunistic pathogens but also to the *Lactobacillus species* (Figure. 2.8a, b). However considerable reduction was not observed in the viability of opportunistic pathogens when compared with direct contact inhibition assay. Furthermore, the test hydrogel has the

property to selectively reduce the viability of opportunistic pathogens but not the

Lactobacillus spp.

Table 2.11 Microbial zone of inhibition

Bacteria	Gentamicin in cm	25 mg RISUG® in cm	p value	50 mg RISUG® in cm	p value	100 mg RISUG® in cm	p value
E. coli	2.9±0.2	0.60±0.3	0.0002	1.8±0.2	0.0008	1.8±0.2	0.0003
P. auregenosa	3.3±0.1	0.73±0.3	0.0001	1.8±0.5	0.006	1.8±0.2	0.0003
S. aureus	2.0±0.2	0.47±0.7	0.004	1.2±0.7	0.01	1.3±0.3	0.01
L. fermentum	1.7±0.1	0.0	-	0.0	-	0.0	-
L. planatarium	1.5±0.1	0.0	-	0.0	-	0.0	-

The p values (ANOVA) for the microbial zone of inhibition was obtained by comparing the zone of inhibition values of test sample (25, 50, 100 mg) with Gentamicin

2.4.14 *In vitro* cytotoxicity studies

2.4.14.1 Cell Proliferation assay and Real time-PCR

The effect of RISUG® conditioned media on the viability of primary rat uterine cell line was compared by measuring the activity of mitochondrial dehydrogenases. This mitochondrial dehydrogenase acts as a representative for both cytostatic and cytotoxic effects of RISUG® conditioned media on rat primary uterine cell lines. The test was performed after 24, 48 and 72 hours exposure of RISUG® conditioned media to rat primary uterine cell lines. The MTT result has not shown any significant reduction ($p > 0.05$) in mitochondrial dehydrogenase activity (Figure. 2.9a).
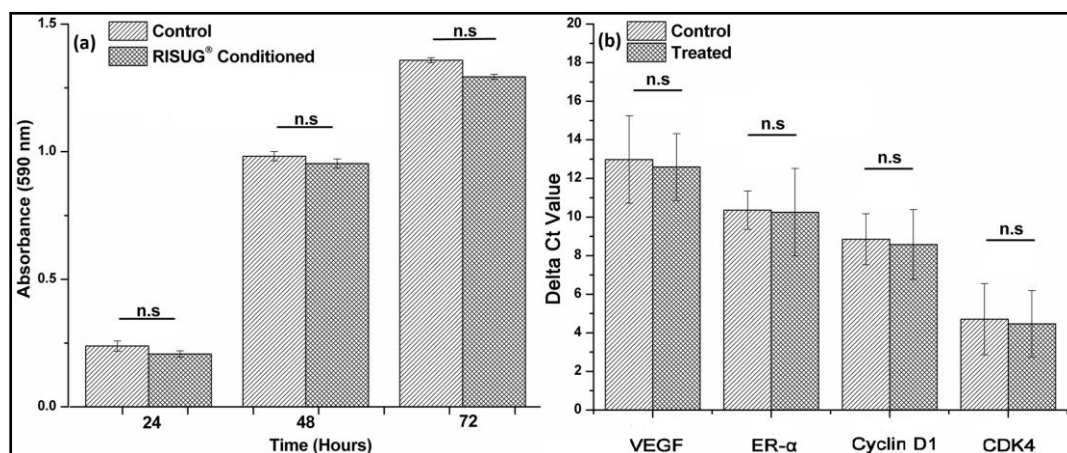
Figure 2.9. (a) MTT assay **(b)** RT-PCR results for control and RISUG® conditioned media treated rat uterine primary cell lines. All the experiments were carried out in triplicates. Values which have not shown significant difference with p > 0.05 were mentioned as "n.s"

The population of uterine cell lines increased with increase in time duration. RISUG® conditioned media has not reduced the growth of primary rat uterine cell line in all the tested time intervals when compared with control media. Moreover, it was observed that there was no significant difference in the morphology of both control and treated primary rat uterine cell lines grown in conditioned media. RISUG® conditioned media treated rat primary uterine cell lines has not shown any significant change in the expression of ER-α and VEGF genes (Figure. 2.9b). Further, the expression level of cell cycle regulators Cyclin D1 and CDK4 of RISUG® conditioned media treated uterine cell lines has not shown any significant change (p > 0.05) compared to control cell lines.
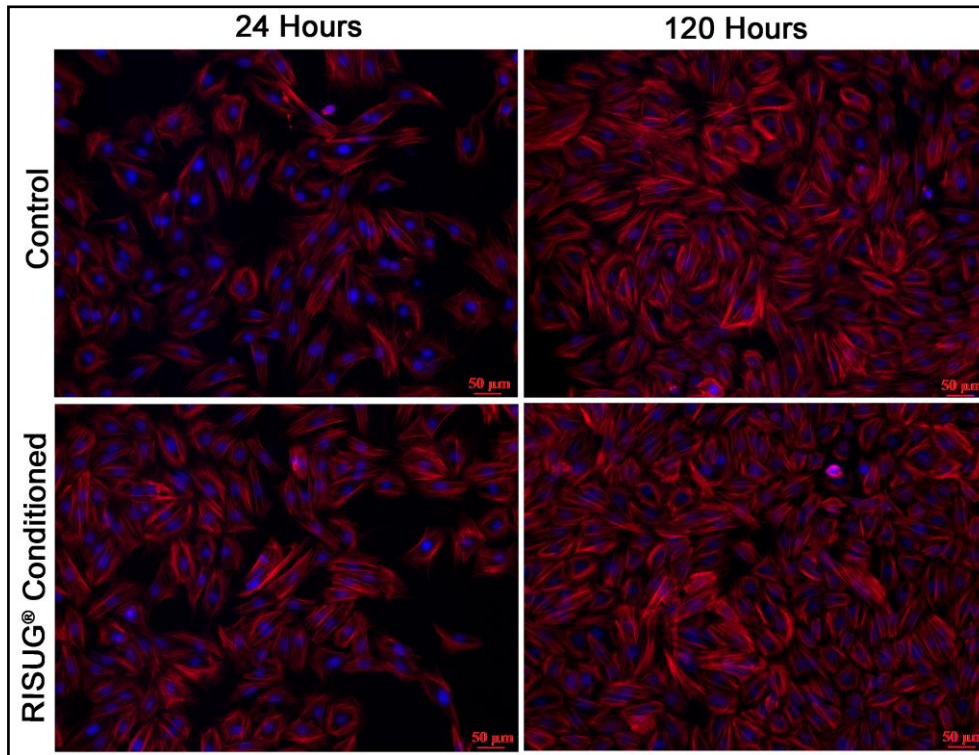
Figure 2.10. Rhodamine and DAPI stained control and RISUG® conditioned media treated rat uterine primary cell lines

2.4.14.2 Cellular morphology and proliferation analysis

The morphological analysis of rat primary uterine cell lines grown in conditioned media has not shown damage in their extracellular or intracellular morphology (Figure. 2.10, 2.11). The rat primary uterine cell lines grown in conditioned media exhibited well extended cytoskeleton as same as the control cell lines. Moreover, the uterine cell lines were capable of making cellular contact with one another.
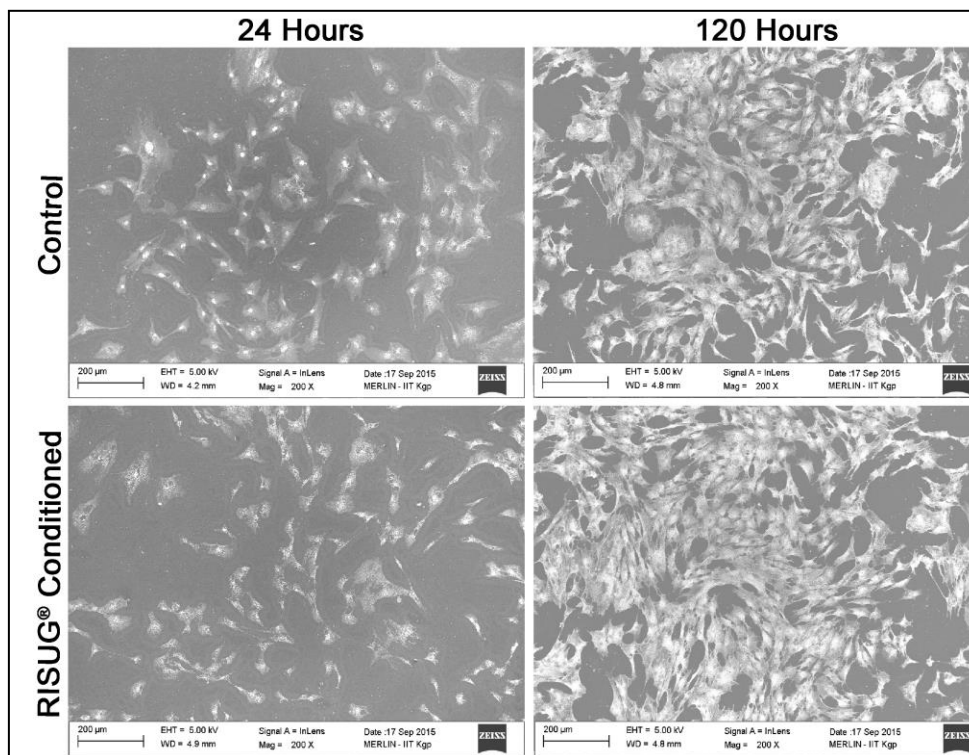
Figure 2.11. SEM of control and RISUG® conditioned media treated rat uterine primary cell lines

2.4.15 *In vivo* studies

2.4.15.1 Gross anatomical macroscopic observation

Test hydrogel implanted uterine isthmuses have not shown any indication of implant oriented swelling, dilation, discontinuation, contraction or any abnormal growth in the external surface when compared with control uterine tissues. The cornua posteromedially extended from the ovary dorsal to the urinary bladder and they normally united to form the corpus as flexible tubular structure. The smooth uterine horns were suspended from the dorsal body wall by heavy wide elastic ligaments through which,

blood vessels and nerves lined without any irregular pattern over the tubular surface of both test and control uterine tissues (Fig. 2.12).
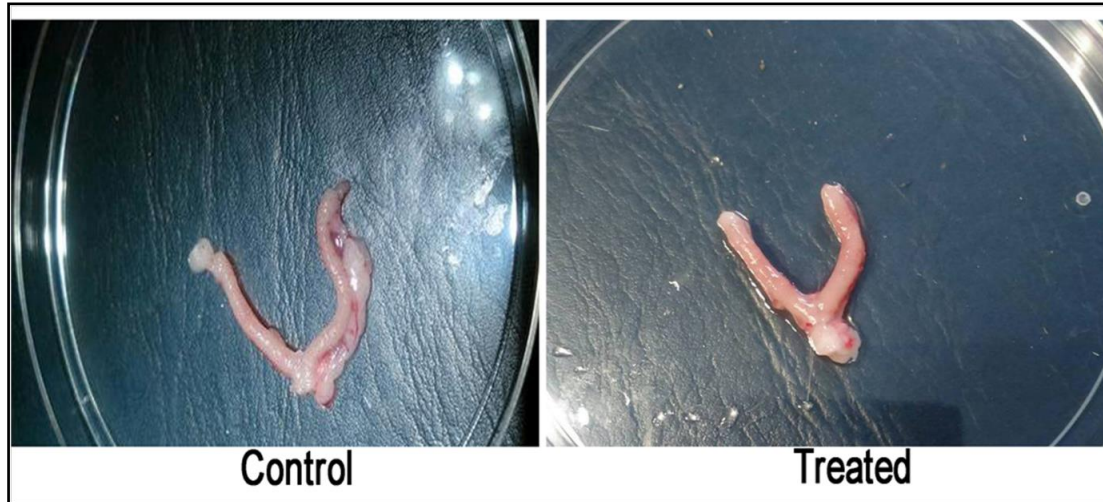
Figure 2.12. Gross anatomical macroscopic observation of control and treated uterine tissue   samples

2.4.15.2 Microscopic anatomical observation

Histological analysis of control and treated rat uterine tissues sample showed no significant alterations in the uterine morphology (Figure. 2.14). The compact architecture of the uterine cells was well defined with prominent nucleus located within the cells in both control and treated uterine tissues. The simple columnar epithelial cells of both control and treated tissue samples normally extended in to branched tubular glands projected in to stroma without any significant morphological change. The stroma of both control and treated uterine tissue samples had many polyhedral cells which has not shown any implant oriented microscopic change when compared with control samples [35]. The microscopic architecture of myometrial muscular layer consisting of inner and outer

differential polyhedral cells lined with loosely connective stratum vasculosum has not shown any significant change in both control and treated tissue samples.
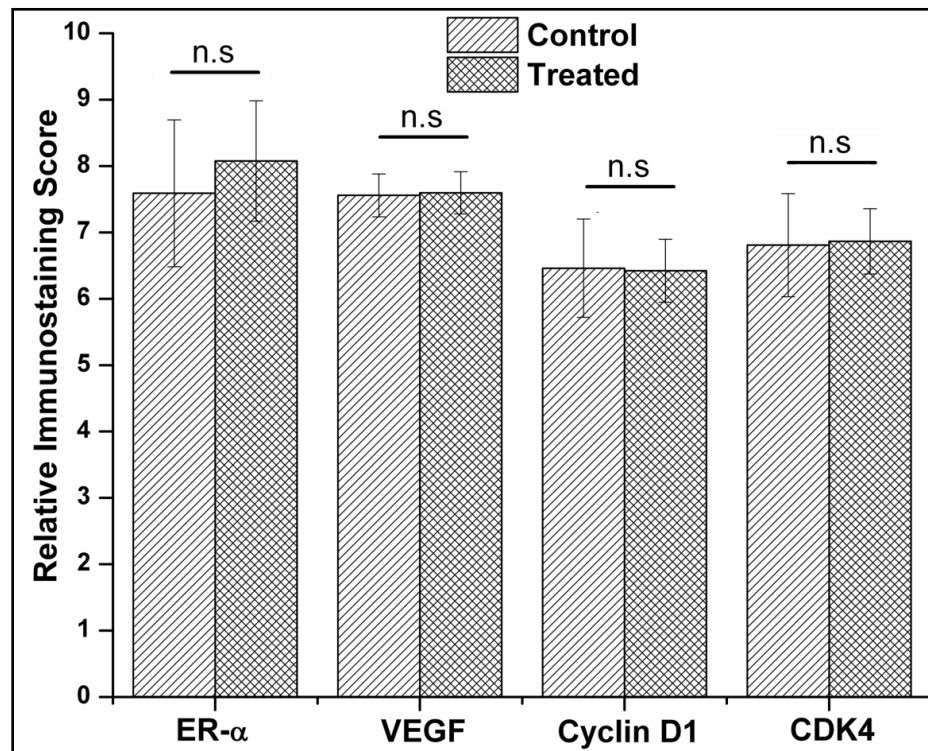
Figure 2.13. Immunohistochemical staining scores of control and RISUG® treated rat uterine tissue samples expressing ER-α, VEGF, CyclinD1 and CDK4 proteins. All the experiments were carried out in triplicates. Values which have not shown significant difference with p > 0.05 were mentioned as "n.s"

2.4.15.3 Immunohistochemical observation

The effect of test hydrogel on expression of ER-α on uterine tissue samples was investigated through immunohistochemical localization of ER-α receptor (Figure. 2.14). Both test and control tissue samples expressed ER-α without any significant change [36]. The control and treated uterine tissue samples showed immunoreactivity to VEGF in agreement with the expression of ER-α. The test hydrogel has not exerted any implant oriented deleterious effects on VEGF expression. To check the effect of test hydrogel on

cell cycle in uterine tissue samples, the expression of cell cycle regulators Cyclin D1 and CDK4 were investigated. Both the cell cycle regulators have not shown any significant difference in their expression when compared with 29 days control and test tissue samples [37]. The test hydrogel has not shown any significant changes ($p > 0.05$) in the expression of estrogen-responsive ER-α and VEGF and also in cell cycle regulators among both control and test uterine tissue samples at 29 days duration. The quantitative method for immunohistochemistry was obtained by scoring the stained areas (epithelial cells, blood vessels and the stroma) of uterine tissue samples. Stained areas in immunohistochemistry express the presence of epitope molecule for the attachment of respective antibodies (Figure. 2.13).

2.4.15.4 Organ pathology

Pathological changes in organs after 29 days of test hydrogel treatment of both control and treated samples were investigated (Figure. 2.15). Heart, Lungs, Liver, Spleen and Kidney were collected and sliced for haematoxylin and eosin staining. The microscopic anatomy of cardiac tissue sample has not shown any sign of interfibrillar hemorrhages, infiltration congestion, or focal disruption of cardiac muscle of both control and treated cardiac tissue samples.
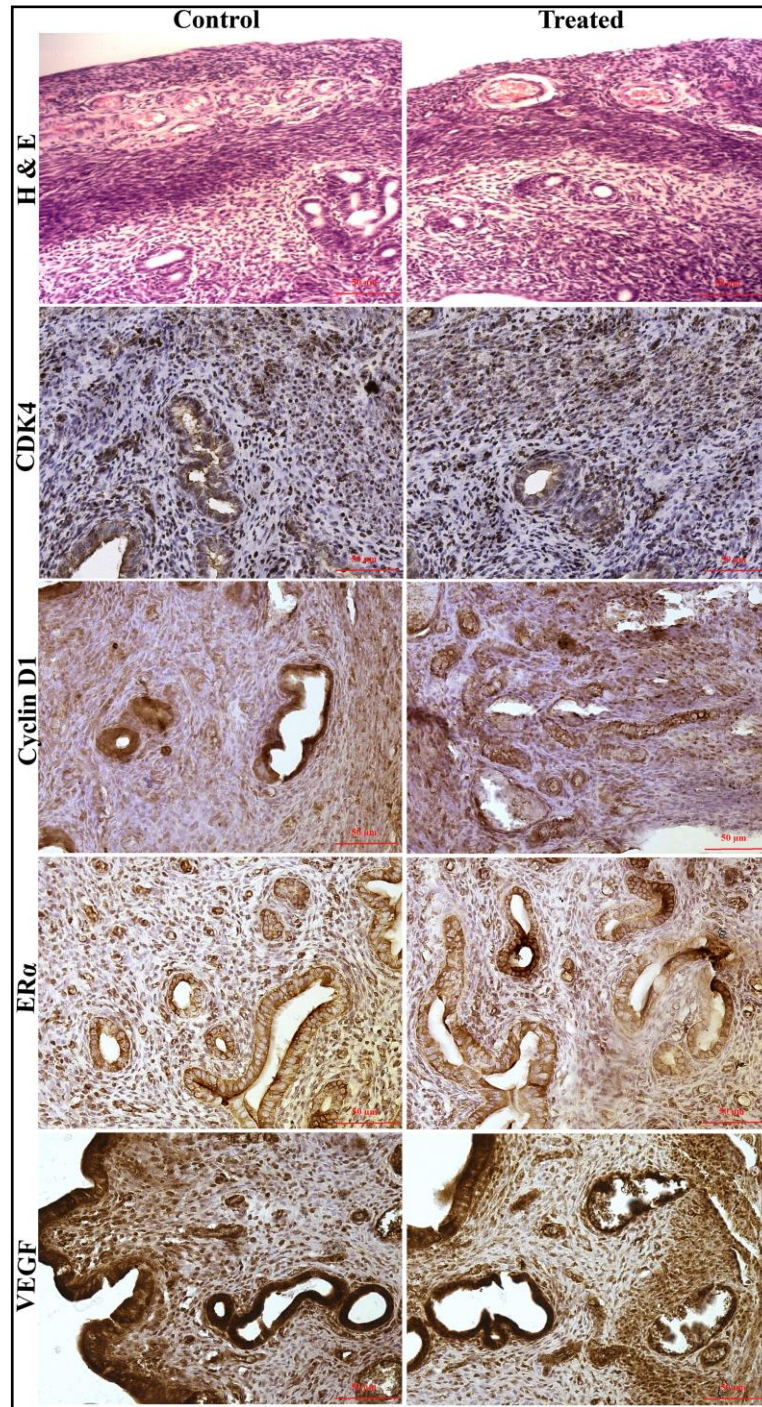
Figure 2.14. Hematoxylin and Eosin stained control and RISUG treated rat uterine tissue samples and Immunohistochemical staining of ER-α, VEGF, CyclinD1 and CDK4 and their receptors in control and RISUG treated rat uterine tissue samples

Microscopic anatomy of both control and treated animal lungs samples were observed

since, implant-associated stress may deprive the respiration of rat due to the formation of

free radicals. Alveolar septa with rich capillarization were visible. The flat alveolar cells and the large granulated pneumocytes were distributed among the tissue sections without any morphological damage. The test hydrogel has not shown any signs or symptoms of respiratory insufficiency in 29 days lungs sample of both control and treated animals. The normal sinusoids in liver assure that the implant has not exerted any change in even distribution of blood to the liver. The hepatic parenchymal cells were observed normal with prominent nuclei. There were no signs of implant-associated ductal hyperplasia in liver sample of both control and treated animals. Both control and treated spleen tissue samples have shown normal inward projecting smooth muscle cells filled trabeculae with a network of reticular fibers with oriented framework. There were no signs of inflammation or fibrosis was observed in kidney sample of both control and treated animals. Both the cortex and medulla of the kidney parenchyma have not shown any morphological damage. Healthier straight tubule segments were evenly arranged as medullary rays. Both outer and inner medullary stripes were distinguishable and had not shown any structural alteration in both control and treated tissue sections [38].

2.4.15.5 Hematology and blood biochemistry

Hematology results have not shown any significant alteration in both control and treated animals (Figure. 2.16a, b, c and d). The critical indicators WBC, RBC and PLT of control rats have not shown considerable differences when compared with untreated rats ($p > 0.05$). All the other hematology markers like MCV, MCH, MCHC, HGB and HCT also had not shown any toxicological change in treated rats when compared ($p > 0.05$) with control. These results inferred that test hydrogel had not shown any biological systemic toxicological effect post-implantation inside the uterus. Blood biochemical

parameters for general metabolic function, kidney and liver function were investigated and compared with 29 days treated animals along with their controls. There was no significant difference in the 29 days treated samples when compared with their respective controls [39].

2.5 Discussion

In vitro characterizations especially σ_y values of gel strength analysis have inference that RISUG® expresses high mechanical strength which could help in resisting expulsion in the upper reproductive tract for an extended duration after implantation. In fact, we have shown that upon dilution with (SUF), RISUG® forms intermolecular H-bonding and exhibited instantaneous gelation as a result of its' viscoelastic nature. It has been shown that water-mediated intermolecular H-bonding between maleic anhydride group of RISUG® and SUF is responsible for surface roughness and mechanical strength of RISUG®. Crystallite size estimated from broadening peaks by Scherer equation has proved that RISUG® after experiencing the dilution by SUF has not shown a structural change in its polymeric structure. The viscosity curves obtained at different shear rate indicate the shear thinning behavior of RISUG® and its dilutions with power-law exponent n ranging to 0.46 from 0.53 at 37ºC.
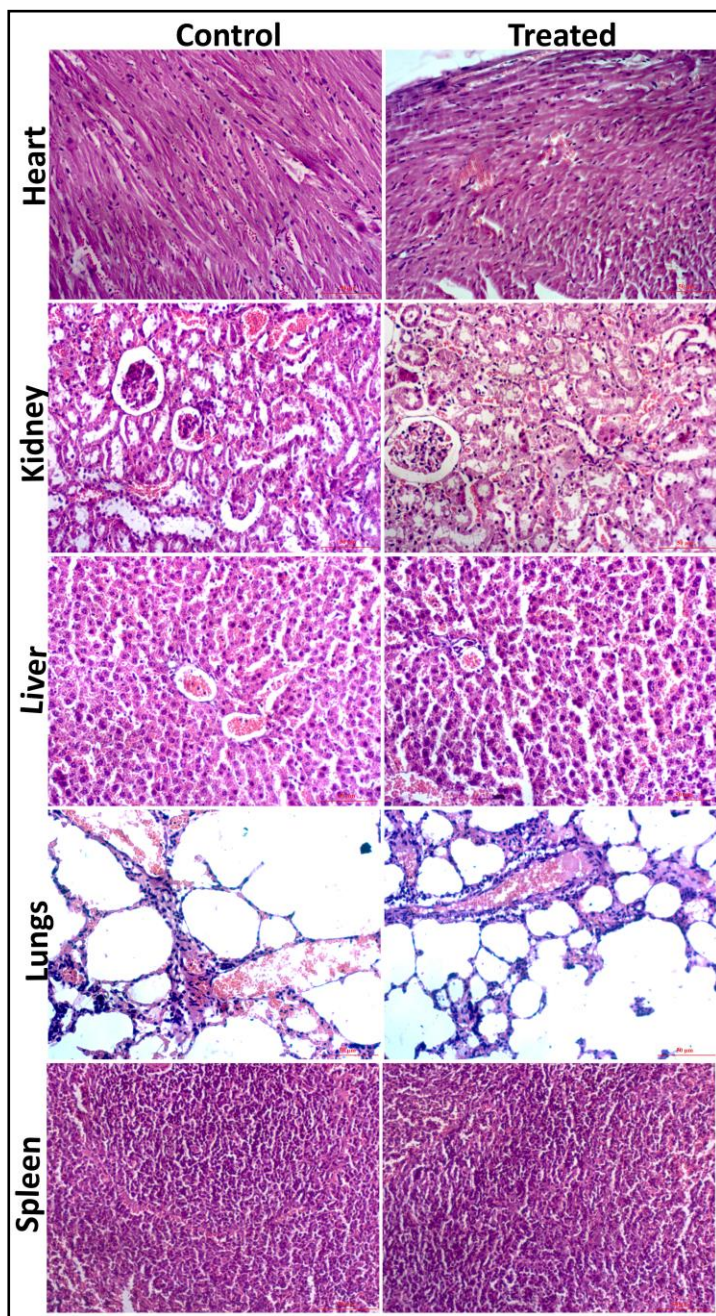
Figure 2.15. Hematoxylin and Eosin stained Heart, Lungs, Liver, Spleen and Kidney of control and RISUG treated rat tissue

The viscoelastic property of RISUG® and its dilutions increases with increase in the interaction of SUF (upon increasing the amount of SUF). These results suggested that mechanical strength of RISUG® depends upon the intermolecular H-bonding interaction

with SUF. This work has demonstrated that these rheological results can be correlated with the composition of the RISUG® and therefore with its retention and also with their stability and compliance.
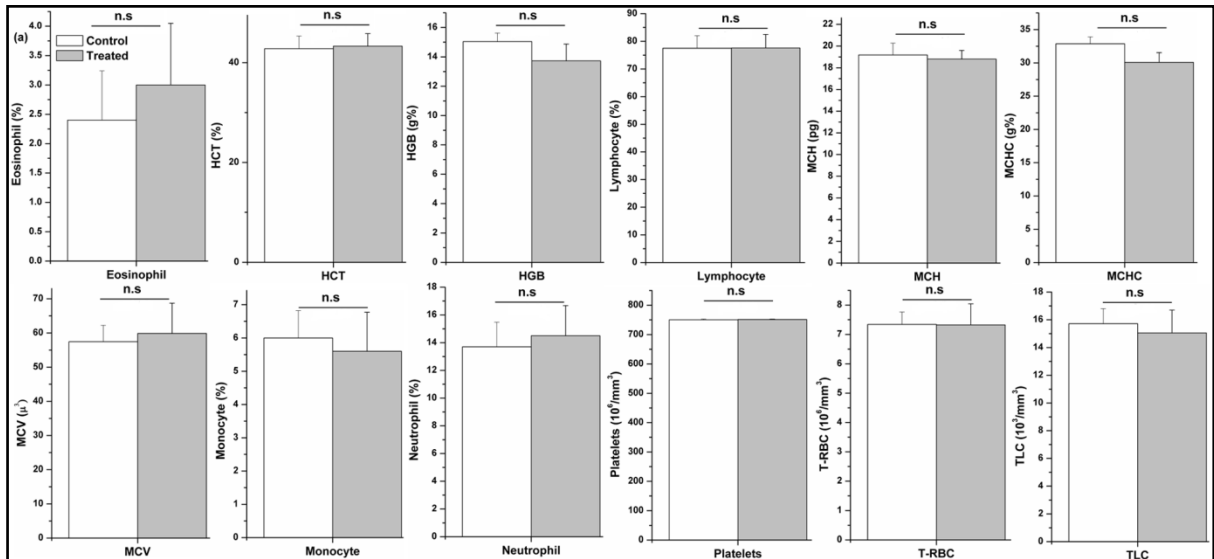
Figure 2.16. (a) Haematological parameters of control and RISUG® treated rat. All the experiments were carried out in triplicates. Values which have not shown significant difference with p > 0.05 were mentioned as "n.s"
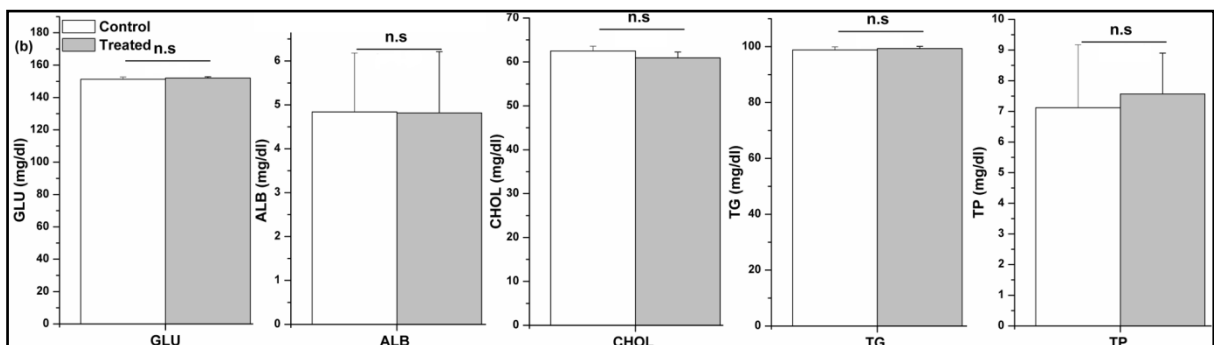
Figure 2.16. (b) General metabolic function of control and RISUG® treated rat. All the experiments were carried out in triplicates. Values which have not shown significant difference with p > 0.05 were mentioned as "n.s"
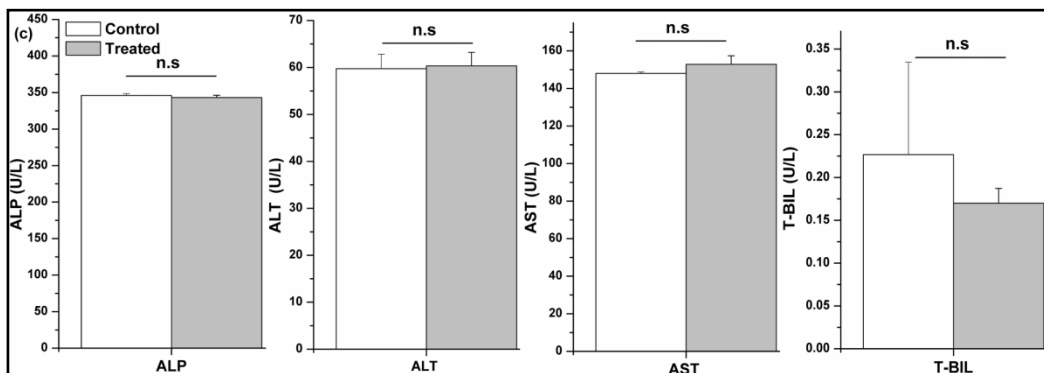
Figure 2.16. (c) Liver function of control and RISUG® treated rat. All the experiments were carried out in triplicates. Values which have not shown significant difference with p > 0.05 were mentioned as "n.s"
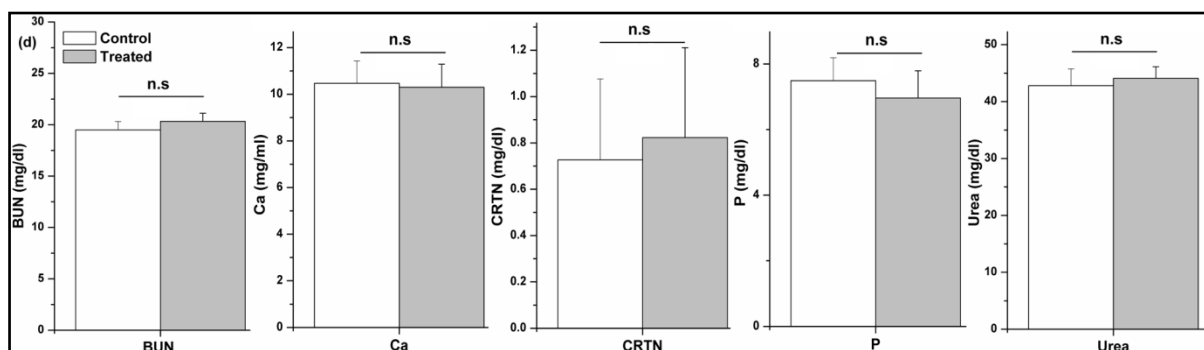
Figure 2.16. (d) Kidney function of control and RISUG® treated rat. All the experiments were carried out in triplicates. Values which have not shown significant difference with p > 0.05 were mentioned as "n.s"

The test hydrogel, when implanted inside the uterus, should provide antimicrobial activity around the reproductive tract to efficiently prevent implant associated bacterial infections without disturbing the beneficial *Lactobacillus spp*. The test hydrogel RISUG® established selective antimicrobial activity against opportunistic pathogens while having limited consequence over the growth of *Lactobacillus spp*. The exact selective mechanism for the antimicrobial activity is still unknown but specific mechanism may be hypothesized. Female reproductive tracts naturally have body fluids like uterine, cervical and vaginal fluid. These body fluids will be replenished continuously [40] at any

particular time intervals. The test hydrogel may exert ionic dispersion into the biological fluids that render unfavorable environment only to pathogenic microbial growth. Further, the dispersed ions in the biological fluid from the three-dimensional structure of test hydrogel may cause morphological damage, lipid peroxidation or DNA damage to the micro-organisms. During the process of exchange of ions and solvent between biological media and RISUG®, a polymeric network of RISUG® hydrogel may generate carbooxyl radicals due to intermolecular H-bonding between maleic anhydride and SUF [40].

Polymeric hydrogel acquires particular attention in biomedical application. When a polymeric hydrogel was synthesized for serving as a biological implant, biocompatibility characterization is of utmost importance. *In vitro* cell culture study is a useful tool for monitoring the cytotoxicity of the synthesized hydrogel. *In vitro* biocompatibility assessment is more important for reducing the suffering of animals during *in vivo* toxicity studies. Furthermore the sensitivity produced by primary cell lines and established cell lines were significantly different. To reduce the sensitivity *in vitro* cytotoxicity assay was performed using rat uterine primary cell lines. The test hydrogel RISUG® has not shown any significant damage to the rat uterine primary cell lines during the period of *in vitro* toxicological assessment. *In* vivo toxicity results inferred that RISUG® hydrogel implant has not exerted any implant associated toxicity post-implantation inside the uterus. Moreover, the effects of RISUG® hydrogel on the expression of estrogen receptor, the estrogen-responsive gene VEGF, along with cell cycle regulatory proteins were investigated. Estrogen receptors are activated by the action of estrogens in the female reproductive tract. Estrogen receptors alpha (α) and beta (β) are expressed all over the body tissues. However, ER-α is predominantly expressed in uterus,

mammary glands, pituitary, ovarian cells and hypothalamus. Estrogen enzyme distinctively targets the uterine tissue and possesses the significant expression of ER-α all over the estrus cycle. ER-α dependent uterine tissue proliferation was explained in the majority of research works. Since ER-α plays an essential role in maintaining healthy [37] uterine tissue, the effects of test hydrogel in the expression of ER-α in uterine tissues were investigated. Further, the expression of estrogen-responsive gene Vascular Endothelial Growth Factor (VEGF) was evaluated since uterine tissues are nourished with vascular tissue and it is well known that it responds primarily to the estrogen in uterine tissues. The change in ER-α expression may significantly affect the cell cycle regulators. So the expression of cell cycle regulators cyclin D1 and CDK4 has also investigated in test hydrogel treated uterine tissues. The test hydrogel has not inferred any change in the expression of ER-α, VEGF and cell cycle regulators (Cyclin D1 and CDK4) which are primarily responsible for estrogen signaling pathway.

Organ tissue pathology studies have shown no significant damage observed in the organs during the entire treatment period. It was described that implant-associated infection or inflammation might alter the biochemical parameters. The test hydrogel has not shown any significant change in any of the biochemical parameters during the treatment phase. The observed hematology and blood biochemical study depicts that the RISUG® does not have any interaction with the systemic biological system. The test hydrogel only has physiological interaction with the implanted site post-implantation. Finally, the results presented here extend these observations to explain that RISUG® can be used as a novel non-hormonal female contraceptive fallopian tube hydrogel implant.

2.6 Conclusion

The authors conclude from the evidence represented by the above research work that, the styrene maleic anhydride based polymeric hydrogel RISUG® is highly applicable for the development of a new improved form of IUCDs as an uterine implant.

References

[1] B.E. Lai, A.R. Geonnotti, M.G. Desoto, D.C. Montefiori, D.F. Katz, Semi-solid gels function as physical barriers to human immunodeficiency virus transport in vitro, Antiviral Res, 88 (2010) 143-151.

[2] R.M. Machado, A. Palmeira-de-Oliveira, J. Martinez-De-Oliveira, R. Palmeira-de-Oliveira, Vaginal films for drug delivery, J Pharm Sci, 102 (2013) 2069-2081.

[3] E.N. Zare, M.M. Lakouraj, M. Mohseni, Biodegradable polypyrrole/dextrin conductive nanocomposite: synthesis, characterization, antioxidant and antibacterial activity, Synthetic Metals, 187 (2014) 9-16.

[4] E.N. Zare, M.M. Lakouraj, M. Mohseni, A. Motahari, Multilayered electromagnetic bionanocomposite based on alginic acid: Characterization and biological activities, Carbohydrate polymers, 130 (2015) 372-380.

[5] V. Hasantabar, M.M. Lakouraj, E.N. Zare, M. Mohseni, Innovative magnetic tri-layered nanocomposites based on polyxanthone triazole, polypyrrole and iron oxide: synthesis, characterization and investigation of the biological activities, RSC Advances, 5 (2015) 70186-70196.

[6] V. Hasantabar, M.M. Lakouraj, E.N. Zare, M. Mohseni, Synthesis, Characterization, and Biological Properties of Novel Bioactive Poly (xanthoneamide-triazole-ethersulfone) and Its Multifunctional Nanocomposite with Polyaniline, Advances in Polymer Technology, 36 (2017) 309-319.

[7] R.B. Scott, Critical ilness and deaths associated with Intrauterine Devices, Obstetrical and gynecology, 31 (1968) 322-327.

[8] L.R. Weekes, Complications of intrauterine contraceptive devices, Journal of the National Medical Association, 67 (1975) 1.

[9] G.H. Silveira, M.A.P. De Oliveira, C.P. Crispi, M. Lamblet, Hysteroscopic Permanent Female Sterilization, Brazilian journal of videoendoscopic surgery 3(2010) 200-208.

[10] T.P. Cleary, N.K. Tepper, C. Cwiak, M.K. Whiteman, D.J. Jamieson, P.A. Marchbanks, K.M. Curtis, Pregnancies after hysteroscopic sterilization: a systematic review, Contraception, 87 (2013) 539-548.

[11] V. Brache, H. Croxatto, R. Sitruk-Ware, R. Maguire, J.C. Montero, N. Kumar, A.M. Salvatierra, A.S. Tejada, L. Cochon, M.L. Forcelledo, P. Lahteenmaki, F. Alvarez, A. Faundes, Effect of a single vaginal administration of levonorgestrel in Carraguard gel on the ovulatory process: a potential candidate for "dual protection" emergency contraception, Contraception, 76 (2007) 111-116.

[12] S. Banerjee, S.K. Guha, RISUG: a potential candidate for the entry inhibitor group of antiretroviral drugs, Med Hypotheses, 73 (2009) 150-152.

[13] F. Alvarez, P.L. Schilardi, M.F. de Mele, Reduction of the "burst release" of copper ions from copper-based intrauterine devices by organic inhibitors, Contraception, 85 (2012) 91-98.

[14] S. Xu, V.L. Cavera, M.A. Rogers, Q. Huang, K. Zubovskiy, M.L. Chikindas, Benzoyl peroxide formulated polycarbophil/carbopol 934P hydrogel with selective antimicrobial activity, potentially beneficial for treatment and prevention of bacterial vaginosis, Infect Dis Obstet Gynecol, 2013 (2013) 909354.

[15] M. Alyane, G. Barratt, M. Lahouel, Remote loading of doxorubicin into liposomes by transmembrane pH gradient to reduce toxicity toward H9c2 cells, Saudi Pharm J, 24 (2016) 165-175.

[16] Y. Zhang, M. Hu, F. Meng, X. Sun, H. Xu, J. Zhang, P. Cui, N. Morina, X. Li, W. Li, X.K. Wu, M. Brannstrom, R. Shao, H. Billig, Metformin Ameliorates Uterine Defects in a Rat Model of Polycystic Ovary Syndrome, EBioMedicine, 18 (2017) 157-170.

[17] A. Prigent-Tessier, U. Barkai, C. Tessier, H. Cohen, G. Gibori, Characterization of a Rat Uterine Cell Line, UIII Cells:Prolactin (PRL) Expression and Endogenous Regulation of PRL-Dependent Genes; Estrogen Receptor b, a2-Macroglobulin, and Decidual PRL Involving the Jak2 and Stat5 Pathway*, Endocrinology, 142 (2001) 1242-1250.

[18] K. Verma, M.M. Misro, H. Singh, S. Mahajan, A.R. Ray, S.K. Guha, Histology of the rat vas deferens after injection of a non-occlusive chemical contraceptive*, Journal of Reproduction and Fertility, 63 (1981) 539-542.

[19] A. Chatterjee, U. Chatterji, All-trans retinoic acid protects against arsenic-induced uterine toxicity in female Sprague-Dawley rats, Toxicol Appl Pharmacol, 257 (2011) 250-263.

[20] U. Schmidt, S. Zschoche, C. Werner, Modification of Poly(octadecene-alt-maleic anhydride) Films by Reaction with Functional Amines, Journal of Applied Polymer Science, 87 (2001) 1255-1266.

[21] H. Xuemei, Y. Hao, Fabrication of Polystyrene/Detonation Nanographite Composite Microspheres with the Core/Shell Structure via Pickering Emulsion Polymerization, Journal of Nanomaterials, 2013 (2013) 1-8.

[22] M. Baghayeri, E.N. Zare, R. Hasanzadeh, Facile synthesis of PSMA-g-3ABA/MWCNTs nanocomposite as a substrate for hemoglobin immobilization: application to catalysis of H2O2, Materials Science and Engineering: C, 39 (2014) 213-220.

[23] M. Baghayeri, E.N. Zare, M. Namadchian, Direct electrochemistry and electrocatalysis of hemoglobin immobilized on biocompatible poly (styrene-alternative-maleic acid)/functionalized multi-wall carbon nanotubes blends, Sensors and Actuators B: Chemical, 188 (2013) 227-234.

[24] P.N. Moghadam, E.N. Zareh, Synthesis of conductive nanocomposites based on polyaniline/poly (styrene-alt-maleic anhydride)/polystyrene, e-Polymers, 10 (2010).

[25] M. Selvakumar, P. Srivastava, H.S. Pawar, N.K. Francis, B. Das, G. Sathishkumar, B. Subramanian, S.K. Jaganathan, G. George, S. Anandhan, S. Dhara, G.B. Nando, S. Chattopadhyay, On-Demand Guided Bone Regeneration with Microbial Protection of Ornamented SPU Scaffold with Bismuth-Doped Single Crystalline Hydroxyapatite: Augmentation and Cartilage Formation, ACS Appl Mater Interfaces, 8 (2016) 4086-4100.

[26] E.N. Zareh, P.N. Moghadam, Synthesis and characterization of conductive nanoblends based on poly (aniline-co-3-aminobenzoic acid) in the presence of poly (styrene-alt-maleic acid), Journal of Applied Polymer Science, 122 (2011) 97-104.

[27] E. Nazarzadeh Zare, M. Mansour Lakouraj, P. Najafi Moghadam, R. Hasanzadeh, Novel conducting nanocomposite based on polypyrrole and modified poly (styrene-alt-maleic anhydride) via emulsion polymerization: Synthesis, Characterization, Antioxidant, and heavy metal sorbent activity, Polymer Composites, 36 (2015) 138-144.

[28] O.G. Atici, A. Akar, R. Rahimian, Modication of Poly(maleic anhydride-co-styrene) with Hydroxyl Containing Compounds, Turkish journal of chemistry, 25 (2001) 259-266.

[29] S. Sepúlveda-Guzmán, L. Lara, O. Pérez-Camacho, O. Rodríguez-Fernández, A. Olivas, R. Escudero, Synthesis and characterization of an iron oxide poly(styrene-co-carboxybutylmaleimide) ferrimagnetic composite, Polymer, 48 (2007) 720-727.

[30] S.K. Guha, Biophysical mechanism-mediated time-dependent effect on sperm of human and monkey vas implanted polyelectrolyte contraceptive, Asian J Androl, 9 (2007) 221-227.

[31] S. Mohanty, A.P. Rameshbabu, S. Dhara, J. Smialek, α-Alumina Fiber with Platelet Morphology Through Wet Spinning, Journal of the American Ceramic Society, 95 (2012) 1234-1240.

[32] A. Pal, J. Dey, Water-induced physical gelation of organic solvents by N-(n-alkylcarbamoyl)-L-alanine amphiphiles, Langmuir, 27 (2011) 3401-3408.

[33] T. Patra, A. Pal, J. Dey, Birefringent physical gels of N-(4-n-alkyloxybenzoyl)-L-alanine amphiphiles in organic solvents: the role of hydrogen-bonding, J Colloid Interface Sci, 344 (2010) 10-20.

[34] S. Samai, J. Dey, K. Biradha, Amino acid based low-molecular-weight tris(bis-amido) organogelators, Soft Matter, 7 (2011).

[35] Y. Zhang, X. Sun, X. Sun, F. Meng, M. Hu, X. Li, W. Li, X.-K. Wu, M. Brännström, R. Shao, H. Billig, Molecular characterization of insulin resistance and glycolytic metabolism in the rat uterus, Scientific Reports, 6 (2016).

[36] H. Wang, H. Eriksson, L. Sahlin, Estrogen Receptors a and b in the Female Reproductive Tract of the Rat During the Estrous Cycle1, Biology of Reproduction, 63 (2000) 1331-1340.

[37] A. Chatterjee, U. Chatterji, RAesresarechnic abrogates the estrogen-signaling pathway in the rat uterus, Reproductive Biology and Endocrinology, 8 (2010) 2-11.

[38] Z. Zhuo, J. Hu, X. Yang, M. Chen, X. Lei, L. Deng, N. Yao, Q. Peng, Z. Chen, W. Ye, D. Zhang, Ailanthone Inhibits Huh7 Cancer Cell Growth via Cell Cycle Arrest and Apoptosis In Vitro and In Vivo, Sci Rep, 5 (2015) 16185.

[39] X.-D. Zhang, J. Chen, Y. Min, G.B. Park, X. Shen, S.-S. Song, Y.-M. Sun, H. Wang, W. Long, J. Xie, K. Gao, L. Zhang, S. Fan, F. Fan, U. Jeong, Metabolizable Bi2Se3Nanoplates: Biodistribution, Toxicity, and Uses for Cancer Radiation Therapy and Imaging, Advanced Functional Materials, 24 (2014) 1718-1729.

[40] S.K. Guha, S. Ansari, S. Anand, A. Farooq, M.M. Misro, D.N. Sharma, Contraception in male monkeys by Intra-vas deferens injection of a pH lowering polymer, Contraception, 32 (1985) 109-118.

Chapter 3

Polyvinyl Alcohol and Styrene-Maleic Anhydride blend polymeric gels as intra-vaginal female contraceptives

3.1 Introduction

Women are provided rights to choose the suitable contraceptive technique on their own to control the child birth for establishing effective contraception according to the global movement, "the family planning 2020 (FP2020)". This FP2020 movement set their bench mark to make 120 female individuals residing in poor countries as additional contraceptive users to access modern contraceptive techniques. An increase of 80 million population was observed every year was recorded as current population statistics all over the world which may lead to overall increase of 9-10 million in world population by the year of 2050 [1]. Such an increase in the populations has resulted in extensive environmental destruction, poverty and starvation. Among many reasons for the population explosion, unintended pregnancy has played a prime role all over the world [2]. The rate of unintended pregnancy could be prevented by implementing adequate access to prevailing contraceptive techniques.

Among the various contraceptive techniques, non-hormonal female contraceptive techniques are considered to be safe and effective. Commercially available vaginal contraceptives encompass detergents such as isonyl-phenyl-polyoxyethylene ether, p-menthanyl-phenyl-polyoxuethylene ether and isooctyl-phenyl-polyoxyethylene ether which have the ability to disrupt cell membranes of the sperms [2]. Other class of surfactants include benzalkonium and dioctyl sodium sulfosuccinate which show direct effects on vaginal epithelial cells and beneficial microflora colonising in the lower female reproductive tract [3-5]. However, recurrent use of these contraceptives has been related with the irritation and ulceration of the female reproductive tract along with the alteration in the population of beneficial micro-organisms of female reproductive tract, thereby

leading to increased threat of opportunistic infections [6-8]. Due to these prevailing side effects, an ideal vaginal contraceptive which poses tissue safety needs to be developed [9-11].

In a determination to develop a new form of spermicidal non-hormonal intra-vaginal contraceptive, RISUG® comprising of SMA and Styrene maleic acid could be a suitable alternative. RISUG® is presently under phase three clinical trial as male contraceptive vas deferens implant [12]. Upon implantation in the vas deferens, it reduces the pH of the surrounding medium, thereby causing damage to the acrosome of the sperms [13, 14]. However, RISUG® cannot directly be implanted into the female reproductive tract due to precipitation property of the polymer. The polymer when in contact with biological fluids it gets precipitated followed by reducing the pH of the medium at its immediate vicinity [15]. This flaky property of the polymer may develop a maze inside the vagina of the female individual that may ultimately result in inconvenience to the individual. Due to this precipitation and flaky properties of RISUG® it can be used as long term contraceptive implant as explained in chapter 2. However, these physiological properties of RISUG® limit its application as short term vaginal contraceptive implant. To overcome these limitations, it needs to be blended with some biocompatible and biodegradable polymer.

In this regard, we have blended RISUG® with Polyvinyl alcohol (PVOH) to formulate films. PVOH was selected since majority of the presently available vaginal film products use PVOH in their formulation and has been regarded safe for vaginal use by U.S. Food and Drug Administration [16, 17]. Furthermore, the bio-degradability and bio-compatible property of PVOH is significantly more in order to make vaginal

contraceptive film. This new for of formulation will aid application of RISUG as a vaginal contraceptive film for fulfilling the purpose of developing short term female contraceptive polymeric film. The presence of strong electronegative oxygen of RISUG® polymeric hydrogel accounts for its robust adhesive features with pendent hydroxyl group of PVOH. We further evaluated RISUG®/Polyvinyl alcohol (PVOH) blended films extensively for their physiochemical characteristics, *in vitro* and *in vivo* biocompatibility and *in vitro* spermicidal activity. To the best of our knowledge, there is no report on using RISUG®-based composite polymeric films for intra-vaginal female contraceptive application. This RISUG®-based composite polymeric films could establish short term contraceptive effect for female individual as a non-hormonal and non-surfactant new form of contraceptive film. This may confort female individuals in order to establish short term female contraception without any side effects and mental stress.

3.2 Materials and methods

3.2.1 Materials

PVOH (GHOSENOL-GH-17-R, Singapore) [18] with saponification degree (mole %) of 86.5 – 89.0 was used in this study to prepare polymeric blends with RISUG® hydrogel. RISUG® polymeric hydrogel was synthesized following standard procedure [15]. The solvents used for this study were procured from Sigma Aldrich. Cell culture media, antibiotics and Fetal Bovine Serum Albumin (FBS) were purchased from thermo fisher scientific, India.

3.2.1.1 Synthesis of RISUG®

Synthesis of RISUG® was done by following the protocol explained in chapter 2 section 2.2.1. Briefly, maleic anhydride and styrene was taken in the ratio of 1:1 and dissolved in ethyl acetate under nitrogen atmosphere in order to avoid the formation of peroxy radicals during polymerization. Ethyl acetate solution containing equal proportion of styrene and maleic anhydride was subjected to γ-irradiation. Irradiation was provided at 0.2 megarad dose for every 40 g to the polymerization solution in sealed glass bottle. The irradiation dose rate was maintained as 30 to 40 rad/sec using cobalt as γ-irradiation source. The irradiated polymer was precipitated using 60/80 grade petroleum ether. The unreactive monomers were removed by dissolving the polymer in 1,2 dichloro ethane followed by precipitation and drying. Dried SMA was dissolved in medical grade Dimethyl Sulfoxide (1:2 ratio) under controlled atmosphere to obtain final SMA hydrogel.

3.2.2 Methods

3.2.2.1 Preparation of polymeric blends

PVOH polymer was dissolved in dual solvent mixture of DMSO and distilled water (H_2O) at proportion of 108g and 27g respectively [19] and in order to make 10% (w/w) homogenous solution PVOH polymer in dual solvent mixture was heated at 95 ºC with continuous stirring.. Weight ratio of PVOH in DMSO:H_2O was maintained constant and RISUG® was added at four different concentrations with reference to PVOH as indicated in Table 3.1.

Table 3.1 Compositions of PVOH/ RISUG® hydrogel polymeric films

Sample description	PVOH concentration	RISUG® concentration
R0	10%	0
R0.5	10%	2.5%
R1	10%	5.0%
R1.5	10%	7.5%
R2	10%	10%

The polymeric blends were mixed using magnetic stirrer for 8 h to make homogenous solution followed by freezing at -20 ℃ overnight. The frozen polymeric films were gently peeled off and immersed in excess ethanol at 25 ℃ for 72 h (ethanol was changed periodically) in order to remove solvents from the polymeric film. Further ethanol was removed by vacuum drying for 48 h. The dried polymeric films were used for further testing and characterization.
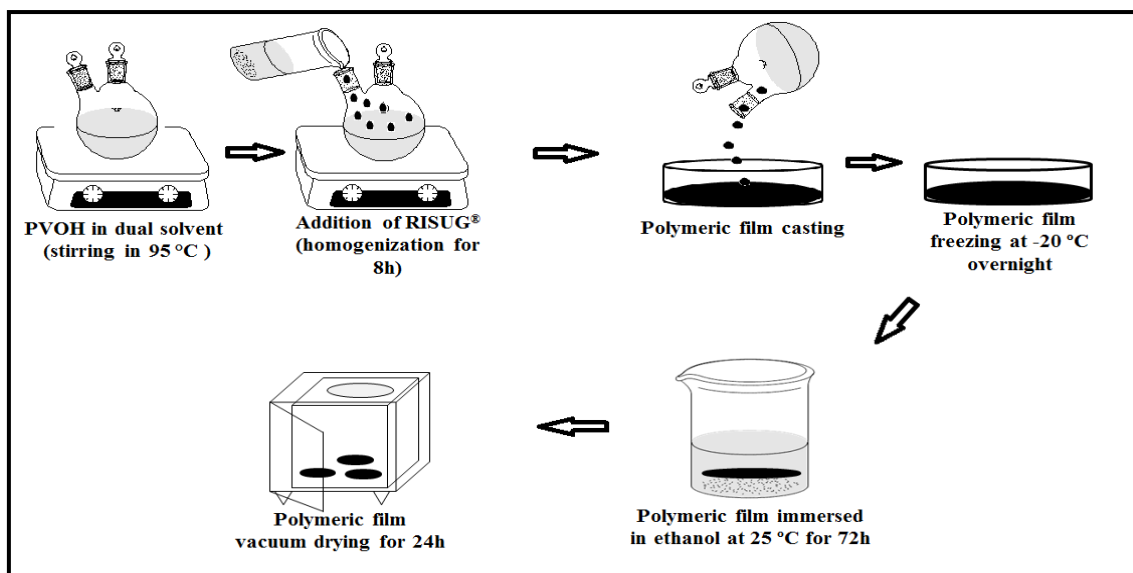
Figure 3.1. Schematic representation of Polymeric film preparation

3.2.2.2 Rheological characterization of polymeric blends

For rheological evaluation, the homogenous solution of polymeric blends was analysed with rheometer with diameter of 50 mm plate diameter and 1° cone-plate geometry. The

polymeric blends were subjected to thermal equilibrium at 35 ℃ (the average normal body temperature) before starting the rheological experiment. The steady state rheological measurements were carried out at 35 ℃ and at shear rates ranging from 0.01 to 1000 S^{-1}. Frequency sweep measurements were carried out at 35 ℃ at frequency ranging from 0.1 to 100 rad/s.

3.2.2.3 FTIR spectroscopy

Infrared spectra for virgin polymer and the polymeric blends were documented by ATR mode FTIR spectrometer (NICOLET 6700 Thermo fisher scientific instruments) in the wavenumber region ranging from 4000 – 400 cm^{-1}. The readings were recorded with a spectral resolution of 0.5 cm^{-1}.

3.2.2.4 Differential Scanning Calorimetry (DSC)

Crystallinity percent, glass transition temperature (T_g) for polymeric films were recorded using differential scanning calorimetry (Perkin Elmer Pyris Diamond DSC). All the polymeric samples were weighed ($\approx$ 10 mg) and scanned in aluminum pans for scanning under a controlled dynamic nitrogen atmosphere at 10 ℃/min from the temperature range of -150 to 250 ℃. All the samples underwent initial scanning procedure to remove any residual elemental stress. Initial run for the virgin polymer and the polymeric blends consist of heating from ambient temperature to 150 ℃ at a rate of scanning at 10 ℃/min. The second run consists of reducing the temperature to -150 $^{\circ}$C followed by heating the polymer samples from -150 to 250 ℃. The results of the second run for the polymeric samples (-150 to 250 ℃) were recorded for further characterization of the polymeric samples. Crystallinity percent for all the polymeric samples were determined by measuring the area under the DSC peak by using the formula given below,

$$P_c = \left[\Delta H_f \Big/ W_i * \Delta H_{f100\%} \right] * 100 \; eqn \; (1)$$

where, P_C is crystallinity percent, ΔH_f is calculated melting enthalpy of polymeric samples (J g^{-1}), W_i is taken as weight fraction of the polymeric samples used for the experiment, $\Delta H_{f100\%}$ is the theoretical melting enthalpy of pure PVOH at its crystalline phase (138.7 J $^{g-1}$) [20, 21].

3.2.2.5 X-Ray Diffraction (XRD) Spectroscopy

The variation in crystal structure of polymeric blends and their alteration in crystallinity were studied using an Philips PW-1710 X-ray diffractometer (Eindhoven, The Netherlands) having crystal monochromator CuK$_\alpha$ radiation (λ=1.540598 Å) having accelerating voltage of 40 kV with beam current of 20 mA for the angular range of 10–80° (2θ). Areas under the peaks of crystalline and amorphous part of the polymers were identified in arbitrary values using X`pert highscore plus 2.1 and Origin Pro 8.5 software in order to identify the degree of crystallinity. The values for degree of crystallinity (X_C), interchain distance (r) and interplanar distance (d) and average crystallite size were calculated using the following equations (2,3,4,5).

$$X_c = [{}^{I_c}/_{I_a + I_c}]*100 \text{ eqn (2)}$$

Where, X_C is degree of crytallinity, I_a is an integrated intensity corresponding to amorphous peak and I_c is an integrated intensity corresponding to crystalline peak of the polymeric samples. The average crystallite size (C_s) for all the polymeric samples were identified using Full Width at Half Maximum (FWHM) values of diffraction peaks using Scherre's equation 5. Furthermore the interchain distance (r) and interplanar distance (d) were also calculated[2] by using the respective formulas (3,4):

$$r = \frac{5\lambda}{8Sin\theta} \text{ eqn (3)}$$

$$d = \frac{\lambda}{2Sin\theta} \text{ eqn (4)}$$

$$C_s = \frac{K\alpha}{\beta\, Cos\theta}\; eqn\ (5)$$

3.2.2.6 *In vitro* degradation study of polymeric blends

In vitro degradation study was performed by monitoring the changes in weight of pre-weighed polymer sample as a function of the incubation time in Simulated Vaginal Fluid (SVF). Dry pre-weighed (10 mg) polymeric sample was incubated in SVF at 37 °C with a regular change every 3rd day. The SVF was prepared with a composition previously described elsewhere [22]. The composition of SVF was described in Table 3.2. Prepared SVF was adjusted to pH 4.2 with the help of lactic acid which is normally prevalent in the female reproductive tract produced by vaginal lactobacilli. Polymeric samples were retrieved at defined time interval, dipped in distilled water three times to remove excess SVF and vaccum dried in order to obtain dry weight. The percentage remaining (R%) of the polymeric samples were calculated [23] using the formula 6,

$$R\% = 100 - \left[\frac{W_i - W_t}{W_i} * 100\right] eqn\ (6)$$

Where, W_i is the initial dry weight of polymeric blends (10 mg) and W_t is the dry weight of polymer sample at respective time interval.

Table 3.2 Compositions of SVF in distilled water

Compositions of SVF in water	Quantity (g/L)
Potassium hydroxide	1.40
Calcium hydroxide	0.23
Sodium chloride	3.51
Bovine Serum Albumin (BSA)	0.01
Acetic acid	1.00
Lactic acid	2.00
Glycerol	0.16
Glucose	5.00
Urea	0.40

3.2.2.7 Morphological analysis of polymeric blends

Morphological analysis of the polymeric blends was carried out using scanning electron microscope (SEM, EVO, ZEEIS, Carl Zeiss SMT AG, Oberkochen, Germany) at an accelerating 20 kV voltage. The polymeric samples were sputter coated with gold and successively examined under SEM. Surface topology of the polymeric blends was evaluated using atomic force microscopy (AFM, Agilent 5500 Scanning Probe Microscope) by intermittent contact mode. The force constant and the resonance frequency of AFM tip was 48 Nm^{-1} and 146-236 kHz respectively having tip radius and stiffness of 10 Nm and 40 Nm^{-1} respectively

3.2.2.8 *In vitro* toxicological assay

In vitro cytotoxic effects of each polymeric blend were investigated in HeLa cell line. The cells were maintained in minimal essential media supplemented with 10% FBS, 1x non- essential amino acid solution, and 1x antibiotic-antimycotic solution with regular passage upon 90% confluency. The cells were seeded in 96 well plates at a concentration of 5X 10^4 cells/well and incubated overnight for cell adhesion. Thereafter the cells were treated with the conditioned media which was prepared by dissolving polymeric film in media at a concentration of 1mg/mL for 24 h followed by cell viability analysis using standard MTT assay. Viability percentage (V%) of vaginal primary cell lines were calculated using the equation (7)

$$V\% = \left[\frac{A_t}{A_c}\right] * 100 \ eqn \ (7)$$

where, A_t is absorbance of the test at 590 nm and A_c is absorbance of control at 590 nm [24].

Furthermore, live/dead staining was also performed using calcein AM/ethidium homodimer as instructed by the manufacturer. The imaging was performed using fluorescence microscopy (Olympus X171).

3.2.2.9 *In vitro* spermicidal activity of polymeric blends

Human semen samples were obtained from healthy individuals following 2-3 days of abstinence. Sterile polyethylene containers were used to collect and transfer the semen samples. Semen samples were allowed to liquefy followed by diluting (1:10) in HEPES buffer supplemented with 10% Bovine Serum Albumin (BSA). The diluted semen samples were incubated in conditioned media for 15 minutes [25]. Control samples were incubated with PBS. *In vitro* spermicidal activity of the polymeric films was evaluated as per protocol defined elsewhere [25] with slight modification.

3.2.2.10 *In vivo* toxicological study

3.2.2.10.1 Maintenance of experimental animals

Adult female Sprague-Dawley rats were procured and maintained in an ambient environment containing 25 ± 2 ℃ and $50 \pm 15\%$ as relative humidity. Normal photoperiod of 12 h dark and light was maintained inside the animal house. The experimental animals were provided with sterilized food and water *ad libitium*. Estrus cycles for the experimental animals were examined through vaginal lavage. The experimental procedure for *in vivo* toxicological study was approved by institute animal ethical committee. Two groups of experimental animals each group containing 5 animals were randomly selected.

3.2.2.10.2 Intravaginal administration of polymeric blend

The experimental animals were anesthetized using ketamine and xylazine (75 and 100 mg/Kg intraperitoneal injection respectively). The anesthetic stage was confirmed by toe withdrawal reflex. About 4% (w/v) of the respective polymeric blend was dissolved in sterile PBS in aseptic condition. Anesthetized animals which received 200 μL of polymeric blend solution were included as treated and control animals received 200 μL of sterile PBS . All the animals were consecutively treated with polymeric blend solution for four days in order to complete a single estrus cycle. After completing the treatment all the experimental animals were sacrificed by using chloroform inhalation. Blood from both control and treated animals were collected for hematological and blood biochemical study. Organs like kidney, spleen, liver, heart, and lungs were isolated for histological studies. The vaginal tissues of the experimental animals were aseptically removed and washed three times in 0.9% (w/v) saline and fixed using 4% formalin. Formalin-fixed tissues were subjected to gradient dehydration in ethanol (from 70%to 100%). Dehydrated tissue samples were embedded in paraffin [26, 28].

3.2.2.10.3 Haematology and blood biochemical study

Throughout the study period, all the experimental animals were daily observed for signs of abnormal behavioral changes, reaction to treatment or ill health. Animals were also observed for signs of changes in skin, fur, eyes and general activity. Blood samples from the experimental animals were collected through cardiac puncture of anesthetized animals prior to sacrifice. Eosinophil (E), haemoglobin (HBG), lymphocyte, mean corpuscular hemoglobin (MCH), mean corpuscular hemoglobin concentration (MCHC), mean corpuscular volume (MCV), monocyte, neutrophil, platelets, total red blood cell

count (T-RBC), total leucocyte count (TLC) and packed cell volume (PCV) or haematocrit (HCT) were estimated for standard hematology marker. Glucose (GLU), cholesterol (CHOL), triglycerides (TG), total proteins (TP) and albumin (ALB)], blood urea nitrogen (BUN), creatinine (CRTN), phosphorus (P), calcium (CA) and urea were estimated to elucidate general metabolic functions. Alkaline phosphatase (ALP), alanine aminotransferase (ALT), aspartate aminotransferase (AST) and total bilirubin (TBL) were examined for liver function.

3.2.2.10.4 Histological and Immunohistochemical examination

Paraffin tissue sections of approximately 3 μm were double stained with hematoxylin and eosin by following the manufacturer's protocol. For the purpose of immunohistochemical staining, the tissue sections were deparaffinized, hydrated and exposed to the process of antigen retrieval using EZ-Retriever System V.2; BioGenex, San Ramon, California, USA for 20 min in 0.1 M sodium citrate buffer (pH 6.0). The tissue sections were immunostained by the chromogenic method. Primary antibodies like Anti-ER-α, anti-Cyclin D1, anti-VEGF and anti-CDk4 (Santa Cruz Biotechnology, CA, 1:250) were used for immunohistochemistry. Goat anti-rabbit HRP-conjugated secondary antibody (1:1000) was used. Immunohistochemical scoring was performed following the protocol explained before in **Chapter 2.10.4**.

3.2.3 Results and discussion

3.2.3.1 Rheological characterization

Rheological characterization of the PVOH and other polymeric blends showed a steady increase in the viscosity with an increase in the shear rate (Figure 3.2A). Sample

R0 showed the least viscosity, followed by R0.5, R1.0, and R1.5. Such an increase in viscosity could provide a hint regarding the intermolecular interaction between the polymers. On the contrary, sample R2 showed a decreased viscosity than that of sample R1.5. Similar flow behavior was observed in frequency sweep curve. Both, storage and loss modulus of the polymeric blends had ascending trend till R1.5. At higher concentration of RISUG® (R2), the polymeric blends attained the saturation reaction point which may alter the rheological parameters of the corresponding polymeric blend. The slopes of the linear regression of angular frequency (ω) against elastic (G') and viscous (G") moduli (Figure 3.2A, B) helps to mathematically calculate the viscosity of gels through following the power type affiliation using the formula,

$$G' \, or \, G'' \, = \, K\omega^n \, eqn \, (8)$$

Where K is the intercept and n is the slope of the equation (8). The true gel is considered by the slope of the power law model having a positive value. In our case also, all the polymeric blends had positive slopes which confirm all of them are true gel having viscous nature (Table 3.3). Generally it is explained that, the homogenisity of any polymeric mix or solutions can be pervaded using Cole-Cole plot. Cole-Cole plot is the graphical representation of G' values versus G" values. The slope value of the plotted graph of G' versus G" for the polymeric solutions at about 2 signifies that, the polymeric solution is homogenous. The slope value lesser that 2 signifies that the polymeric solutions or mix exhibit heterogenesity of the polymeric mix. In our experimentation results of the Cole-Cole plot (Figure 3.2C) depicted that all the polymeric blends except R1, had a slope value of 2, thereby indicating homogeneity in their solutions. For, sample

R1, the slope value of 1.77 was observed which may be due to greater intermolecular hydrogen bonding interaction between the polymeric samples [19].

Table 3.3 Rheological Slope values for the polymeric blends

Sample	Slope of ω Vs G'	Slope of ω Vs G"	Slope of G' Vs G"
R0	1.35	0.64	2.07
R0.5	1.41	0.60	2.05
R1	1.42	0.67	1.77
R1.5	1.45	0.57	2.03
R2	1.51	0.60	2.09
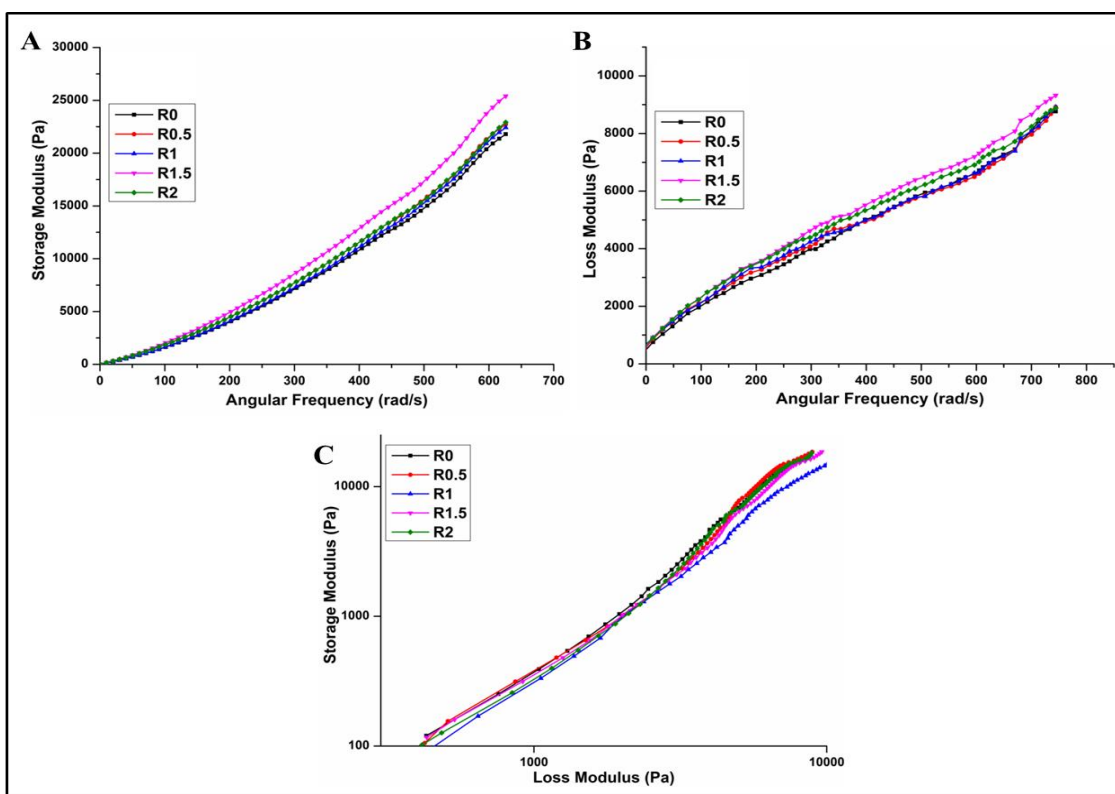
Figure 3.2. (A) Storage modulus of polymeric blends; **(B)** Loss modulus of polymeric blends; **(C)** Cole-Cole plot of polymeric blends

3.2.3.2 Fabrication of RISUG® and PVOH polymeric blend films

The polymeric films blending PVOH and RISUG® were successfully formed. A visual inspection revealed that R0 (without RISUG®) appear more flexible, softer and smoother as compared to those containing RISUG®. Increase in the concentration of the RISUG® resulted in a reduction of the flexibility and smoothness of the polymeric samples. Sample R2 had the roughest surface among all the blends.

3.2.3.3 FTIR spectroscopy

FTIR spectroscopy is an appropriate method to investigate chemical interactions between the molecules of polymeric blends. The IR spectra of virgin PVOH and polymeric films are shown in Figure 3.3B. The specific molecular peak assignments are revealed in Table 3.6. The results showed significant alterations in the carbonyl and CH rocking peaks of RISUG® and PVOH respectively (Figure 3.3a, b). With an increase in the RISUG® concentration, the carbonyl peak of RISUG® at 1716 cm^{-1} in the polymeric blends portrayed a band shift from 1716 cm^{-1} to 1721 cm^{-1} and CH rocking peak of PVOH at 1250.26 cm^{-1} shifted from 1250.26 cm^{-1} to 1233.35 cm^{-1}. Shifting of these peaks clearly specifies the interaction between PVOH and RISUG® via means of intermolecular hydrogen bonding. The maleic anhydride group of RISUG® hydrogel have a strong electronegative oxygen which extends its affinity towards PVOH through hydrogen molecular bonding, where –OH group of PVOH plays the role of proton donor and –COO$^-$ of SMA plays the role as proton acceptor [30]. An in-depth evaluation of these peak shifts revealed that the reaction enthalpy of the polymeric blends is negative as both, carbonyl stretching and CH rocking peaks of IR spectra shifted to lower wavenumber, thereby providing negative values for ΔHs in case of polymeric blends.

This present study comprehended the molecular interaction between PVOH and SMA hydrogels by using Fowkes equation. Fowkes equation is the tool to relate IR associated peak position change with that of enthalpy of the molecular interaction between the individual phase in dual polymeric system like polymeric blends or polymeric composites [4]. Enthalpy of molecular interaction of polymeric blends were identified using the formula (9),

$$\Delta H = 0.236 \times \Delta v \; eqn\,(9)$$

Where, enthalpy of the interacting polymers in dual polymeric system, Δv is the change in the corresponding peak position of functional group of polymer involved in molecular interaction like hydrogen bonding. The change in free energy of the polymeric blend post mixing of two different polymers can be expressed as,

$$\Delta G^{P1} = \Delta H^{P1} - T\Delta S^{P1} \; for \; polymer \; 1 \; eqn\,(10)$$

$$\Delta G^{P2} = \Delta H^{P2} - T\Delta S^{P2} \; for \; polymer \; 2 \; eqn\,(11)$$

In the above discussed equations (9 & 10) the super scripts P1 and P2 corresponds to polymer system 1 and polymer system 2 in dual polymeric system. With the help of equations (10 & 11), the total free energy change in the dual polymeric system can be obtained as,

$$\Delta G_S = \Delta H_S - T\Delta S_S = \Delta H_S - T(\Delta S^{P1} + \Delta S^{P2}) eqn\,(12)$$

Both PVOH and SMA hydrogels will be mutually miscible when the value of ΔH_S falls negative and ΔS_S falls positive in order to promote a thermodynamically favourable reaction between the polymers. This favourable interaction of both the polymers ultimately results in negative value of ΔG_S. Since the reaction enthalpy of the

polymeric blends is negative, both carbonyl stretching along with CH rocking peaks of IR spectra is shifted to lower wave number (Table 3.4, 3.5). The polymeric blend composition provides negative values for ΔH_S. The calculated ΔH_S values for corresponding carbonyl stretching peaks lie in-between the range from 1.891 to 3.990 kcal/mol and the values corresponding to CH rocking peaks lie in-between the range from 0.16 to 1.18 kcal/mol. Increase in the values of ΔH_S also increases the values of ΔG_S. Since the randomness of the dual polymeric blend system grows upon blending, the value of ΔS falls negative for blending of two different polymers. Thus the value of ΔH is a best hallmark for the miscibility of two different polymers. Thus it can be concluded that all the polymeric blends shows good miscibility at all the blend proportions through this thermodynamic calculation. It has been reported that the miscibility of the polymeric blends may be due to intermolecular hydrogen bond between C=O of maleic anhydride and hydrogen group of PVOH.

Table 3.4 Carbonyl peak position shift of RISUG® polymer and corresponding enthalpy of SMA and PVOH interaction in polymeric blends

RISUG (wt)	Wave Number of C=O Stretching (cm^{-1})	Δv of C=O Stretching (cm^{-1})	ΔH (Kcal mol^{-1})
R2g	1721	0	0
R1.5g	1720.31	-0.69	-0.16284
R1g	1718.19	-2.81	-0.66316
R0.5g	1717.63	-3.37	-0.79532
R0g	1716	-5	-1.18

Table 3.5 CH rocking peak position shift of PVOH polymer and corresponding enthalpy of SMA and PVOH interaction in polymeric blends

RISUG (wt)	Wave Number of CH Rocking Band (cm^{-1})	Δv of CH Rocking Band (cm^{-1})	ΔH (Kcal mol^{-1})
R0g	1250.26	0	0
R0.5g	1242.55	-7.71	-1.81956
R1g	1239.57	-10.69	-2.52284
R1.5g	1236.14	-14.12	-3.33232
R2g	1233.35	-16.91	-3.99076
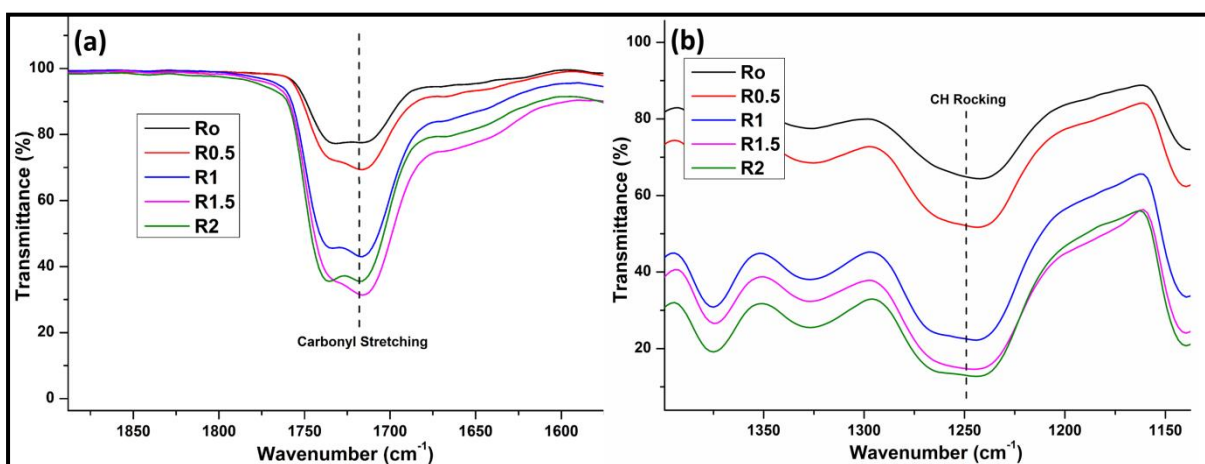
Figure 3.3. (a) Carbonyl peak position shift of RISUG® polymer; **(b)** CH rocking peak position shift of PVOH polymer

Table 3.6 Specific molecular assignments of virgin polymers

Peak wave number (cm^{-1})	Corresponding Functional group
3327	OH stretching of PVOH
2942	CH vibrational stretching of PVOH
1727	C = O stretching vibration of PVOH
1432	CHOH stretching vibration of PVOH
1090	CO vibrational stretching
840	C-C ring and side group vibration of PVOH
3424	OH stretching of sulfoxide group of RISUG®
1724	C=O stretching vibration of RISUG®
1415	Stretching frequency of organic sulftaes

3. 2.3.4 Differential scanning calorimetry

Endothermic peaks of polymeric bends were obtained using DSC (Figure 3.4D) calorimetric parameter values like crystallinity temperature (T_c) and glass transition temperature (T_g) were evaluated thereafter (Table 3.7). The DSC curve of R0 showed a first endothermic peak between 50-150 °C which may be due to the relaxation of crystalline domains of PVOH [31]. This peak may also be correlated with the presence of water molecules in free form in PVOH. However, the peak is not close to boiling point (100 °C) of pure water because less number of free water molecules may be associated with PVOH. The second endothermic peak was observed between 150 °C which might be due to melting and relaxation of crystalline domains of PVOH. Interestingly, upon addition of RISUG® to PVOH, a reduction in T_c of the polymeric blends along with a slight increase in the T_g was observed. The increase in T_g might be attributed to an intermolecular hydrogen bond between the polymeric blends. Again due to this intermolecular hydrogen bonding between PVOH and RISUG, formation of crystallion region within PVOH has been hindered (Table 3.7) resulting fall in T_c in the polymeric blends. The presence of single T_g in all the polymeric blends depicts that the polymeric blends were miscible mixtures. These results reveal about the occurrence of chemical synergy between PVOH and RISUG® at the molecular level, thereby promoting mutual miscibility of both the polymers. The intensity of DSC curves of the polymeric blends showed continuous reduction upon increasing the concentration of RISUG®. This inference may be discussed as the three-dimensional crystal growth of PVOH polymer is hindered by the increased concentration of RISUG® within its molecular chains.

Table 3.7 Crystalization temperature, Glass transition temperature and Crystallinity % properties of polymeric films

Sample	Crystalline %	Tg	Tc
R0	5.39	77	153.81
R0.5	2.21	80	131.80
R1	1.48	80.63	116.83
R1.5	1.03	81.71	116.03
R2	0.958	82.4	116.03

3. 2.3.5 XRD analysis

The X-ray diffractogram showed a single sharp crystalline peak at the 2θ range of 19.3° corresponding to (101) plane was present in all the cases (PVOH and all other polymeric blends) (Figure 3.4C). However, the addition of RISUG® to PVOH resulted in significant peak broadening and a decrease in the degree of crystallinity (X_c) (Table 3.8). This may be attributed to the intermolecular interactions including hydrogen bonding as discussed previously in the DSC data. Initial increase in crystalline size may be due increased hydrogen bonding between RISUG and PVOH, but overall crystallinity decreases for the same reason.

Table 3.8 XRD results of the polymeric films

Sample	Xc %	C_s	r	d
R0	84.82	1.76	5.74	4.59
R0.5	80.14	1.98	5.85	4.68
R1	79.76	1.76	5.81	4.65
R1.5	79.42	1.57	5.80	4.64
R2	75.56	1.57	5.77	4.62

3. 2.3.6 Morphological analysis of polymeric blends

The morphological micrographs revealed the presence of single phase morphology in all the samples without any evidence of phase separation, agglomeration

or precipitation, especially in the polymeric blends (Figure 3.5). This, in turn, validated out FTIR, XRD and DSC analysis regarding the complete miscibility of both the polymers in all proportions. However, there was a visual increase in the surface roughness with the increase in RISUG® concentration. To validate this we performed AFM analysis (Figure 3.5). The surface of polymeric blends provides increased roughness with increasing the concentration of RISUG®. In general, AFM tapping mode data was used to assess the distribution homogeneity of H-bond of polymeric blends [32, 33]. The regions of H-bonds on the surface of polymeric blends can be characterized by the spatial variations. These spatial variations occur due to the interaction of the AFM tip with the polymeric surfaces in which the interaction is longer with the softer material that results in dark color phase images and H-bond regions possess bright color phase images. The PVOH polymer surface provides dark color phase images whereas the bright colored phase images started developing in the polymeric blends with sample R2 showing the most bright colored phase images. Increased adhesion of RISUG® polymer through intermolecular interactions increases the roughness of the polymeric blends was evidenced by these observations.

3. 2.3.7 *In vitro* degradation study

Polymer degradation parameter is the important factor in order to establish the polymer as vaginal formulation. *In vitro* degradation study revealed significant alteration in the degradation kinetics of the polymeric blends (Figure 3.4E). The virgin PVOH polymer (R0) showed a complete degradation within 10 h of incubation in SVF. Interestingly, upon addition of RISUG®, there was a significant reduction in the rate of degradation of the polymeric films with R0.5 and R1 showing complete degradation in 13

and 19 h respectively. The polymeric blends, R1.5 and R2 did not degrade completely even after 30 hours of incubation. This could be explained in terms that the polymeric blends, R0.5 and R1 established a loose network architecture that resulted in their faster degradation than R1.5 and R2. Furthermore, R1.5 and R2 had a larger proportion of RISUG® that restricted the flow of solvent molecules into their three-dimensional architecture, thereby resisting the degradation of the polymeric blends. In accordance with the *in vitro* degradation study, sample R1.5 and R2 was neglected for cytotoxicity studies since vaginal contraceptive films reciding in female vagina may leads to discomfort to the female individuals.
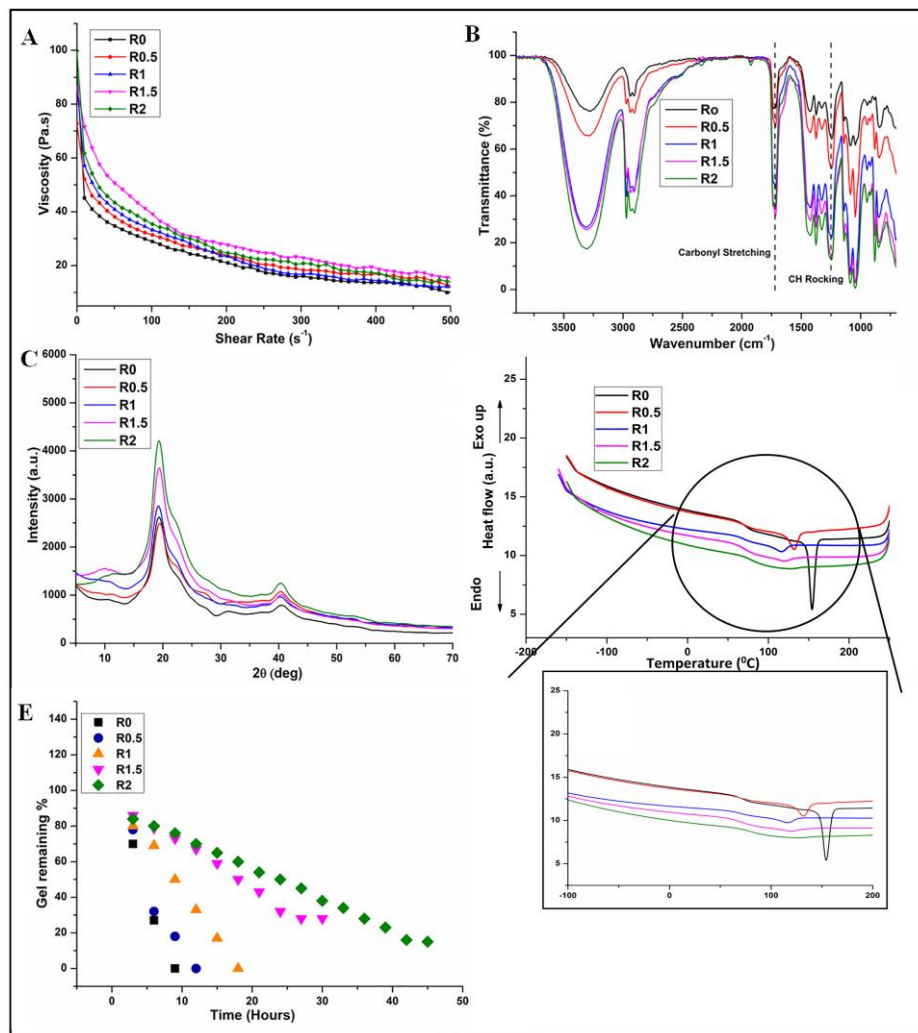
Figure 3.4. Physico-chemical characterization of the polymeric blends. (A) Viscosity vs. shear rate for the polymeric samples. (B) FTIR spectroscopic profile for the polymeric films. (C) XRD profile for the polymeric films. (D) DSC profile of the polymeric films. (E) *In vitro* degradation profile for the polymeric films
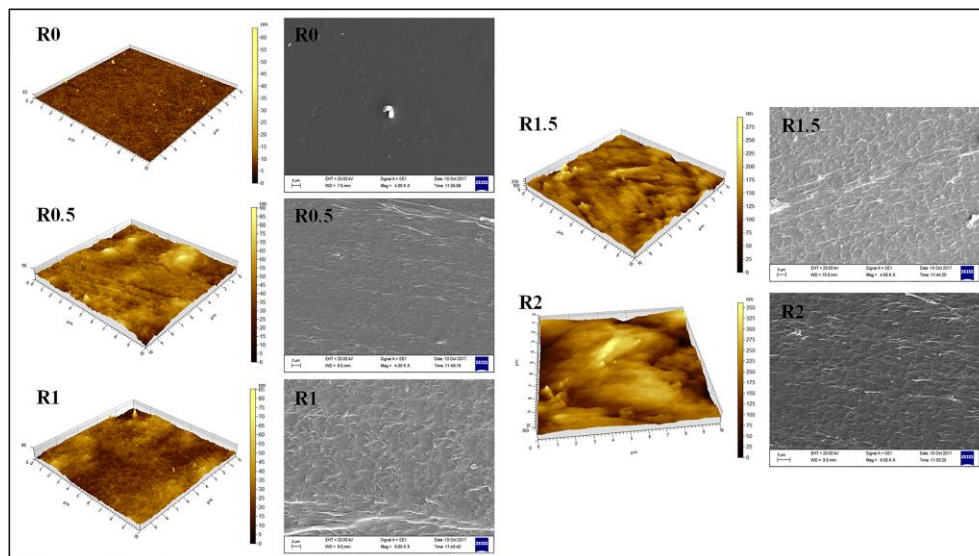
Figure 3.5. Representative images of atomic force microscopy (AFM) and scanning electron microscopy (SEM) of the polymeric films. AFM profile for all the samples was obtained for an area of 100 µm^2. The SEM micrographs have the scale bar of 3 µm.

3.2.3.8 *In vitro* cytotoxicity, cellular morphological and spermicidal activity of polymeric blends

In vitro cytotoxicity assay using MTT assay revealed that neither of the polymeric blends showed any significant toxicity. Percentage viability in case of R0, R0.5, and R1 were **97%, 95% and 92% respectively** with respect to tissue culture plate. To further validate our results, we performed calcein/ethidium homodimer staining. Fluorescent micrographs revealed no significant increase in the number of dead cells in comparison to control (Figure 3.6A). The cells retained their normal spread morphology in all the cases (control and treated). Further, we checked for the spermicidal activity of the blend films. The results revealed significantly high number dead sperms (PI positive) in semen samples treated with R1 followed by R0.5 and R0 (Figure 3.6B). These results confirm that RISUG® retained its spermicidal activity even after it was blended with PVOH in the

films. Based on these results we used sample R1 to check it's *in vivo* biocompatibility

and hemocompatibility in adult female Sprague-Dawley rat models.
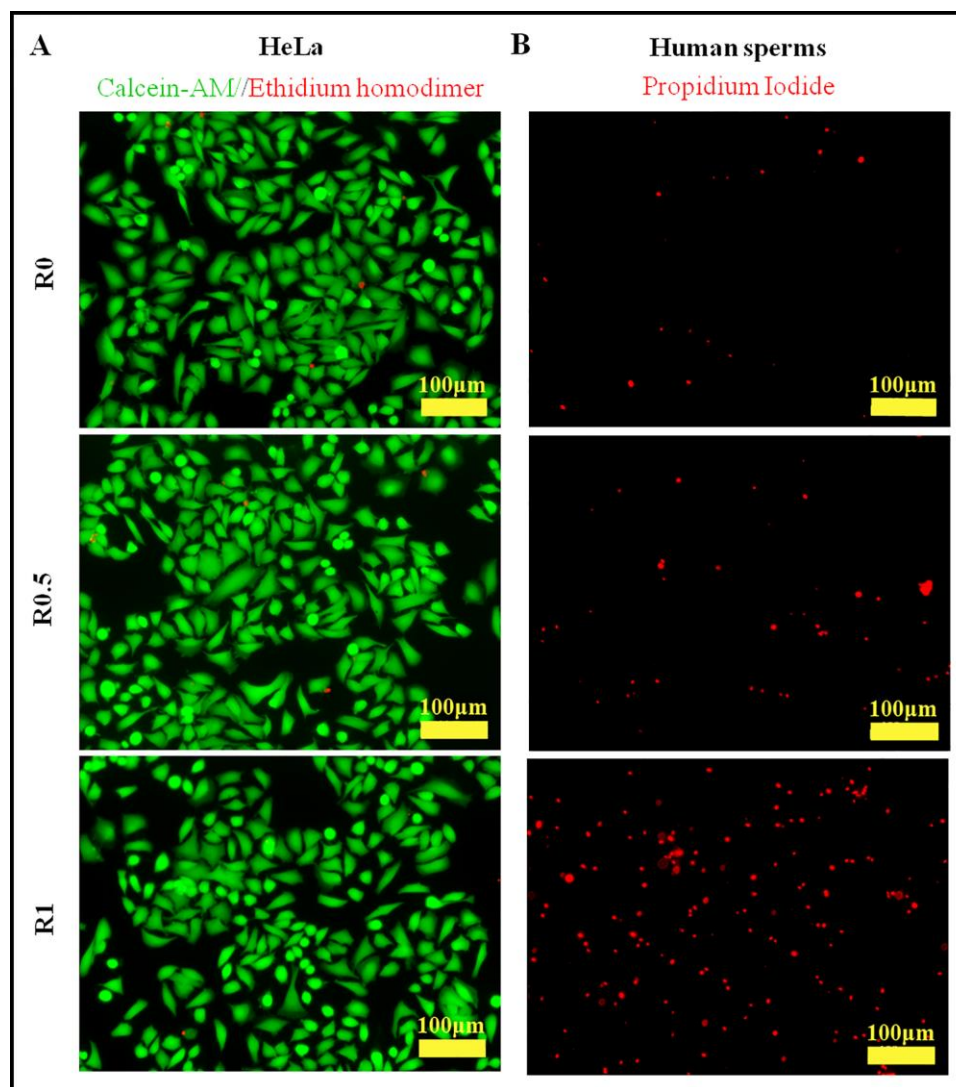
Figure 3.6. (A) *In vitro* biocompatibility evaluation of the polymeric blends in HeLa cells using calcein-AM/ethidium homodimer-1 based live/dead assay. (B) *In vitro* sperm killing efficiency of the polymeric films using propidium iodide staining. The scale bar represents 100 μm.

3. 2.3.9 *In vivo* toxicological study

3. 2.3.9.1 Haematology and blood biochemistry

Upon regular intravaginal administration of polymeric solution for four consecutive days, the safety of the fabricated polymer was assessed. Both the treated and control groups did not show any variations in their general health and behavior. The hematological studies showed no significant changes in the critical blood test analysis, like platelets, WBC (TL) and RBC (TR) in control and treated group. In addition, no alterations in the levels of AST, ALP, and bilirubin were observed in the treated set as compared to control. General metabolic markers including glucose, urea, albumin, creatinine, phosphate, calcium, cholesterol and triglyceride also did not change significantly in trated set compare to control. These results together confirm haemocompatibility of blended film (Figure 3.7A, B).

3. 2.3.9.2 Histological studies to determine organ pathology

Further, we evaluated the histopathological alterations in the architecture of organs like heart, kidney, liver, spleen, and lungs (Figure 3.7C). No morphological changes like infiltration congestion or of interfibrillar hemorrhages in the heart tissue sections were observed. Both control and treated animal lungs have shown well distributed granulated pneumocytes and flat alveolar cells. The normal prominent nucleus was observed in hepatic parenchymal cells in both control and treated animals. The kidney of both control and treated animals has not shown any signs and symptoms of fibrosis or inflammation. The parenchymatic cells of the kidney have shown the good orientation of cortex and medulla in treated animals when compared with control. The well-oriented framework of reticular fibers smooth muscles projected inwards in the

spleen of both control and treated animals were observed. These results together confirm that the polymeric solution did not show any toxicological effect to organs of the treated animals when compared to the control.
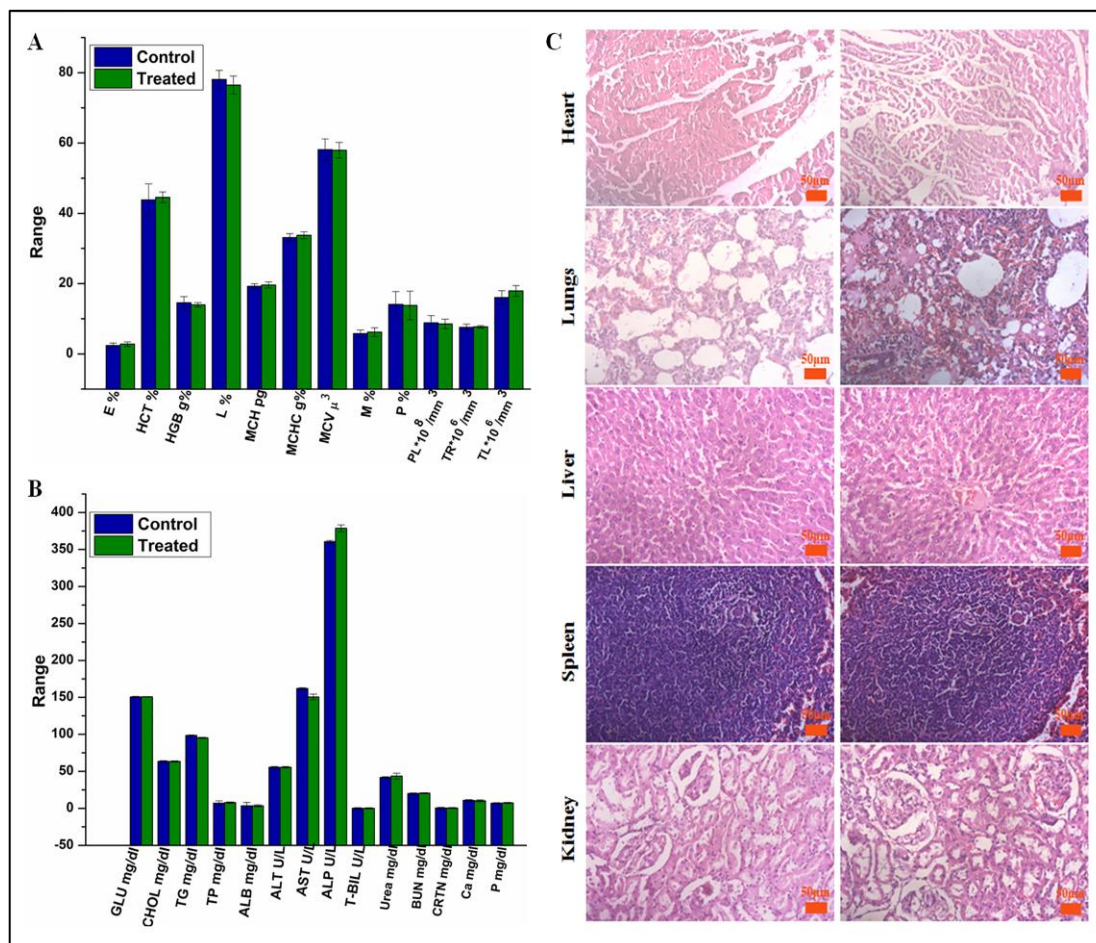
Figure 3.7. (A) Haematological and (B) serum biochemical parameters of control and treated groups of rats after 4 days of sample injections. (C) Histological images of the heart, lungs, liver, spleen, and kidney from control and treated groups of rats after 4 days of sample injections to evaluate organ pathology. The scale bar represents 50 μm.

3. 2.3.9.2 Histological and immunohistological observation of vaginal tissues

Upon evaluation of the vaginal tissue from both the groups, we found no observable difference in their architecture with similar epithelial layer thickness and tissue weight. A well-established stratum corneum (arrowhead) along with large anuclear

cornified epithelium (CE) were observed in both control and treated tissue samples. In both and control tissue sections, dehiscence of stratum corneum occurred without any significant difference, thereby exposing the underlying stratum granulosum (SG) which releases a number of cornified epithelial cells into the lumen of vagina [27]. We further evaluated the expression of estrogen-responsive genes including ER-α and VEGF within the vaginal epithelium using immunohistological studies (Figure 3.8). The results did not reveal any evidence of implant oriented variations in their expression in both the groups [28]. Change in ER-α responsive genes expression may result in tissue irritation and tissue aberration but the histochemical evaluation provided an inference that the polymeric blend has not shown any significant level of toxicity in vaginal epithelial tissues.
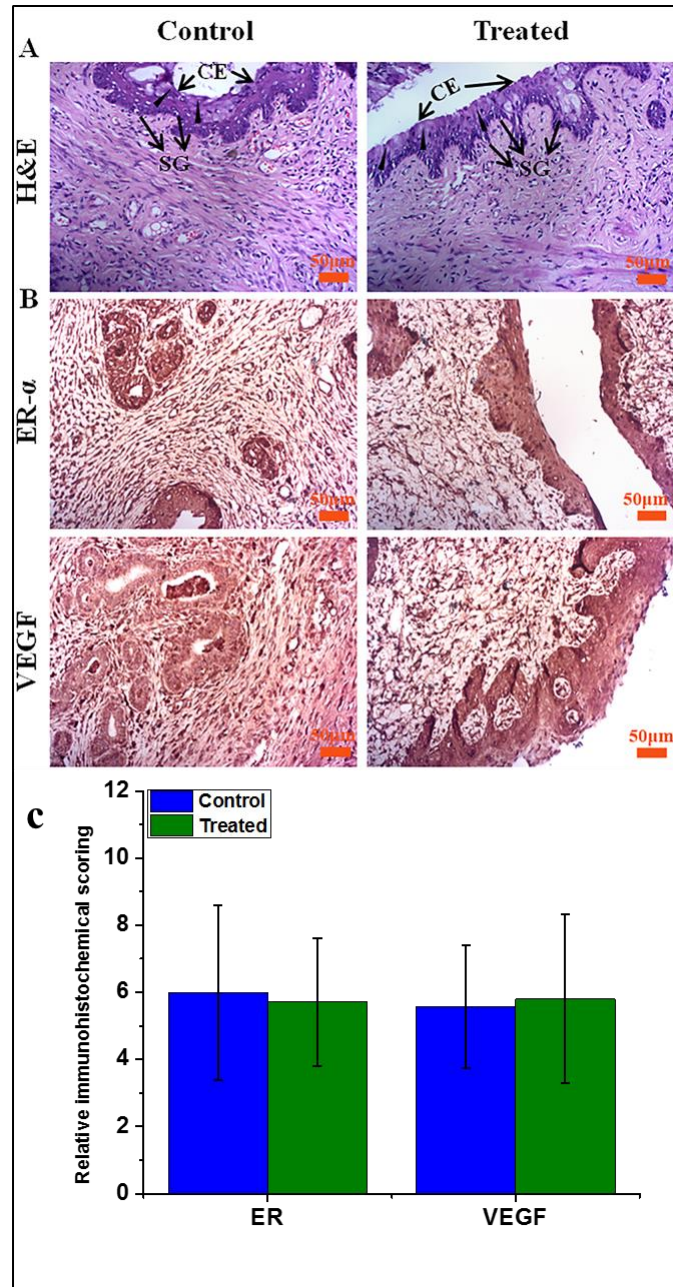
Figure 3.8. (A) Histological evaluation of the vaginal tissue sections derived from control and treated rats. CE and SG represent large anuclear cornified epithelium and stratum granulosum present in the vaginal tissue respectively, while the arrowheads show the presence of well-established stratum corneum. The scale bar represents 50 μm. (B) Immunohistological staining of the vaginal tissue sections from control and treated groups against estrogen receptor α (ER-α) and VEGF. The scale bar represents 50 μm. (C) Immunohistochemical scoring of ER and VEGF immunostained images.

3.2.4 Conclusions

The authors would like to conclude that from the present research work that the SMA based polymeric hydrogel RISUG® can also be formulated as non-hormonal vaginal contraceptive film by blending with PVOH polymer at suitable above explained concentration. The future work of the research team will focus on *in vivo* release kinetics of RISUG® from polymeric blends post implantation of the polymeric blends in large animals.

5.0 References

[1] F. Bray, A. Jemal, N. Grey, J. Ferlay, D. Forman, Global cancer transitions according to the Human Development Index (2008–2030): a population-based study, The Lancet Oncology, 13 (2012) 790-801.

[2] H.R. Baradaran, B. Hamdela, A. G/mariam, T. Tilahun, Unwanted Pregnancy and Associated Factors among Pregnant Married Women in Hosanna Town, Southern Ethiopia, PLoS ONE, 7 (2012).

[3] O.J. D'Cruz, M.-J. Shih, S.H. Yiv, C.-L. Chen, F.M. Uckun, Synthesis, characterization and preclinical formulation of a dual-action phenyl phosphate derivative of bromo-methoxy zidovudine (compound WHI-07) with potent anti-HIV and spermicidal activities, Molecular human reproduction, 5 (1999) 421-432.

[4] O.J. D'Cruz, T.K. Venkatachalam, F.M. Uckun, Structural requirements for potent human spermicidal activity of dual-function aryl phosphate derivative of bromo-methoxy zidovudine (compound WHI-07), Biology of reproduction, 62 (2000) 37-44.

[5] O.J. D'Cruz, F.M. Uckun, Novel derivatives of phenethyl-5-bromopyridylthiourea and dihydroalkoxybenzyloxopyrimidine are dual-function spermicides with potent anti-human immunodeficiency virus activity, Biology of reproduction, 60 (1999) 1419-1428.

[6] O.J. D'Cruz, T.K. Venkatachalam, F.M. Uckun, Novel thiourea compounds as dual-function microbicides, Biology of reproduction, 63 (2000) 196-205.

[7] S. Klebanoff, Effects of the spermicidal agent nonoxynol-9 on vaginal microbial flora, Journal of Infectious Diseases, 165 (1992) 19-25.

[8] O.J. D'Cruz, S.H. Yiv, F.M. Uckun, GM-144, a novel lipophilic vaginal contraceptive gel-microemulsion, AAPS PharmSciTech, 2 (2001) 4-13.

[9] J. Aggarwal, V. Prabha, Contraceptive effect of sperm-agglutinating factor isolated from Staphylococcus aureus in mouse, BJOG, 113 (2006) 1039-1043.

[10] N.D. Digenis GA, Mohammadi F, Darwazeh NB, Anwar HS, Zavos PM, Novel Vaginal Controlled-Delivery Systems Incorporating Coprecipitates of Nonoxynol-9, Pharmaceutical Development and Technology, 4 (1999) 421-430.

[11] R.K. Jain, A. Jain, J.P. Maikhuri, V.L. Sharma, A.K. Dwivedi, S.T. Kumar, K. Mitra, V.K. Bajpai, G. Gupta, In vitro testing of rationally designed spermicides for selectively targeting human sperm in vagina to ensure safe contraception, Hum Reprod, 24 (2009) 590-601.

[12] S. Roy, D. Ghosh, S.K. Guha, Polyelectrolyte polymer properties in relation to male contraceptive RISUG action, Colloids Surf B Biointerfaces, 69 (2009) 77-84.

[13] S. Sharma, P. Sen, S.N. Mukhopadhyay, S.K. Guha, Microbicidal male contraceptive—Risug induced morphostructural damage in E. coli, Colloids and Surfaces B: Biointerfaces, 32 (2003) 43-50.

[14] S. Banerjee, S.K. Guha, RISUG: a potential candidate for the entry inhibitor group of antiretroviral drugs, Med Hypotheses, 73 (2009) 150-152.

[15] S.K. Guha, Biophysical mechanism-mediated time-dependent effect on sperm of human and monkey vas implanted polyelectrolyte contraceptive, Asian J Androl, 9 (2007) 221-227.

[16] A.B. Sassi, M.R. Cost, A.L. Cole, A.M. Cole, D.L. Patton, P. Gupta, L.C. Rohan, Formulation development of retrocyclin 1 analog RC-101 as an anti-HIV vaginal microbicide product, Antimicrob Agents Chemother, 55 (2011) 2282-2289.

[17] A. Akil, M.A. Parniak, C.S. Dezzuitti, B.J. Moncla, M.R. Cost, M. Li, L.C. Rohan, Development and Characterization of a Vaginal Film Containing Dapivirine, a Non-nucleoside Reverse Transcriptase Inhibitor (NNRTI), for prevention of HIV-1 sexual transmission, Drug Deliv Transl Res, 1 (2011) 209-222.

[18] P. Datta, J. Chatterjee, S. Dhara, Phosphate functionalized and lactic acid containing graft copolymer: synthesis and evaluation as biomaterial for bone tissue engineering applications, J Biomater Sci Polym Ed, 24 (2013) 696-713.

[19] D. Gupta, M. Jassal, A.K. Agrawal, The electrospinning behavior of poly(vinyl alcohol) in DMSO–water binary solvent mixtures, RSC Advances, 6 (2016) 102947-102955.

[20] M. Selvakumar, A. Mahendran, P. Bhagabati, S. Anandhan, Thermodynamic Miscibility and Thermal and Mechanical Properties of Poly(ethylene-co-vinyl acetate-co-carbon monoxide)/Poly(vinyl chloride) Blends, Advances in Polymer Technology, 34 (2015) n/a-n/a.

[21] S. Gaidukov, I. Danilenko, G. Gaidukova, Characterization of Strong and Crystalline Polyvinyl Alcohol/Montmorillonite Films Prepared by Layer-by-Layer Deposition Method, International Journal of Polymer Science, 2015 (2015) 1-8.

[22] M.R.C. Marques, R. Loebenberg, M. Almukainzi, Simulated Biological Fluids with Possible Application in Dissolution Testing, Dissolution Technologies, 18 (2011) 15-28.

[23] S. Nanda, N. Sood, B.V.K. Reddy, T.S. Markandeywar, Preparation and Characterization of Poly(vinyl alcohol)-chondroitin Sulphate Hydrogel as Scaffolds for Articular Cartilage Regeneration, Indian Journal of Materials Science, 2013 (2013) 1-8.

[24] K. Dhaouadi, F. Raboudi, C. Estevan, E. Barrajon, E. Vilanova, M. Hamdaoui, S. Fattouch, Cell viability effects and antioxidant and antimicrobial activities of Tunisian date syrup (Rub El Tamer) polyphenolic extracts, J Agric Food Chem, 59 (2011) 402-406.

[25] A.V. Makarevich, E. Kubovicova, A.V. Sirotkin, J. Pivko, Demonstration of the effect of epidermal growth factor on ram sperm parameters using two fluorescent assays, Veterinární Medicína, 55 (2018) 581-589.

[26] A. Awaad, Histopathological and immunological changes induced by magnetite nanoparticles in the spleen, liver and genital tract of mice following intravaginal instillation, The Journal of Basic & Applied Zoology, 71 (2015) 32-47.

[27] C. Cunha-Reis, A. Machado, L. Barreiros, F. Araujo, R. Nunes, V. Seabra, D. Ferreira, M.A. Segundo, B. Sarmento, J. das Neves, Nanoparticles-in-film for the combined vaginal delivery of anti-HIV microbicide drugs, J Control Release, 243 (2016) 43-53.

[28] A. Chatterjee, U. Chatterji, All-trans retinoic acid protects against arsenic-induced uterine toxicity in female Sprague-Dawley rats, Toxicol Appl Pharmacol, 257 (2011) 250-263.

[29] S. Bag, M. Pal, A. Chaudhary, R.K. Das, R.R. Paul, S. Sengupta, J. Chatterjee, Connecting cyto-nano-architectural attributes and epithelial molecular expression in oral submucous fibrosis progression to cancer, J Clin Pathol, 68 (2015) 605-613.

[30] N.-x. Chen, J.-h. Zhang, The role of hydrogen-bonding interaction in poly(vinyl alcohol)/poly(acrylic acid) blending solutions and their films, Chinese Journal of Polymer Science, 28 (2010) 903-911.

[31] M. Mohsin, A. Hossin, Y. Haik, Thermal and mechanical properties of poly(vinyl alcohol) plasticized with glycerol, Journal of Applied Polymer Science, 122 (2011) 3102-3109.

[32] J. Bhadra, N.K. Madi, N.J. Al-Thani, M.A. Al-Maadeed, Polyaniline/polyvinyl alcohol blends: Effect of sulfonic acid dopants on microstructural, optical, thermal and electrical properties, Synthetic Metals, 191 (2014) 126-134.

[33] G.H. Kim, D. Lee, A. Shanker, L. Shao, M.S. Kwon, D. Gidley, J. Kim, K.P. Pipe, High thermal conductivity in amorphous polymer blends by engineered interchain interactions, Nat Mater, 14 (2015) 295-300.

Chapter 4

Poly-Caprolactone (PCL) and Styrene-Maleic Anhydride blend polymeric formulations as biodegradable Intrauterine contraceptive Device (IUD)

4.1 Introduction

Population growth is the major global socio-economic problem that can have direct or indirect effect on environment, wealth, land-use, health and education of the society. Unintended pregnancy plays a major role for the cause of population increase. The effect of unintended pregnancy has led to unsafe abortion in many countries which ultimately resulted in damage to the health of female individuals and even led to their mortality [1]. Providing effective and reliable methods of contraception plays a vital role in empowering women to have sway over their reproductive lives. As discussed in the earlier chapters, long-acting reversible method of contraceptives like IUD or Intrauterine System (IUS), contraceptive implants and contraceptive injections are considered as effective methods for female contraception, which are reported to have their own side effects to the practitioners [2]. There is a need for developing a new non-hormonal contraceptive in order to encourage the female practitioners to use contraceptive and thus to reduce population explosion.

The present aim of this study is to fabricate a novel biodegradable flexible block copolymeric scaffold grafted with RISUG® for establishing bio-degradable form of IUCD. Implantation of RISUG® in fallopian tube (Chapter 2) is a surgical method that requires cut and stitch in order to achieve non-hormonal contraception by female individuals. Vaginal formulation of RISUG® (chapter 3) polymer can be used as non-hormonal female contraceptive implant only for a short duration of time. By considering these limitations of chapter 2 and 3, this study focuses on developing a new form of female non-hormonal intrauterine implant to provide female contraception for long duration of time. The technical advancement of this present study is that the RISUG®

grafted intrauterine contraceptive implant has complete biodegradable property. Furthermore, the implant could establish long time contraception and can be implanted as similar to commercially existing any form of IUDs. Furthermore this biocompatible RISUG® grafted intrauterine contraceptive implant is biodegradable which does not require any surgical method to remove it [3].

Considerable attraction has been provided to biodegradable hydrogels for past decades for their application in biomedical uses since they do not require any surgical procedures to remove after the system achieves its objective. Furthermore, the rate of degradation can be customized by altering the physico-chemical parameters of the hydrogel system. This alteration in the hydrogel system provides flexibility in fabrication of the biomedical devices blended with target drug or pharmacologically active ingredient to achieve specific goal post implanting the device inside human body. Majority of the polymeric hydrogels uses physical or chemical cross-linking methods to blend natural water-soluble polymers or segmented block co-polymers comprising both hydrophilic and hydrophobic segments. Practice of using segmented block co-polymers is the improved way to regulate the physical and chemical properties of the fabricated hydrogels including their biodegradability [4]. Polyether-polyester block co-polymer contributes major application in fabricating biomedical hydrogels. More particularly poly(ε-caprolactone) (PCL) have been comprehensively investigated in fabricating biocompatible and bio-degradable polymeric scaffolds. The crystallinity factor of PCL inhibits their biodegradability. However, copolymerization of PCL with other monomers is the best way to overcome the problem of biodegradability. Radical crosslinking of PCL with Polyethylene glycol (PEG) terminated by diacrylate (DA) groups provided a

multipurpose tool to have control over the biodegradability and biocompatibility of the crystalline PCL. The present study focuses on fabricating a novel biodegradable flexible block copolymeric scaffold composed of PCL-DA: PEG-DA blend grafted with different concentrations of RISUG®. The fabricated polymeric scaffolds were further investigated for their physico-chemical properties, mechanical property, sperm killing ability, *in-vitro* biodegradability, *in-vitro* and *in-vivo* toxicological property required for the application as new form of implantable non-hormonal biodegradable intrauterine contraceptive device [5].

4.2 Materials and Methods

4.2.1 Materials

Polycaprolactone diol (PCL diol) with average Mn~2,000, benzene anhydrous with 99.8% purity, triethylamine with 99.5% purity, anhydrous grade DMSO were procured from Sigma-Aldrich (Bangalore, Karnataka, India). Acryloyl chloride stabilized with phenothiazine was procured from Merck Millipore, India. Azobisisobutyronitrile (AIBN) synthesis grade was procured from JUNSEI chemicals Japan. Polyethylene glycol diacrylate (PEG-DA) polymers were procured from Sigma-Aldrich (Bangalore, India). All the chemicals procured were used without further purification.

4.2.2 Synthesis of PCL diacrylate (PCL-DA)

PCL diacrylation was performed by following the method described elsewhere [5]. Briefly, 4 mmol of PCL diol was dissolved in anhydrous grade benzene. After completely dissolving PCL diol under magnetic stirrer in round bottom flask, 10 mmol of triethylamine and acryloyl chloride was added to the solution under nitrogen atmosphere. The solution mixture was heated at 80 °C for 3 h with continuous stirring. The reaction solution containing triethylamine hydrochloride as a by-product was separated by filtering the solution. PCL diacrylate was precipitated from the filtrate using cold *n*-hexane. The precipitated product was further subjected to drying in vacuum oven.

4.2.3 Synthesis of RISUG®

RISUG® polymer was synthesised by following the procedure described in chapter 2 section 2.2.1. Briefly, styrene and maleic anhydride monomers were equally mixed in the ratio of 1:1 in a borosil glass bottle. Ethyl acetate (≥99%) was used as a solvent to mix the monomers under pure nitrogen atmosphere. A calculated dose of Gamma irradiation (0.3 Gy/s) was provided to obtain SMA copolymer. The SMA copolymer was precipitated using petroleum ether. The impurities in the polymer were removed using soxhlet distillation process by adding 1,2-dichloroethane. Purified form of Styrene Maleic Anhydride (SMA) copolymer was powdered and kept in sterile glass tubes. SMA was mixed with DMSO (1:2) to get the ultimate product RISUG® [6].

4.2.4 Polymeric scaffold preparation

Calculated amount amounts of PEG-DA and PCL-DA were taken in polypropylene conical tube. Both the diacrylate polymers were dissolved in 5 mL of DMSO. The ratio of PEG-DA and PCL-DA was maintained constant as 20% with determined feed ratio of 7:3 (PEG-DA:PCL-DA). The complete polymer concentration was determined to 2 g. With this fixed amount of PEG-DA:PCL-DA polymer, SMA hydrogel was added at four different concentrations. The compositions of polymeric scaffolds along with their descriptions were given in Table 4.1.

Table 4.1 Compositions of polymeric scaffolds along with their descriptions

Sample description	PEG-DA:PCL-DA concentration	SMA hydrogel concentration
S0	2 g	0
S0.5	2 g	0.5 g
S1	2 g	1 g
S1.5	2 g	1.5 g
S2	2 g	2 g

To the polymeric mixture 0.1% of AIBN was added as an initiator. Immediately after adding initiator the solution was kept inside convection oven holding temperatire of 70 °C for 12 h. The polymeric scaffold formed was removed from the polypropylene tubes and immersed in ethanol solution to remove residual debris for 24 h. The polymeric scaffolds were removed from the ethanol solution and subjected to freeze drying for 36 h after washing in distilled water.

4.2.5 Preparation of Simulated Uterine Fluid (SUF)

By following the standard protocol elsewhere [7] SUF was prepared. The compositions used for the preparation of SUF were given in Table 4.2. The final pH of SUF prepared was adjusted to 7.3 by adding 1M hydrochloric acid.

Table 4.2 Compositions of SUF

Composition Name	Amount (mg/L)
Sodium bicarbonate	250
Sodium dihydrogen phosphate	72
Calcium chloride	167
Potassium chloride	224
Sodium chloride	4970
Glucose	50
Urea	48

4.2.6 Nuclear Magnetic Resonance (NMR) and Fourier Transform Infrared (FTIR) Spectroscopy

Both ^1H and ^{13}C NMR spectrum of the PCL-DA were recorded by 400 MHz Bruker spectrometer using deuterated DMSO (DMSO-d^6) as solvent along with internal standard as tetramethylsilane (TMS). Attenuated total reflectance (ATR) mode FTIR spectra for the nude and polymeric blends were recorded in Nexus-870 FTIR spectrometer. Every spectrum of the corresponding sample were collected and co-added with 1.5 cm^{-1} spectral resolution after 36 scans. Before reporting the results, background spectra obtained using Zinc selenide ATR crystal was subtracted from the sample spectra in the wavenumber region of 4000-400 cm^{-1}.

4.2.7 Differential Scanning Calorimetry (DSC)

Differential scanning calorimeter (Perkin Elmer Pyris Diamond DSC) was used to record the percent crystallinity (C%) and glass transition temperature (T_g) of nude polymers and polymeric scaffolds (S0, S0.5, S1, S1.5 and S2). The polymeric samples were weighed before locking them inside aluminium pans associated with differential scanning calorimeter for scanning the samples. The calorimeter was operated under

controlled oxygen free nitrogen atmosphere from the temperature range of -150 to 250 ℃ and at scanning rate of 10 ℃ min^{-1}. Initial scanning procedure was carried out for all the samples in order to eliminate any residual elemental stress. All the samples were subjected to three thermal runs, heating run (ambient temperature to 150 ℃), cooling run (150 ℃ to ambient temperature) and final heating run (from -150 to 250 ℃). The rate of scanning (10 ℃ min^{-1}) was maintained constant for all the thermal runs. The calorimetric data of second thermal heat run was recorded for further analysis. The % of inaccuracy linked with the measurement of the distinctive temperatures was with $\pm 1\%$. The percent crystallinity for all the polymeric samples were calculated by determining the area under the curve formula for the endothermic DSC curves by using the following equation 1,

$$\%C = \left[\frac{\Delta H_e}{W_F * \Delta H_{e100\%}} \right] * 100 \; eqn \; (1)$$

Where, %C is crystallinity percent, ΔH_e is melting enthalpy of samples (J g^{-1}), W_F is weight fraction of the polymeric samples, the theoretically reported melting enthalpy of pure PCL at its crystalline phase (139.3 J $^{g-1}$) is, $\Delta H_{e100\%}$ [8].

4.2.8 X-Ray Diffraction (XRD) Spectroscopy

XRD is the best tool to identify the crystal structure of the polymeric samples. Variation in the crystallinity of sample polymers due to blending with SMA hydrogel was identified using Philips PW-1710 X-ray diffractometer (Eindhoven, The Netherlands). The crystal monochromator with $\lambda = 1.540598$ Å of CuK$_\alpha$ radiation with accelerating voltage of 40 kV having 20 mA beam current for 10-80° (2θ) angular range was used to accomplish WXRD experiment. The degree of crystallinity (D$_c$) for all the samples were identified by measuring area under the peaks of the crystalline and amorphous peaks using X`pert

highscore plus 2.1 and Origin Pro 8.5 softwares. The calculated values were substituted

in the following equation 2,

$$D_C = [{C_I}/{A_I + C_I}]*100 \; eqn \, (2)$$

Where, D_C is calculated degree of crytallinity, C_I is an integrated intensity of

corresponding amorphous peak and C_I is an integrated intensity corresponding crystalline

peak of the samples. The Full Width at Half Maximum (FWHM) values obtained using

the X`pert highscore plus 2.1software from the diffraction peaks of the samples, which

were used to calculate the average crystallite size (C_s) of all the samples. In addition to

that the interchain distance (r) and interplanar distance (d) for the samples were

calculated using the following equations 3, 4 and 5 [9],

$$r = \frac{5\lambda}{8Sin\theta} \; eqn \, (3)$$

$$d = \frac{\lambda}{2Sin\theta} \; eqn \, (4)$$

$$C_s = \frac{K\alpha}{\beta \, Cos\theta} \; eqn \, (5)$$

4.2.9 Morphological analysis of polymeric blends

The corresponding morphological analysis for the samples was recorded using

Scanning Electron Microscope (SEM, EVO, ZEEIS, Carl Zeiss SMT AG, Oberkochen,

Germany) predominantly at an accelerating voltage of 20 kV. The samples were subjected to sputter coating with gold and consecutively inspected under SEM. Atomic Force Microscopy (AFM, Agilent 5500 Scaning Probe Microscope) using intermittent contact mode was used to evaluate surface morphology for the samples. The AFM tip was having force constant as 48 Nm^{-1} and resonance frequency as 146-236 kHz respectively. The polymeric films were prepared as thin films for subjecting them to perform AFM study at devising tip radius of 10 NM and stiffness of 40 Nm^{-1} [9].

4.2.10 *In-vitro* degradation study

The changes in weight of polymer sample at corresponding incubation time were monitored to investigate the *in-vitro* degradation study for all the polymeric samples. All the polymeric samples were pre weighed (3 g) and incubated in SUF at 37 ℃. The SUF was changed periodically during the experimental procedure. At respective time intervals the polymeric samples were taken out from the SUF and excess simulated fluid was driven out before weighing the sample. The percentage remaining (%S) of the samples were calculated by the equation 6,

$$\%S = \left[\frac{I_W - T_W}{I_W} * 100 \right] eqn\ (6)$$

Where, I_W is the initial weight of polymeric sample (10 mg) and T_W is the weight of polymeric sample at corresponding time interval [6].

4.2.11 *In-vitro* toxicological study

Primary rat uterine cell lines were used to investigate *in-vitro* toxicity of the polymeric samples. The primary rat uterince cell lines having passage number three were used for the study. Primary rat uterine cell lines were isolated from the female Sprague-Dawley by following the method described elsewhere [10] with some alterations. The animals were euthanized by following the ethical guidelines and the uterine horns were removed aseptically. Aseptically removed uterine tissues were washed with Phosphate Buffered Saline (PBS) to remove excess blood and were subjected to enzymatic digestion using 0.2% of collagenase type I mixed in DMEM and Ham's F-12 (Thermo Fisher Scientific, India) at equal proportion. The tissues were incubated for an hour provided with continuous shaking. The enzyme digested tissue samples were neutralized using of DMEM/F12 cell culture enumeration media having 10% of charcoal stripped Fetal Bovine Serum (FBS). The neutralization media is also provided with 1% penicillin-streptomycin, 1 nmol/L β-estradiol, 100 nmol/L progesterone and 10 mmol/L HEPES. In order to collect the viable cells, the tissue suspension was subjected to filtration using 100 and 40 μm strainer respectively followed by centrifugation at 250 g for 5 minutes (4°C). Finally the cells were seeded on to Nun^{TM} EasYFlask^{TM} cell culture flasks (Thermo Fisher Scientific) until desired passage number was obtained. Non adherent cells were removed by periodical changing of the cell culture media. *In-vitro* toxicological study was performed in cell culture enumeration media conditioned with respective polymeric samples and also in normal media without conditioning with polymeric sample. MTT (3[4,5-dimethylthiazol-2-yl]-2,5-diphenyltetrazolium bromide) toxicological assay was carried out to investigate the toxicological effect of polymeric samples on primary cell

lines. The efficiency of viable primary rat uterine cell lines to cleave tertrazolium ring in order to form blue colour was measured calorimetrically to evaluate *in-vitro* toxicity. The polymeric conditioned media was prepared by incubating the respective polymeric samples in cell culture media under aseptic condition (1 mg/mL) and allowing the sample to completely dissolve in the media. The primary rat uterine cell lines were seeded on to 24 well cell culture plates (density of 10,000 cells per well) and incubated under controlled environment provided with 95% air humidified atmosphere and 5% of CO_2 at 37 ℃ for 12 and 24 h. The viability of primary rat uterince cell lines were calorimetrically quantified by measuring the absorbance at 590 nm. The percent viability (V%) of the rat uterine cell lines were calculated by using the equation 7,

$$V\% = \left[\frac{A_t}{A_c}\right] * 100 \; eqn \; (7)$$

Where, A_t is absorbance of media containing cells grown in conditioned media at 590 nm and A_c is absorbance of control (cells grown in normal media) at 590 nm [11].

4.2.12 Quantitative rt-PCR

Twenty four hours grown uterine cell lines cultivated in normal and conditioned media were taken in RNA later (Qiagen) and kept in controlled environment for extracting cellular RNA. With the help of Hipure Kit (Himedia, Mumbai, India) total RNA was extracted from primary rat uterine cell lines and the purity of extracted RNA was verified spectrometrically. By following manufacturer's protocol cDNA synthesis was carried out using High-Capacity cDNA Reverse Transcription kit (Applied Biosystems) in GeneAmp® PCR system 2720 Thermal Cycler (Applied Biosystems). By

using Light Cycler® 480 SYBR Green I Master from Roche Diagnostics GmbH, Mannheim, Germany the reactions of Estrogen Receptor-α (ER-α), Vascular Endothelial Growth Factor (VEGF), Cyclin D1 and Cyclin-dependent Kinase 4 (CDK4) genes were amplified (endogenous control as Glyceraldehyde 3-phosphate dehydrogenase (GAPDH)). About 1 µL of 10 X diluted cDNA template was used in a total reaction volume of 10 µL for amplification. Each set of PCR assay includes a negative control without template [12, 13]. The primers for each gene including their cycling settings are stated in the Table 2.3.

4.2.13 Spermicidal activity of polymeric blends

The spermicidal activity of polymeric blends was performed based on the method explained in chapter 3 section 3.2.3.8.

4.2.14 *In-vivo* toxicological analysis

4.2.14.1 Experimental animal maintenance

Adult female Sprague-Dawley rats were purchased and maintained under ambient environmental condition with $50 \pm 15\%$ relative humidity and 25 ± 2 ℃ temperature. Photoperiod of 12 h dark and light was continued inside the animal house. Sterilized food and water *ad libitium* was provided to the experimental animals. Estrus cycles for the female rats were inspected through vaginal lavage. *In-vivo* toxicological experimental procedure was permitted by institute animal ethical committee. Two experimental groups of animals each containing 5 female rats were arbitrarily selected.

4.2.14.2 *In-vivo* implantation of test polymer inside rat uterus

Surgical anaesthesia was induced using ketamine and xylazine (75 mg/Kg and 100 mg/Kg intraperitoneal injection respectively). The state of surgical anaesthesia was confirmed by toe withdrawal reflex of the animals. The uterine horns of the animals were located by making ventro-median incision in the middle of the last teats with sterile scalpel. The isthmus regions of the uterine horns were held upright with the help of sterile cotton swab. A small key hole was made using blunt end sterile scissor. The polymeric sample was inserted inside the uterine horns of the animals with the help of double lumen central venous catheter kit (Polymed). The incision was closed using 8-0 Vicryl plus absorbable suture. The control non treated animals were injected with sterile PBS. From treated and control groups five animals were euthanized and the uterine tissues were removed aseptically after 142 days by following the *in-vitro* rate of degradation of polymer. The tissues were fixed in 4% formalin solution. The control and treated tissue samples were further processed for both immunohistochemical and histological analysis.

4.2.14.3 Histological and Immunohistochemical study

The formalin fixed tissue samples were cleared using xylene and further dehydrated in graded alcohol solution from 70 to 100% subsequently. The tissue sections were stained using hematoxylin-eosin double staining by following the manufacturer's protocol. The hematoxylin-eosin double stained tissue sections were observed under microscope. The uterine tissue sections were subjected to antigen retrieval procedure using EZ-Retriever System V.2; BioGenex, San Ramon, California, USA in 0.1M sodium citrate buffer (pH 6.0) following the deparaffination and hydration for the purpose of

immunohistochemical analysis. The tissue sections were immunostained by chromogenic method. The primary antibodies used in this study were Anti-ER-α, anti-Cyclin D1, anti-VEGF and anti-CDk4 (Santa Cruz Biotechnology, CA, 1:250). Goat anti-rabbit HRP-conjugated was used as secondary antibody (1:1000) [12].

4.2.14.4 Immunohistochemistry scoring

The immunohistochemical staining was quantitatively measured by scoring the staining intensity of the tissue sections. Ten random areas of the tissue sections were selected to score the stain intensity by a person who does not have any information about the group of the tissue sample. Scoring values were semi-quantitatively allotted from 0 to 10 (0 = the tissues were not stained, 2.5 = less than one third of the total tissue area stained, 5 = only one third of the total tissue area was stained, 7.5 = almost two third of the total tissue area was stained and 10 = more than two third of the total tissue area was stained). For every stained tissue samples, the areas of epithelial, stromal and blood vessel portions were scored separately and the scores of the tissue areas were summed to estimate the mean score value [15].

4.2.14.5 Hematology, blood biochemistry and organ pathology studies

All the animals were observed daily for any change in their behaviour or any signs and symptoms of infection during the treatment procedure. Body weight of each rat was recorded at the beginning and end of the study. In order to perform standard haematological analysis blood samples from all the animals were collected by cardiac puncture from heart of anaesthetized rats afore sacrifice. Regular haematological indicators like Eosinophil, Haemoglobin (HBG), Lymphocyte, Mean Corpuscular

Hemoglobin (MCH), Mean Corpuscular Hemoglobin Concentration (MCHC), Mean Corpuscular Volume (MCV), Monocyte, Neutrophil, Platelets, Total Red Blood Cell Count (T-RBC), Total Leucocyte Count (TLC) and Packed Cell Volume (PCV) or Haematocrit (HCT) were analysed and compared between the control and treated animals. General metabolic function elucidation was analysed by measuring blood biochemical markers like Glucose (GLU), Cholesterol (CHOL), Triglycerides (TG), Total proteins (TP) and Albumin (ALB) for both control and treated group of animals. Kidney function of the control and treated group animals were analysed by measuring the Blood Urea Nitrogen (BUN), Creatinine (CRTN), Phosphorus (P), Calcium (CA) and Urea. Finally Alkaline phosphatase (ALP), Alanine aminotransferase (ALT), Aspartate aminotransferase (AST) and Total Bilirubin (TBL) were analysed to identify the liver function of the control and treated animals. Kidney, Spleen, Liver, Lungs and Heart of both control and treated animals were isolated and stained with hematoxylin and eosin to evaluate implant associated toxicological effect.

4.3 Results

4.3.1 Characterization of PCL Diacrylate

Figure 4.1 A and B shows the qualitative (^{1}H) and quantitative (^{13}C) NMR spectrum of the synthesised PCL-di Acrylates (PCL-DA) to confirm the proposed structure. In figure 1, a small doublet peak at 6.1 ppm (H-1) is assigned to the CH= proton of the acryloyl chloride moieties of the polymerization reaction. A prominent intense signal was received at 3.9 ppm (H-2) corresponding to the methylene proton attached to the oxygen next to the carbonyl group (C=O) of the PCL backbone chain. The combined methylene protons of the main chain (H-3 and H-5) were received at 1.5 with intense triplet peak signal. A peak at 2.2 ppm (H-6) corresponds to the end methylene proton of the main chain and peak at 1.5 ppm (H-4) assigned to the mid methylene proton (−CH$_2$−) of the PCL main chain. 13C NMR spectrum of the synthesized PCL-di Acrylates (PCL-DA) is shown in figure 2.

In figure 2, a convincing intense peak at 173 ppm corresponding to the carbonyl carbon of the PCL main chain (C-1). Likewise, number of intense peaks at 24, 25, 28, 33 and 63ppm were also observed, corresponding to the different carbons of the PCL main chain: (C-2), (C-3), (C-4), (C-5), and (C-6), respectively. The appearance of these all intense peaks from the ^{1}H and ^{13}C NMR spectrums authorises the proposed structure of the synthesised PCL-di Acrylates (PCL-DA) copolymer [16].
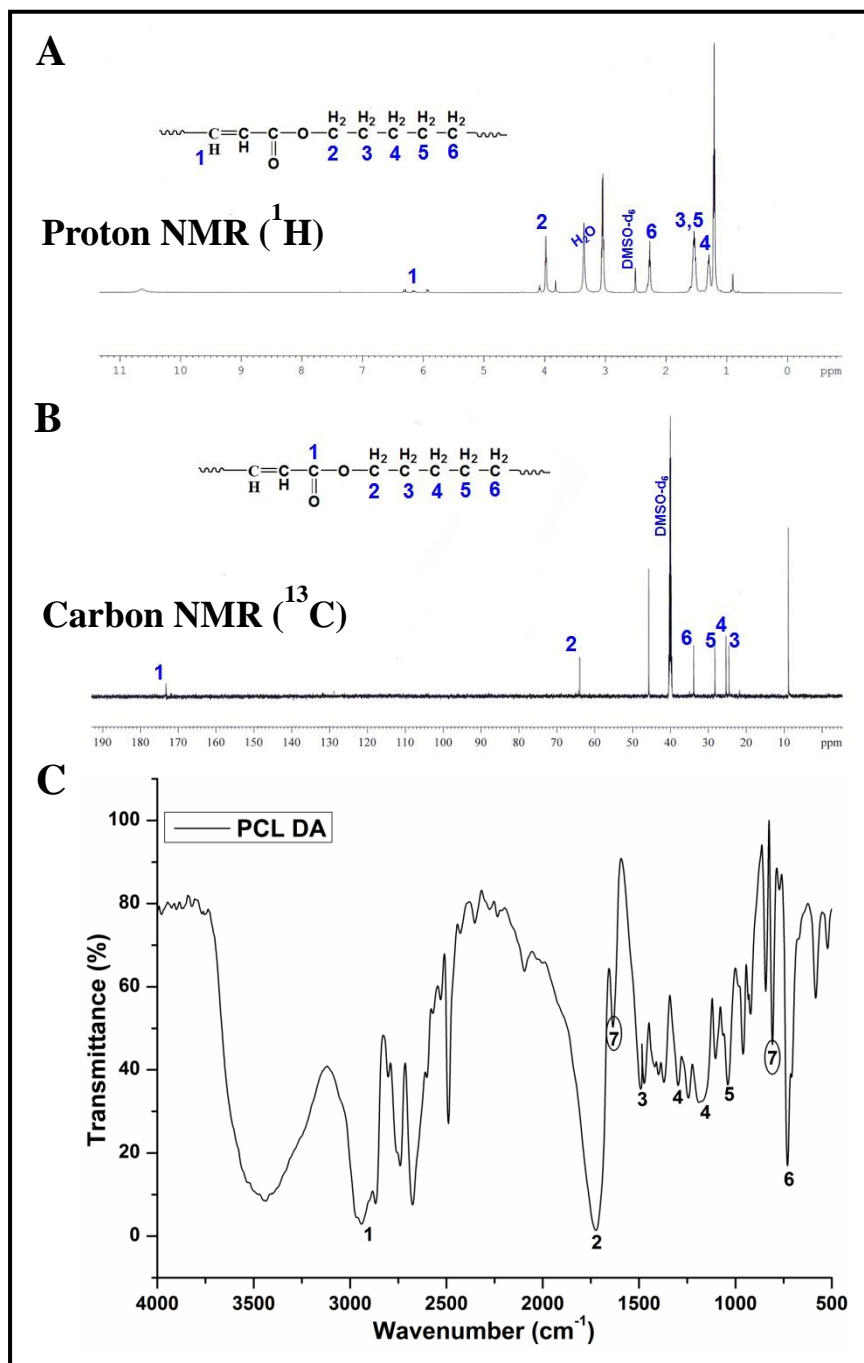
Figure 4.1. Structural elucidation of synthesised PCL-DA polymer (A) ^{1}H NMR spectrum of PCL-DA. (B) ^{13}C NMR spectrum of PCL-DA. (C) FTIR spectroscopy of PCL-DA.
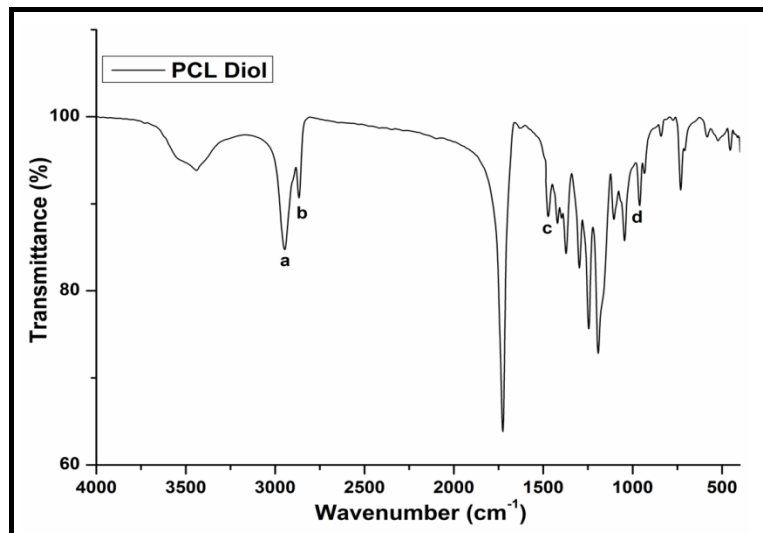
Figure 4.2. FTIR spectroscopy for PCL diol

4.3.2 FTIR Spectroscopy

IR results of PCL-DA, RISUG® and polymeric blends were represented in Figure 4.3.A. The IR peak distributions are in agreement with the reports described elsewhere. The FTIR spectrum of PCL-diol (Figure 4.2) shows spectral peaks a, b which attributes to asymmetrical and symmetrical stretching of C − H bonds. Peak c attributes to CH_2 bending and peak d attributes to C − O − C stretching. The FTIR spectrum of synthesized PCL-DA was similar to previous studies (Figure 4.1.C) which display C − H stretching vibration at peak position 1, C = O stretching at peak position 2, CH_2 bending at peak position 3, (O =)C − O stretching vibration at peak position 4, O − CH_2 stretching bond at its corresponding peak position 5, CH_2 rocking peak position at 6. The process of diacrylation of PCL-diol provided C = C corresponding peak position at 7 [17, 18].

The FTIR spectra recorded for the polymeric blends exhibit well defined peak shifting and peak broadening corresponding to carbonyl stretching of RISUG® polymer and also to the CH rocking of PCL-DA: PEG-DA blend by varying the composition of RISUG® polymer. The decrease in wavenumber was observed by increasing the concentration of RISUG® polymer due to the result of intermolecular interface between the polymers. It was observed that the carbonyl peak at wavenumber (cm⁻¹) 1722 of RISUG® polymer has shifted its appearance towards lower wavenumber as shown in figure 4.3.A for PCL-DA: PEG-DA: RISUG® blends. It was also observed that intermolecular interaction between the polymeric blends resulted in shift in CH rocking peak from the wavenumber (cm⁻¹) regions of 1449 to 1435 (figure 4.3.B). The affinity between different polymeric chains for the polymeric blends was understood using Fowkes equation. The shift in IR peak position due to intermolecular reaction and change in the enthalpy of polymeric affinity due to polymer blending reaction can be interrelated using Fowkes equation 8.

$$\Delta H = 0.236 \times \Delta v \; eqn \, (\,8\,)$$

Whereas ΔH is the enthalpy of affinity between the polymeric blends and Δv is change in peak position. Fowkes equation usually identifies the polymeric affinity in binary phases. Here in this study RISUG® polymer is assumed as one phase and PCL-DA: PEG-DA was assumed as another phase of polymeric system. The shift in wavenumber corresponding to CH rocking and carbonyl stretching resulted in negative enthalpy change which represents that the polymeric affinity happened in thermodynamically favourable environment (Table 4.3 and 4.4). The calculated ΔH

values for corresponding carbonyl stretching peaks lies in-between the range of -0.57 to -0.92 kcal/ mol. The ΔH values corresponding to the peak shift of CH rocking falls in-between the range of -9.44 to -3.29 kcal/ mol. As the negative values for calculated ΔH acts as a good indicator for the polymeric miscibility it was understood that these polymeric blends shows good compatibility at different blending ratios used in this work. This compatibility or miscibility of the polymeric blends may be due to the intermolecular hydrogen bond between the polymeric blends [9].
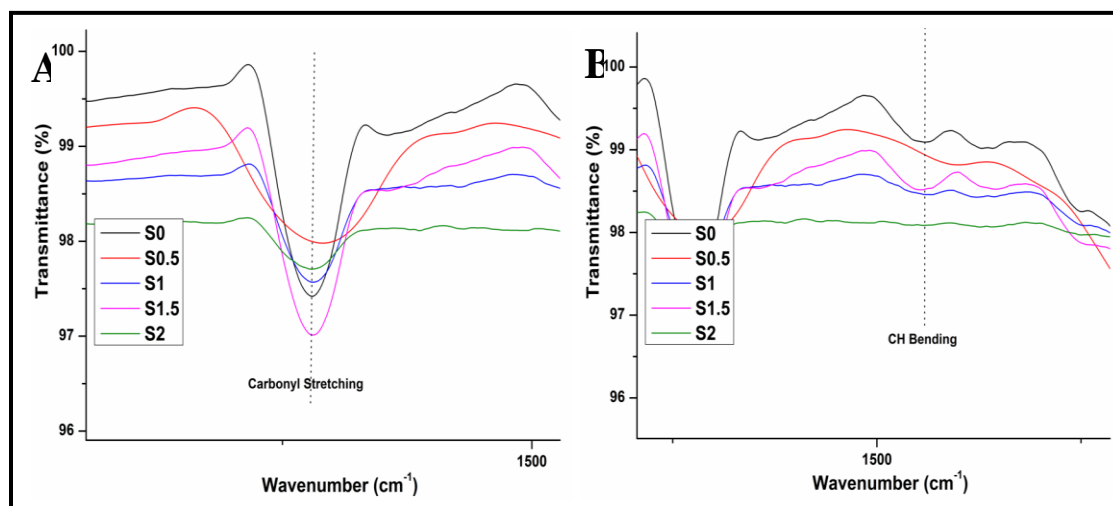
Figure 4.3. (A) Carbonyl stretch in FTIR spectrum. (B) CH bending in FTIR spectrum

Table 4.3 Shift of Carbonyl Stretching Peak in FTIR spectrum of polymeric blends

RISUG (wt)	Wave Number of C=O Stretching (cm-1)	Δ V of C=O Stretching (cm-1)	ΔH (Kcal mol-1)
S2g	1722.66	0	0
S1.5g	1720.21	-2.45	-0.5782
S1g	1719.25	-3.41	-0.80476
S0.5g	1715.47	-7.19	-1.69684
S0g	1718.77	-3.89	-0.91804

Table 4.4 Shift of CH bending Peak in FTIR spectrum of polymeric blends

RISUG (wt)	Wave Number of CH Rocking Band (cm-1)	Δ V of CH Rocking Band (cm-1)	ΔH (Kcal mol-1)
S0g	1449.26	0	0
S0.5g	1409.24	-40.02	-9.44472
S1g	1439.14	-10.12	-2.38832
S1.5g	1436.24	-13.02	-3.07272
S2g	1435.28	-13.98	-3.29928

4.3.3 Differential scanning calorimetry

The melting endotherm along with crystallization temperature of the individual polymers was shown in figure 4.4.C and D. PCL-diol when encapped with acrylate groups at its terminal end reduces both the melting temperature (T_m) and crystallization temperature (T_c). Introducing acrylate group in to the PCL-diol backbone may provide flexibility to the polymer that result in reduction of sharp thermal peaks. The calorimetric values like T_c, T_m, ΔH (heat of fusion), X_c (percent crystallinity) for the polymeric blends were calculated (Table 4.5). By increasing the concentration of RISUG® polymer shift in calorimetric values towards lower temperature was observed. The T_g of the polymeric blends almost falls under the same range which infers that the polymeric blends were equally miscible at all the proportions. The values of T_c, T_m and ΔH had shown significant difference with increasing the concentration of amorphous RISUG® polymer. This may be due to the ability of RISUG® polymer to hinder the crystallization property of PCL-DA: PEG-DA polymeric blend. The polymeric blends tends more towards the region of amorphous region which may be due to (i) inhibition of polymeric backbone chain mobility, (ii) increasing the concentration of amorphous polymer, (iii)

intermolecular interaction between the polymeric blends which may interfere with the free energy nucleation of the polymers, (iv) development of spherulite morphology due to the competition between amorphous and crystalline polymer concentrations which may diffuse the amorphous polymeric materials towards the interfibrillar region. It was observed that T_c of the polymeric blend decreases with increasing the concentration of RISUG® polymer and at higher concentration of RISUG®, T_c tends to vanish. This change observed in T_c may be due to the property of polymeric blends that polymeric blends tends to attain randomness with increase in the concentration of amorphous segment of blend ie RISUG® polymer. The increased concentration of amorphous RISUG® polymer may disturb the T_c of the polymeric blends that results in the disappearance of crystallization peak.

The miscibility of the polymeric blends can also be evidenced by the shift of T_m value. This may be due to the addition of amorphous RISUG® polymer which may disturb the three-dimensional crystal growth of PCL-DA: PEG-DA polymeric blend and thus dropping the lamellar thickness. Furthermore T_m is influenced by T_c in a polymeric system. It is evident that RISUG® polymer reduces the T_c of PCL-DA: PEG-DA that in turn reduces the lamellar thickness and melting property of the PCL-DA: PEG-DA polymeric blend. Both morphological and thermodynamic effect may also contribute to the reduction of T_m of polymeric blend system. As per the mechanism of polymeric miscibility both chemical potential and crystalline polymer free energy decreases with increase addition of amorphous polymer in the polymeric blend system. This reaction may lead to reduction in melting temperature of subsequent miscible PCL-DA: PEG-DA: RISUG® polymeric blends. The polymeric blend R2 displays increase in the T_m in the

DSC thermogram. This may be due to the saturated level of intermolecular interaction between the polymeric blends. The intermolecular reaction gets saturated above 1.5g of RISUG® concentration which shows shift in the value of T_m towards higher temperature [9, 19].

Table 4.5 Glass Transition, Crystallization, and Melting Characteristics of polymeric blends

Sample	X_c	Tg	Tm	T_c
S0	1.7	-36.6	32.5	-21.0
S0.5	1.1	-37.3	31.5	-11.5
S1	0.8	-37.5	31.3	-17.2
S1.5	0.7	-37.8	30.0	-20.4
S2	1.7	-38.2	34.5	-23.5

4.3.4 XRD analysis

XRD peaks for the polymeric blends were shown in Figure 4.4.B. The polymeric blends show XRD peaks at 21.5° and 23.5° of 2θ values that corresponds to (110) and (200) PCL crystallographic planes. The calculated crystallographic values like degree of crystallinity (D_c), crystallite size (C_s) interchain distance (r) and interplanar distance (d) were calculated using respective equations (Table 4.6). A significant change in the D_c was observed by increasing the concentration of RISUG® polymer. The D_c values got reduced upon increasing the concentration of RISUG® polymer which may be due to the intermolecular interaction between the polymeric blends which tends towards amorphous nature. The values of r and d were relatively similar which shows the equal miscibility of the polymeric blends [20].
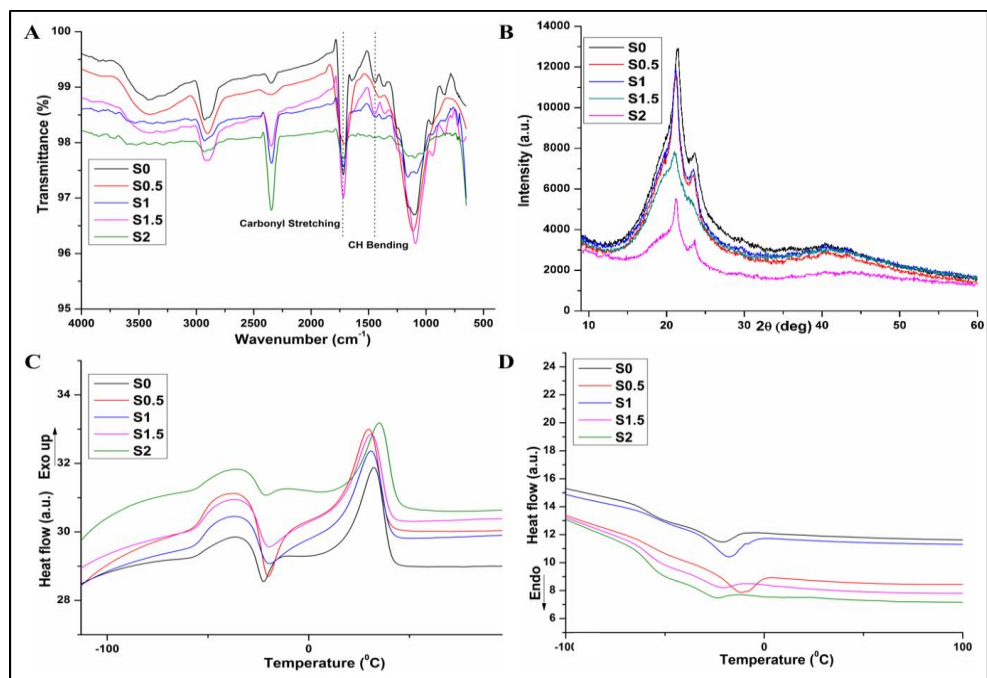
Figure 4.4 Physico-chemical characterization of the polymeric blends. (A) FTIR spectroscopic profile of the polymeric blends. (B) XRD profile for the polymeric films. (C) Exothermic peak of polymeric blends in DSC. (D) Endothermic peak of polymeric blends in DSC.

Table 4.6 Calculated crystallographic values for the polymeric blends

Sample	D_c	C_s	r	d
S0	76.10	3.15	5.16	4.12
S0.5	73.32	1.14	5.18	4.16
S1	70.32	2.36	5.25	4.20
S1.5	66.64	2.83	5.20	4.16
S2	64.95	3.54	5.20	4.16

4.3.5 Mechanical testing

Mechanical strength of the polymeric blends was displayed in Figure 4.5 A. The stress strain curves of the polymeric blends showed an increasing trend upon increasing the concentration of RISUG®. The polymeric blend S2 showed decrease in the stress strain curve. This phenomenon may be due to the saturated level of intermolecular interaction between the polymeric blends. The increase in the tensile strength of the polymeric blends may be due to the property of adhesion of RISUG® polymer with PCL-DA: PEG-DA polymers. The intermolecular interaction may occur by the formation of hydrogen bonds between the polymeric blends by providing more point-bonded sites in the polymeric backbone [21]. Decrease in the crytalinity of the polymer ultimately leads to decrease in their mechanical strength. The regularly ordered molecular chains of the crystalline polymer (PCL-DA: PEG-DA polymers) may start converting themselves to disordered macromolecular assembly upon addition of RISUG® polymer. The decrease in the mechanical strength of the polymer blends by addition of RISUG® may reflect the development of spherulite form in the polymeric backbone of PCL-DA: PEG-DA blends.

4.3.6 *In-vitro* swelling kinetics study

In-vitro swelling kinetics study is considered as vital factor in developing bio-degradable uterine implantable contraceptive formulation. Significant changes were observed in the swelling kinetics of the polymeric blends upon increasing the concentration of RISUG®.
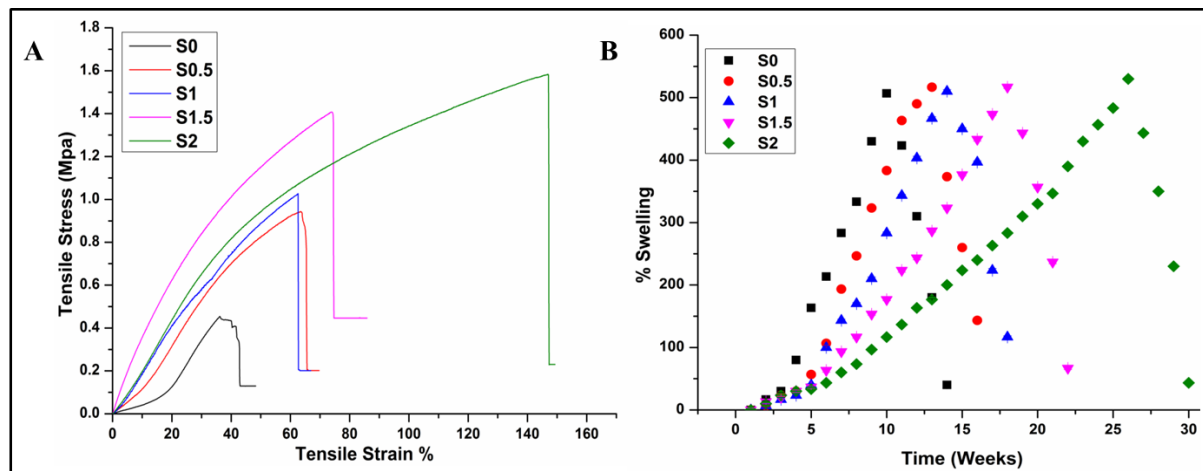
Figure 4.5. (A) Mechanical testing of polymeric blends. (B) *In-vitro* degradation profiles of the polymeric blends.

The polymeric sample S0 without RISUG® attained its maximum swelling at 10 weeks of time duration. The polymeric samples S0.5 and S1 attained maximum swelling at 20 and 21 weeks of time duration respectively. Sample S1.5 and S2 25 and 33 weeks of total time duration in order to achieve maximum of its swelling. This phenomenon of swelling reaction might be due to the intermolecular interaction between the polymeric blends. Upon increasing the concentration of RISUG® polymer, the mechanical stability of the PCL-DA: PEG-DA could increase that ultimately leads to the increase in the time duration for achieving maximum swelling for the polymeric blends. Sample S1 was selected to evaluate acute *in-vivo* toxicological study of the fabricated polymeric blends.

4.3.7 *In-vitro* toxicological study

The calcein-acetoxymethyl (Calcein AM) dye showed (Figure 4.6 B) good retention inside primary rat uterine cell lines. The viability of the cell lines was accessed through the retention ability of (green) fluorescent Calcein AM dye inside the significant number of viable primary rat uterine cell lines, than the DNA binding ethidium

homodimer (red) fluorescent dye. Furthermore the *in-vitro* sperm killing activity of the polymeric blends showed increasing trend of dead sperm by increasing the concentration of RISUG® polymer. Sperm killing activity (Figure 4.6 D) of the sample S2 was also performed inoredr to identify the sperm killing ability of the polymeric blend having RISUG® at maximum concentration. Both cytotoxic and cytostatic effects on primary rat uterine cells by conditioned media were evaluated through the mitochondrial dehydrogenase activity. Observed mitochondrial dehydrogenase (Figure 4.6 A) activity has shown 80% of viability in all the polymeric samples. Based on the MTT and live dead assay results quantitative rt-PCR and *in-vivo* toxicological experiments were performed using sample S1. The change in cycle threshold value (ΔCt) obtained from qRT-PCR (Figure 4.6 C) for the expression levels of ER-α, VEGF, Cyclin D1 and CDK4 genes has not shown any significant changes in the values of both control and treated cells [13, 14, 22].

4.3.8 *In-vivo* toxicological study

4.3.8.1 Microscopic anatomic observation

Hematoxylin and eosin stained uterine sections (Figure 4.7 A) of treated uterine tissue has not shown any morphological changes when compared with control. Tall columnar epithelial cells have not shown any implant associated architectural change. The luminal and glandular epithelium of control and treated uterine tissue showed vacuolar degeneration that represents the oestrus phase of the rat reproductive cycle.
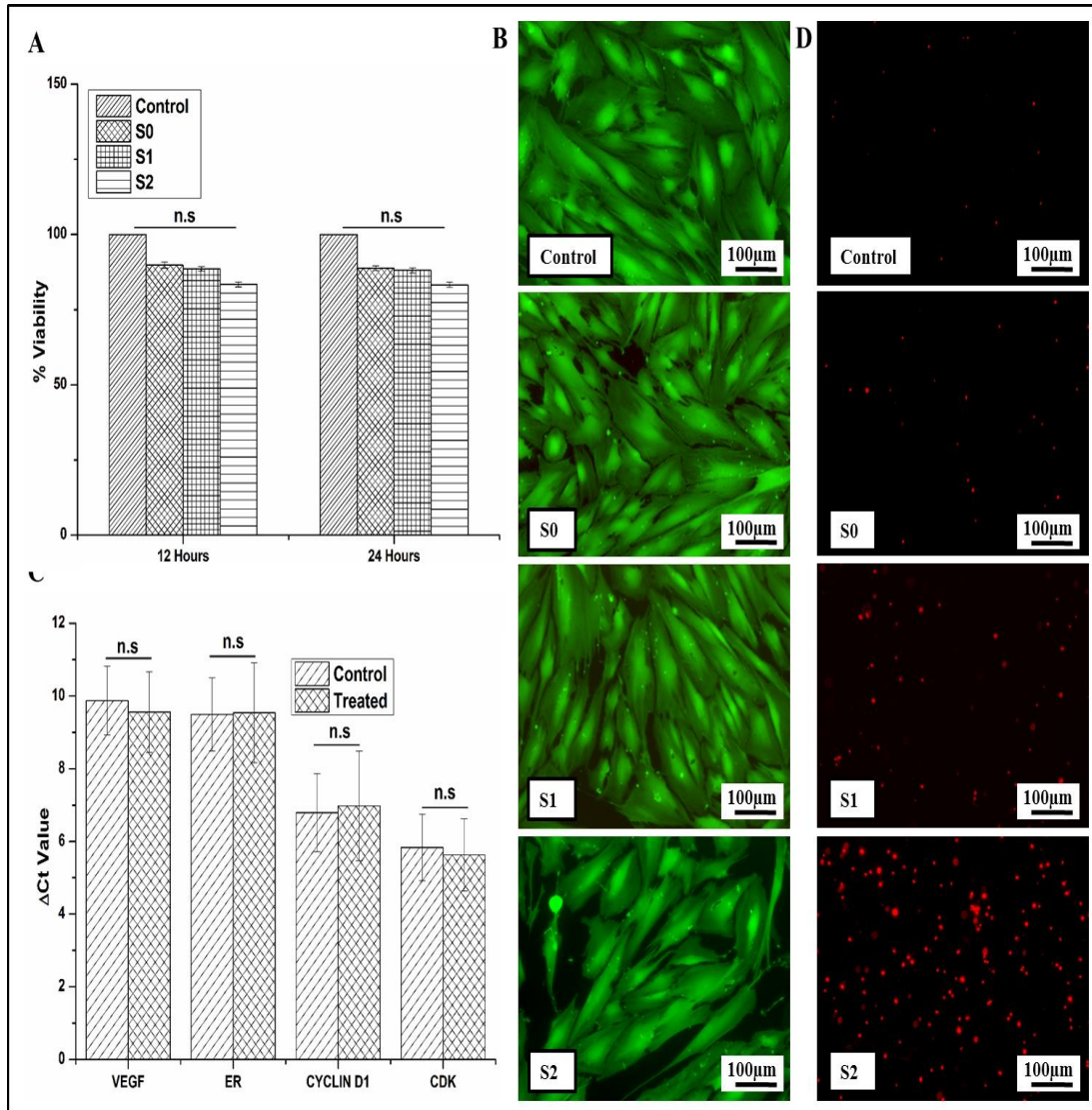
Figure 4.6. (A) *In-vitro* biocompatibility evaluation of the polymeric blends in primary rat endometrial cell lines (A) MTT assay. (B) Calcein-AM/ethidium homodimer-1 based live/dead assay. (C) Quantitative rt-PCR assay "(n.s. signifies that the values has not shown any significant difference). (D). In vitro sperm killing efficiency of the polymeric films using propidium iodide staining.

Furthermore large numbers of polymorphonuclear (N) cells infiltrate the lamina propria and endometrial glands. In both control and treated tissue sections the outer and inner differential polyhedral cells covered with slackly connective stratum vasculosum

containing myometrial muscular layer (D) has not shown implant associated morphological change when compared with control tissue sections [22].

4.3.8.2 Immunohistochemical observation

The polymer implant has not exerted any change in the expressions of Estrogen responsive genes (ER-α, VEGF) when compared with control uterine tissue (Figure 4.7 B). The immunoreactivity of both ER-α and VEGF in both control and treated tissue sections are in good agreement with each other in their expressions. The polymer implant has not altered the vascular development or tissue architecture. It was also observed that the cell cycle receptors (Cyclin D1 and CDK4) (Figure 4.7 B) of treated tissue have not exerted any change in their expression while compared with control tissue. Immunohistochemical results were quantitatively evaluated by scoring the protein expression areas of stroma, blood vessels and epithelial cells of both control and treated tissue sections. Thus the polymer extract in the conditional media has not altered the estrogen responsive protein expressions and cell cycle regulator protein expression [12].

4.3.8.3 Organ pathology

Microscopic anatomical changes in organs (Figure 4.9 A) of control and treated animals were evaluated in order to identify any implant associated stress or toxicological effects. Organs like heart, lung, liver, spleen and kidney were observed after hematoxylin and eosin staining. The heart muscles of treated animals have not expressed any signs and symptoms of interfibrillar depletions, penetration congestion or focal commotion while compared with control heart tissue sections. In order to evaluate implant associated stress generated respiratory deprivation in polymer treated lung tissues, the hematoxylin and

eosin stained tissues of control and treated animals were compared. No signs and symptoms of respiratory insufficiency were observed in treated lungs tissue when compared with control. The polymer implant has not exerted any metabolical change in the animal which was indemnified by the normal sinusoids of liver tissue. Prominent nuclei were observed in both control and treated liver tissue which assure that the polymer implant has not exerted any ductal hyperplasia. The kidney cells have not shown any evidences of inflammation or fibrosis in the treated tissue when compared with control. The morphological orientation of medulla and cortex of treated kidney tissue has not shown any significant change when compared with control. The smooth muscles of spleen filled with trabeculae showed oriented frame work of reticular fibers in treated tissue as like in control tissue. No significant morphological changes were observed in the hematoxylin and eosin stained organs of treated animal.

4.3.8.4 Hematology and blood biochemistry

The hematology and blood biochemistry (Figure 4.9 B and C) has not shown any significant amount of changes in treated animals when compared with control animals. When compared with control animals critical blood indicators like differential leukocyte count (Neutrophil (N), Platelets (Pl), Eosinophil (El), Monocyte (MS), Lymphocyte (LS)), Total RBC (Tr), Total leucocyte (Tl) and Platelets (Pl) has not shown any significant changes. Other haematological markers including Mcv, Mch, Mchc, Hgb and Hct has not shown any significant change in treated animals when compared with control. These haematological markers indicate that polymeric implant has not exerted any significant amount of toxicity in animals. The treated animals have not shown any

significant amount of changes in the general metabolic functions, kidney and liver functions when compared with control animals.
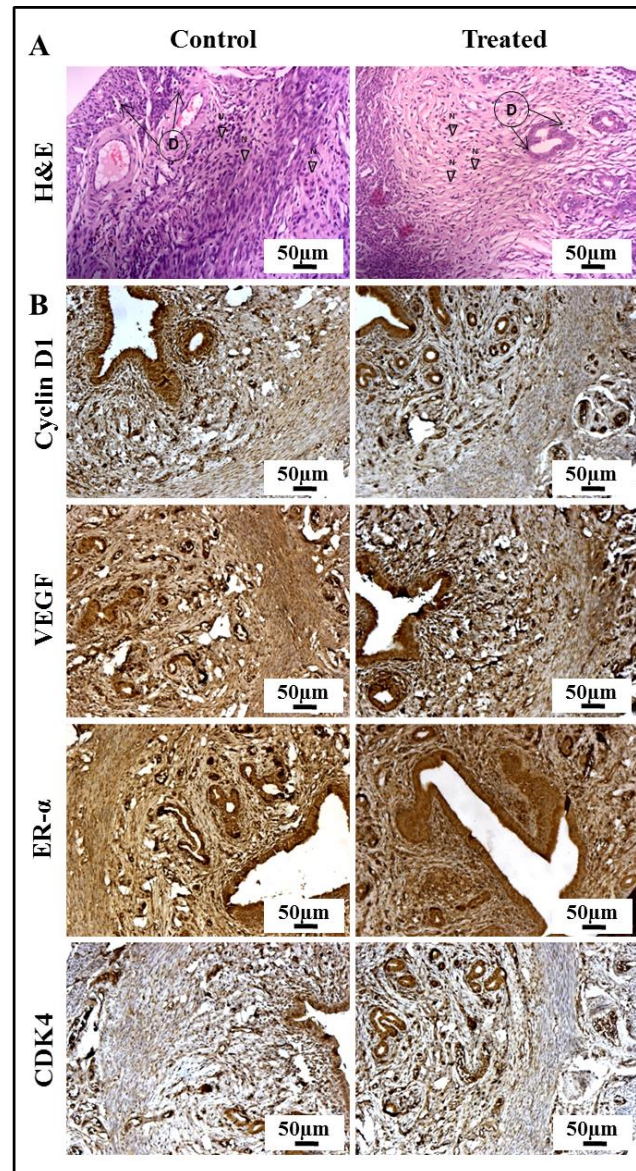
Figure 4.7. (A) Histological evaluation of the uterine tissue sections derived from control and treated rats. N and D represents polymorphonuclear cells and myometrial muscular layer respectively. **(B)** Immunohistological staining of the uterine tissue sections from control and treated groups of rats against cyclin D1, VEGF, estrogen receptor α (ER-α) and CDK4.

4.4 Discussions

Biocompatible form of PCL-DA was synthesized through the process of esterification and with the help of acryloyl chloride. Synthesized PCL-DA was structurally confirmed by NMR analysis. For the purpose of enhancing the hydrophillicity, the PCL-DA was blended with PEG-DA at desired proportion. This PCL-DA and PEG-DA polymeric blends were evaluated for the application of biodegradable form of female contraceptive implant by grafting the polymeric blends with styrene maleic anhydride copolymer male contraceptive RISUG® for the development of nonhormonal female contraceptive implant.
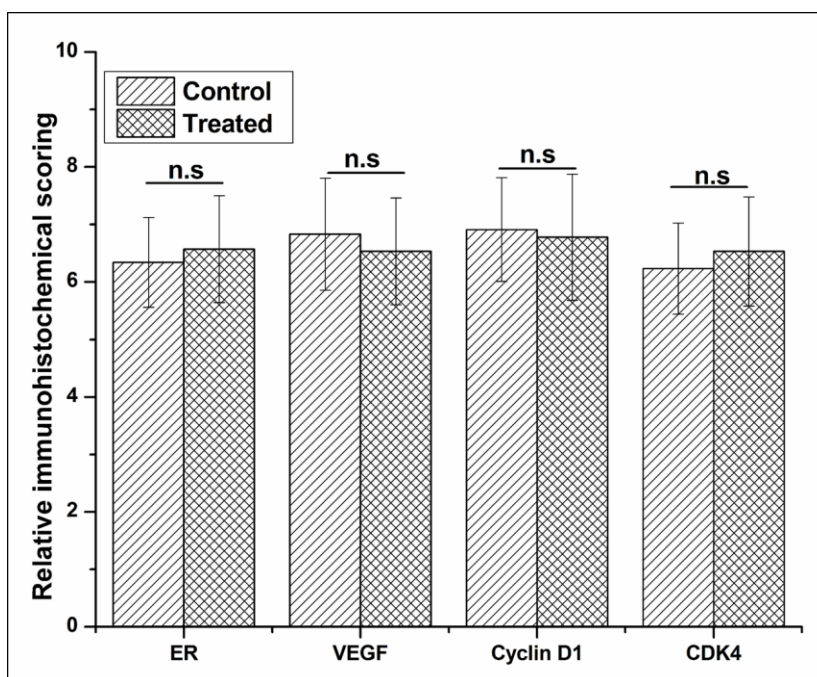
Figure 4.8. Immunohistochemical staining scores of polymeric blend samples compared with treated rat uterine tissue samples expressing ER-α, VEGF, CyclinD1 and CDK4 proteins expression. All the experiments were carried out in triplicates. Values which have not shown significant difference with $p > 0.05$ were mentioned as "n.s"

Physiochemical characterizations like FTIR, DSC, XRD, AFM and SEM studies reveal the nature of interaction between RISUG® and PCL-DA: PEG-DA polymeric blend. Miscibility between the polymeric blends and RISUG® was clearly evidenced by the enthalpy of polymeric affinity (ΔH) between the polymeric mixtures. The peak shift in the regions of carbonyl stretching and CH rocking reveal the nature of intermolecular interaction between the polymeric mixtures after grafting with RISUG®. Furthermore the intermolecular interaction between RISUG® and PEG-DA: PCL-DA polymeric blends altered the melting point (Tm) of the polymeric blends. Increase in the concentration of RISUG® shift T_m towards the amorphous region since RISUG® polymer composed of SMA, is amorphous in nature. Further reduction in crystallization temperature (T_c) may be reduction of lamellar thickness in the polymeric blends due to the addition of RISUG® polymer. Weak hydrogen bond between the strong electronegative oxygen groups in maleic anhydride of RISUG® may interact with hydrogen molecules present in the PEG-DA: PCL-DA polymeric blends. There are possibilities for the establishment of surface interaction of RISUG® over the PEG-DA: PCL-DA polymeric blend. Addition of more amount of amorphous polymer with PEG-DA: PCL-DA polymeric blend resulted in accumulation of RISUG® over the surface of the polymeric blend. The stress versus strain curve of polymeric blends provided information about the mechanical strength of the polymeric blends.
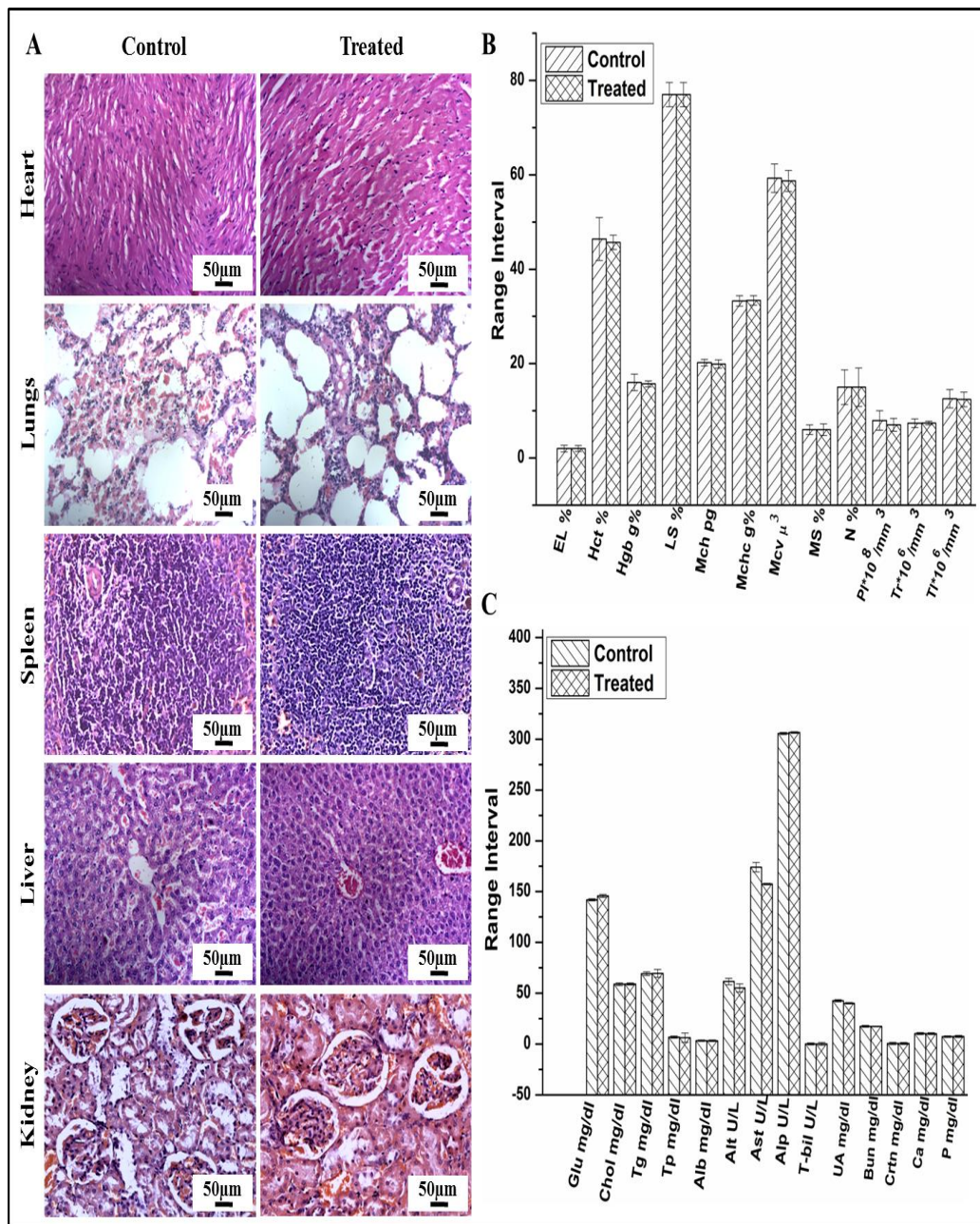
Figure 4.9. (A) Representative histological images of the heart, lungs, liver, spleen, and kidney from control and treated groups of rats to evaluate organ pathology. (B) Haematological and (c) serum biochemical parameters of control and treated groups of rats.

The strength of the polymeric blends increased with increasing concentration of RISUG®, while sample S2 showed a sudden decrease in the curve. The intermolecular interaction between the polymeric blends might have reached the saturation point in which amorphous solid polymer RISUG® surrounds the PEG-DA: PCL-DA polymeric blend that may result in the reduction stress strain curve. Furthermore the exothermic peak of polymeric sample S2 also shows shift towards increasing temperature (34 ºC) which may infer saturated level of intermolecular interaction between the polymeric blends. *In-vitro* toxicological effect of primary rat uterine cell lines treated with conditioned media has not shown significant level of toxicity when compared with control cells. The mitochondrial dehydrogenase activity has not shown any significant level of change in conditioned media treated cells even after 24 hours of treatment. The quantitative RT-PCR results of gene expression (VEGF, ER-α, Cyclin-D1 and CDK4) has not shown any significant level of change in the ΔCt values between control and treated primary rat uterine cell lines. Histochemical and histopathological evaluation of control and treated uterine tissues of rats has not shown any significant levels of difference between them. Implant associated tissue irritation or tissue damage may exert variation in the estrogen responsive gene levels that may in turn directly affect the expression levels of cell cycle regulators CDk4 and Cyclin-D1. But the protein expression on treated tissue sections has not shown any change in their expression levels when compared with control rat uterine sections. Histological evaluation of organs like kidney, liver, spleen, heart and lungs has not shown any evidence of implant associated toxicity. The blood biochemical and haematological parameters of treated animals has not shown any significant change while compared with control animals. The present research

work concludes that biodegradable formulation of intrauterine nonhormaonal contraceptive device can be developed by grafting RISUG® with PEG-DA: PCL-DA polymeric blends at proportion of S1. The future research work of the authors will be focused on analysing release kinetics RISUG® from the polymeric blends at particular time duration.

4.5 Conclusions

The present research work concludes that a new form of biodegradable intra-uterine nonhormonal female contraceptive implant can be formulated by grafting RISUG with suitable proportion of PEG-DA: PCL-DA. This polymeric formulation is biocompatible and may further effectively function as nonhormonal female contraceptive intrauterine implant.

References:

[1] G.S. Susheela Singh, Rubina Hussain, Unintended Pregnancy: Worldwide Levels, Trends, and Outcomes, Studies in Family Planning, 41 (2010) 241-250.

[2] L. Hoggart, V.L. Newton, Young women's experiences of side-effects from contraceptive implants: a challenge to bodily control, Reproductive Health Matters, 21 (2013) 196-204.

[3] S. Banerjee, S.K. Guha, RISUG: a potential candidate for the entry inhibitor group of antiretroviral drugs, Med Hypotheses, 73 (2009) 150-152.

[4] Y.M.C. Su Jin Im, Elango Subramanyam, Kang Moo Huh, Synthesis and Characterization of Biodegradable Elastic Hydrogels Based on Poly(ethylene glycol) and Poly(ε-caprolactone) Blocks, Macromolecular Research, 15 (2007) 363-369.

[5] J.S. Park, D.G. Woo, B.K. Sun, H.M. Chung, S.J. Im, Y.M. Choi, K. Park, K.M. Huh, K.H. Park, In vitro and in vivo test of PEG/PCL-based hydrogel scaffold for cell delivery application, J Control Release, 124 (2007) 51-59.

[6] S. Roy, D. Ghosh, S.K. Guha, Polyelectrolyte polymer properties in relation to male contraceptive RISUG action, Colloids Surf B Biointerfaces, 69 (2009) 77-84.

[7] M.R.C. Marques, R. Loebenberg, M. Almukainzi, Simulated Biological Fluids with Possible Application in Dissolution Testing, Dissolution Technologies, 18 (2011) 15-28.

[8] O.W. Guirguis, M.T.H. Moselhey, Thermal and structural studies of poly (vinyl alcohol) and hydroxypropyl cellulose blends, Natural Science, 04 (2012) 57-67.

[9] M. Selvakumar, A. Mahendran, P. Bhagabati, S. Anandhan, Thermodynamic Miscibility and Thermal and Mechanical Properties of Poly(ethylene-co-vinyl acetate-co-

carbon monoxide)/Poly(vinyl chloride) Blends, Advances in Polymer Technology, 34 (2015) n/a-n/a.

[10] M. Hellstrom, R.R. El-Akouri, C. Sihlbom, B.M. Olsson, J. Lengqvist, H. Backdahl, B.R. Johansson, M. Olausson, S. Sumitran-Holgersson, M. Brannstrom, Towards the development of a bioengineered uterus: comparison of different protocols for rat uterus decellularization, Acta Biomater, 10 (2014) 5034-5042.

[11] K. Dhaouadi, F. Raboudi, C. Estevan, E. Barrajon, E. Vilanova, M. Hamdaoui, S. Fattouch, Cell viability effects and antioxidant and antimicrobial activities of Tunisian date syrup (Rub El Tamer) polyphenolic extracts, J Agric Food Chem, 59 (2011) 402-406.

[12] A. Chatterjee, U. Chatterji, All-trans retinoic acid protects against arsenic-induced uterine toxicity in female Sprague-Dawley rats, Toxicol Appl Pharmacol, 257 (2011) 250-263.

[13] A. Chaudhary, S. Bag, P. Banerjee, J. Chatterjee, Honey Extracted Polyphenolics Reduce Experimental Hypoxia in Human Keratinocytes Culture, Journal of Agricultural and Food Chemistry, 65 (2017) 3460-3473.

[14] T. Agarwal, R. Narayan, S. Maji, S.K. Ghosh, T.K. Maiti, Decellularized caprine liver extracellular matrix as a 2D substrate coating and 3D hydrogel platform for vascularized liver tissue engineering, J Tissue Eng Regen Med, 12 (2018) e1678-e1690.

[15] K. Lozenski, R. Ownbey, B. Wigdahl, T. Kish-Catalone, F.C. Krebs, Decreased cervical epithelial sensitivity to nonoxynol-9 (N-9) after four daily applications in a murine model of topical vaginal microbicide safety, BMC Pharmacology and Toxicology, 13 (2012) 9.

[16] S.J. Im, Y.M. Choi, E. Subramanyam, K.M. Huh, K. Park, Synthesis and characterization of biodegradable elastic hydrogels based on poly(ethylene glycol) and poly(ε-caprolactone) blocks, Macromolecular Research, 15 (2007) 363-369.

[17] Q. Jing, J.Y. Law, L.P. Tan, V.V. Silberschmidt, L. Li, Z. Dong, Preparation, characterization and properties of polycaprolactone diol-functionalized multi-walled carbon nanotube/thermoplastic polyurethane composite, Composites Part A: Applied Science and Manufacturing, 70 (2015) 8-15.

[18] J.Z. Luk, J. Cooper-White, L. Rintoul, E. Taran, L. Grøndahl, Functionalised polycaprolactone films and 3D scaffolds via gamma irradiation-induced grafting, Journal of Materials Chemistry B, 1 (2013).

[19] G. Zhu, Q. Xu, R. Qin, H. Yan, G. Liang, Effect of -radiation on crystallization of polycaprolactone, Radiation Physics and Chemistry, 74 (2005) 42-50.

[20] C. Mahoney, D. Conklin, J. Waterman, J. Sankar, N. Bhattarai, Electrospun nanofibers of poly(epsilon-caprolactone)/depolymerized chitosan for respiratory tissue engineering applications, J Biomater Sci Polym Ed, 27 (2016) 611-625.

[21] R. Zamani, Y. Pilehvar-Soltanahmadi, E. Alizadeh, N. Zarghami, Macrophage repolarization using emu oil-based electrospun nanofibers: possible application in regenerative medicine, Artif Cells Nanomed Biotechnol, DOI 10.1080/21691401.2017.1367689(2017) 1-8.

[22] J.M. Goldman, S.C. Laws, S.K. Balchak, R.L. Cooper, R.J. Kavlock, Endocrine-Disrupting Chemicals: Prepubertal Exposures and Effects on Sexual Maturation and Thyroid Activity in the Female Rat. A Focus on the EDSTAC Recommendations, Critical Reviews in Toxicology, 30 (2000) 135-196.

Chapter 5

Improved Intra Uterine Contraceptive Device (IIUCD) – a new form of polymeric composite as anti-cancerous and anti-HIV female contraceptive implant

5.1 Introduction

Intra Uterine contraceptive Devise (IUD) is considered as an effective method to prevent pregnancy from the year of 1909. The contraceptive mechanism of non-hormonal IUD is not completely elucidated. It was explained that IUD directly interfere with the implantation of fertilized ovum which provides contraception. Furthermore it was also understood that IUD persuades inflammatory response inside uterine cavity. This inflammatory response activates lysosome along with other inflammatory pathways providing lethal environment to the sperm. Copper bearing IUD provides various complications like uterine perforations, Pelvic Inflammatory Disease (PID), expulsion, improper bleeding, cramping pain etc. It was expected that the local inflammatory response exerted by the IUD may results in development of endometrial carcinoma was anticipated due to some known scientific observations [1]. Since IUD invoked prolonged inflammatory responses continue as a chronic effect inside uterine cavity post IUD implantation in could persuade endometrial cancer. When compared with other bio-inert devices the irritation inside uterine cavity by copper makes IUD more susceptible in inducing cancer. IUD alters the uterine tissue sensitivity to hormones like progesterone and oestrogen which is providing the information of cancer induction theoretically. In addition to hormonal changes, IUD also induce loss of epithelial cells over the surface of uterine tissue and also reduce the number of ciliated cells which shows a risk of development of endometrial neoplasm. These IUD associated complications limit their use which ultimately leads to increase in unintended pregnancy which acts as adverse social Impact [2-5].

A new form of IUD which could lower the risk of cancer induction or IUD provided with anti-cancer drug will eradicate the panic of using IUD as a long term contraceptive implant. In order to achieve the objective a new form of IUD called an Improved Intra-uterine Contraceptive Device (IIUCD) comprised of flexible form of polymeric tubelets has been developed. This new form of IUD is provided with contraceptive polymer composed of high and low molecular weight SMA and SMAc polymers dissolved in DMSO. The *in-vitro* and *in-vivo* results of this IUD found to be capable of providing long-term contraception [6].

SMA is an amphiphilic polymer which comprises of critical concentrations of acidic carboxylic group and hydrophobic aromatic groups. When the carboxylic are exposed to low pH, the hydrophilic nature of the polymer undergoes conversation to hydrophobic biologically inert form which ultimately results in destabilization of cellular membranes. This characteristic nature of shift in hydrophilic and hydrophobic form provides a name as pH responsive "smart polymer" [7]. Membrane destabilization may be due to the merge of smart polymers with the lipo-protein membranes of cells. The contraceptive SMA polymer when get exposed to biological environment develops electrical charge over its surface. Electrical charge generation occurs due to hydration of SMA polymer which helps to possess positive and negative charges over the polymeric surface with positive charge occurring more [8]. By having more positive charge around the surface of the polymer it may act as cationic polymer which may activate the "Proton sponge effect" when exposed to acidic pH of cancer cells [9, 10]. The acidic residues on the surface of plasma membrane [11] and around extracellular microenvironment of cancer cells may trigger the SMA polymer to influence proton sponge effect like reaction

[12]. This change in the cellular microenvironment may destabilize the cancer cell membrane which may ultimately results in anticancer activity of SMA polymer.

HIV spread from the male sex partner to the female sex partner is a foremost health predicament. An objective of recommending an intra vas deferens implant of an antimicrobial composite to avert the infection spread is evaluated in HIV infected cell lines. Mode of action for the reticence could comprise inactivating HIV in sperms transient through the vas deferens and drug discharge from the intra vas implant to annihilate HIV spreading into semen from genital structures situated away from the vas deferens. A new drug RISUG$^®$ (Reversible Inhibition of Sperm Under Guidance) which is in advanced phase III clinical trials for its male contraceptive effect has the potency to establish selective antimicrobial activity against opportunistic pathogens. The drug is composed of SMA, SMAc dissolved in DMSO can be developed in to female implantable contraceptive implant as whole as described in Chapter 3 and can also be grafted with biodegradable various forms of female contraceptive implants (Chapter 4 and 5) this SMA is hypothesized to establish entry inhibitory activity against HIV virus by inhibiting the interaction between viral surface protein gp120 and host cell surface protein CD4. Hence SMA is here anticipated as a potential candidate substance for the HIV inhibiting implant when administered in below contraceptive threshold quantity.

5.2 Supporting evidences for the research hypothesis

5.2.1 Interaction of RISUG® with phospholipid membrane:

The basis of this hypothesis lies in the structure, composition and physiochemical characteristics of RISUG® polymer. RISUG® mainly consists of SMA (14). Upon exposure to the biological fluids, it undergoes hydrolysis, thereby, gradually getting converted into SMAc (15). This SMAc is an amphipathic molecule consisting of hydrophobic styrene units and hydrophilic carboxyl/carboxylate (COOH/COO⁻) groups (16, 17). The carboxyl groups of the maleic acid unit have 2 pka values; first at pH 6 and other at pH 10 which plays vital role in determining the charge of the SMAc molecules depending on the pH of the surrounding medium (17).

The interaction between phospholipid membrane and SMAc molecule is driven by the hydrophobic interactions between phenyl group of SMAc and lipid fatty acid chains of phospholipid membrane. This interaction is modulated by the electrostatic forces between anionic charges from partially deprotonated maleic acid groups of the SMAc and phosphate head of the phospholipids (18-20). The binding is followed by insertion of SMAc deeply into the hydrophobic core of the phospholipid membrane. This insertion results in the destabilization of the cellular lipid membrane architecture followed by formation of vesicular intermediates and membrane solubilization to disc-shaped nanostructures. The interaction of RISUG® with lipid membrane is an interplay between the composition of both, RISUG® polymer (ratio of SMAc units) and lipid membrane (phospholipid type and chemical characteristics of fatty acyl chains) (21). In addition, the pH of the surrounding medium also plays a crucial role, thereby affecting the interaction of the polymer with the lipid membrane (Figure 5.1.) (21). At alkaline pH, the carboxyl

groups of SMAc are deprotonated which causes electrostatic forces to dominate over the hydrophobic forces, thereby restricting incorporation of the polymer into the lipid membrane. On the other hand, at acidic pH values, the protonation of the carbonyl groups causes loss of electrostatic repulsion with dominating hydrophobic effect which results in faster incorporation of SMAc molecules with phospholipid membrane.

5.2.2 Interaction of RISUG® with normal and cancerous cells:

Several studies have already shown that the SMAc interacts with the mammalian cells and exerts effects based on cellular microenvironment and architecture (21, 22). In this regard, both normal and cancer cells share a number of differences. We made these differences as the base to validate our hypothesis pertaining to the potential anticancer effect of RISUG® polymer.

5.2.3 Effect of cellular microenvironment on RISUG® incorporation:

Under normal conditions, the ionic and pH homeostasis is maintained with a lower intracellular pH (~7.2) and a higher extracellular pH (~7.4) (23). However, under cancerous conditions, poor vascular perfusion, regional hypoxia, and fermentative glycolysis results in reversed pH gradient with higher intracellular (~7.9 to 7.4) and lower extracellular pH (~6.4 to 6.8). Interaction of SMAc with the acidic external environment of cancer cell would result in the shielding of its negative charges. Such decrease in the charge density would cause dominating hydrophobic forces to induce faster incorporation of the SMAc polymer into the lipid bilayer of the cancerous cells which may leads to cytolysis through membrane destabilization (Figure 5.1.). On the other hand, the external alkaline pH in case of normal cells would resist its incorporation due to the electrostatic repulsion between the negatively charged polymer and negatively charged cell

membrane. Previously Scheidelaar et al. has also demonstrated a similar result wherein a decrease in pH of the medium significantly increases the degree of SMAc incorporation into the phosphatidylcholine (PC) lipid membrane (24). Here, it is important to mention that an optional ratio of SMAc units in the polymer is essential for efficient incorporation into lipid membrane. The variation in the lipid composition significantly alters the physiological behavior of the cells and also alters their response to the chemotherapeutic drugs.

5.2.4 Effect of membrane lipid composition on RISUG® incorporation:

Apart from the differences in their microenvironment, both the normal and cancer cells also differ in their lipid bilayer composition and also vary significantly between the different cancer types (25). In this section, we would discuss the efficacy of RISUG® as an anticancer agent of different cancer types.

5.2.4.1 Drug-sensitive cancer cells v/s normal cells

The cell membrane of cancer cells has marked decrease in the molar ratio of cholesterol (C) to phospholipids (PL) (25). The molar C:PL ratio for healthy normal cells is estimated between 0.6 and 1.0, while for cancer cells, it varies in between $0.31 - 0.46$ (25, 26). Such a reduction in the cholesterol levels results in the fluidity of the plasma membrane. These cancer cells also show an increase in short and unsaturated acyl chains (C16:0 and C18.1, n-9) in the bilayer of the membranes which further provide a hint regarding an increase in their fluidity (26-28). In addition to this, the membranes of the cancerous cells have a disordered symmetrical distribution of lipids (28).
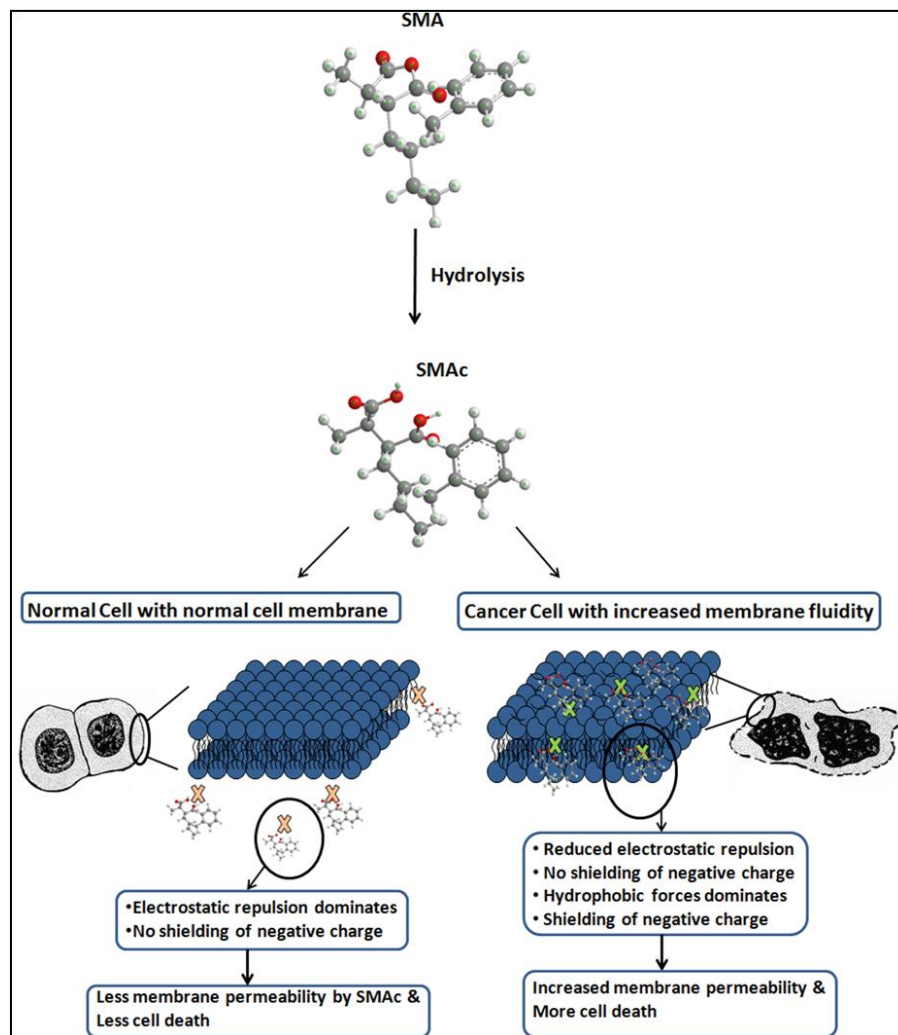
Figure 5.1. Membrane destabilization activity of SMAc derived from SMA in normal and cancer cells.

In normal cells, the phosphatidylethanolamine (PE) and Phosphatidylserine (PS) are exclusively localized in the inner leaflet of the membrane, while in the cancerous cells, both, PE and PS also get distributed to the outer leaflet (28). Such an alteration in the lipid composition and distribution in the bilayer affects its functionality and permeability of the phospholipid membrane. Peetla et. al. has stated that the presence of

high concentration of PE on the outer leaflet increases the membrane permeability of the cancer cells (28).

Another aspect that needs to be highlighted here is that the lipid membrane of the cancer cells have a significant increase in the negative charge density on their surface due to the localization of PS and increased the concentration of sialic and folic acid (29, 30). Such an increase in the negative charges could slightly alter the interaction of SMAc with the bilayer. But the acidic pH of the microenvironment could also protonate these negatively charged groups and reduce the degree of electrostatic repulsion between polymer and cancer cell membrane.

Previous studies have shown that the presence of short chain fatty acid, lower cholesterol levels in the lipid membrane, and reduced electrostatic repulsion between membrane and SMAc allows faster membrane solubilization (25). Based on these ground, we could hypothesize that the increase in membrane permeability along with an increase in membrane fluidity would allow faster incorporation of the SMAc in the drug-sensitive cancerous cells in comparison to the normal cells. This would eventually lead to membrane permeabilization, thereby disrupting the ionic balance and allowing unrestrained flow of molecules inside-out of the cell. Such alteration in the cellular environment would ultimately trigger cellular apoptosis/necrosis (31, 32). A similar membrane destabilization and permeabilization has recently been reported by Tan et. al. as a potential strategy for exerting anticancer effects. The study made use of PE-binding peptides and other small molecules (ophiobolin A) that bind specifically to the ethanolamine head group of PE and facilitate the formation of transmembrane pores and eventually lead to cell death (33).

5.3 Materials and Methods

5.3.1 Polymer extract

The contraceptive polymer SMA and SMAc polymers dissolved in DMSO was incubated in Simulated Uterine Fluid (SUF) (1:5 at 37 °C and pH 7.8) containing Sodium bicarbonate (0.25 g/L), Sodium dihydrogen phosphate (0.072 g/L), Calcium chloride (0.167 g/L), Potassium chloride (0.224 g/L), Sodium chloride (4.97 g/L) and Glucose (0.50 g/L) dissolved in distilled water [1]. The polymeric extract was subjected to freeze drying following the complete dissolution of the polymer in the SUF. This freeze dried polymer extract was further utilized for further experiments.

5.3.2 Cancer cell lines

Two types of cervical cancer cell lines (SiHa and ME-180) were procured from National Centre for Cell Science (NCCS), Pune, India. The cells were cultured as monolayer in MEM medium provided with 1 mM sodium pyruvate, 10% Fetal Bovine Serum (FBS), 10 mM HEPES, 1.5 g/L sodium bicarbonate, 2 mM L-glutamine, and 100 U/ml antibiotic (penicillin-streptomycin) and maintained at 37 °C with 5% CO_2 atmosphere. Cancer cell lines were treated with polymer extract at different concentration ranges (10, 20, 30, 40, 50, 60, 70, 120, 240 µg/ml) and nurtured for duration of 24 h. The cytotoxicity provided by the polymer extract was calculated by MTT assay according to the equation 1. The IC50 values for the polymeric extract were calculated and optimal dosage was used for further experiments [2-4].

5.3.3 Viral cell culture and treatment

CEMss cells were obtained from the National Institutes of Health AIDS Research and Reference Reagent Program. Obtained cells were cultured grown in RPMI 1640 medium supplemented with 10% heat-inactivated fetal bovine serum, 1% L-glutamine, and 1% penicillinstreptomycin at a cell population of 0.6 X 10^6 to 0.8 X 10^6 /ml. Cultured cells were treated with SMA and AZT at different concentrations (a = 3 µg/ml, 6 µg/ml, 20 µg/ml, 90 µg/ml, 200 µg/ml, 1000 µg/ml) . MTT (3[4,5-dimethylthiazol-2-yl]-2,5-diphenyltetrazolium bromide) assay was performed by calorimetric method to determine the viability percentage (V%) of the clls post drug and test sample treatment using the formula,

$$V\% = \left[\frac{A_t}{A_c}\right] * 100 \ eqn \ (1)$$

Where, A_t is absorbance of test at 590 nm and A_c is absorbance of control at 590 nm. The untreated cells were cosnidered as cells having 100% viability.

5.3.4 Plaque reduction assay and antiviral Index

CEM$_{ss}$ cells at density of 1 X 10^5 /ml were cultured in 60 mm tissue culture dishes. The cells were infected with 100 plaque forming units (PFU/0.2 ml) of virus after the cells attain 80 - 90% of confluence. The virus was allowed to adsorb for 1 h at 37 ºC in 5% CO2 atmosphere. The solution was removed and the cells were washed twice with pre-warmed MEM medium. While virus adsorption, drug dilutions were prepared in the overlay medium. The infected cells were overlaid with 5ml 0.8% of nutrient methylcellulose. The plates were incubated at 37 ºC in 5% CO2 atmosphere for three to

five days before fixing with 10 % formalin solution for 30 min. Cells were either stained with 1 ml per well of methylene blue. Stain was removed and rinsed gently three times with tap water and allowed to dry inverted overnight and plaques (dark areas) were counted using low power magnification on a binocular microscope. The percentage of inhibition of plaque formation was calculated using the formula,

$$\left[\frac{Mean\ number\ of\ plaques\ in\ control - Mean\ OD\ plaques\ in\ sample}{Mean\ OD\ of\ plaques\ in\ control}\right] * 100\ eqn\ (2)$$

The value of TC50, which is the concentration of test sample required to inhibit upto 50% of virus growth as compared with the virus control group, were estimated from the graphical plot of the data. Furthermore the antiviral index (AI) was calculated using the formuls,

$$AI = \left[\frac{IC_{50}}{EC_{50}}\right]\ eqn\ (3)$$

Where IC_{50} is the maximum drug concentration which causes cytotoxic effect in 50% of the cultured cells and EC_{50} is the minimum drug concentration which is effective to inhibit virus induced plaque formation or cytopathic changes by 50%.

5.3.5 *In-vitro* toxicological assay

In-vitro toxicological assay of respective polymeric sample was investigated in primary rat vaginal cell lines, having passage number of three after consecutive two passages. The primary rat vaginal cell lines were isolated by the procedure described elsewhere [5]with some changes. Briefly, vaginal tissues from rats were aseptically excised and incubated in DMEM and Ham's F-12 mixed in equal proportion (V/V),

having 0.2% collagenase type I at 37 ℃ for 1 h in a shaker. The tissue containing collagenase solution was added with equal volume of DMEM/F12 cell culture media having 10% Fetal Bovine Serum (FBS stripped with charcoal to remove native hormones). The cell culture media was also added with 1% penicillin-steprtomycin solution, 1 nmolL^{-1} β-estradiol and 10 mmolL^{-1} HEPES. The neutralized tissue sample was filtered through 100 and 40 μm tissue strainer respectively prior to centrifugation at 250 g for 5 minutes at 4 ℃. The pellet containing viable cells were seeded on 6 well plates for further study. Fresh media was frequently added to the growing cells by removing the non-adherent vaginal cells. MTT (3[4,5-dimethylthiazol-2-yl]-2,5-diphenyltetrazolium bromide) assay was performed by calorimetric method. The ability of proliferating and metabolically active primary vaginal cells that can cleave MTT containing tetrazolium ring to form blue coloured formazan crystals was measured. Rat primary vaginal cell lines were incubated in both normal and special media conditioned with polymeric sample. The special conditioned media was prepared by dissolving respective polymeric sample (25 mg in 5 mL) for 3 days under aseptic condition. The cell lines were seeded at a density of 10,000 cells per well on to 24 well plate. The primary cell line was incubated inside 95% air humidified atmosphere having 5% of CO_2 at 37 ℃ for 12 and 24 h. The viability of proliferating cells were quantified by measuring absorbance at 590 nm. The vaginal primary cell lines growing in normal media was considered as 100% viable control cells. The viability percentage (V%) of vaginal primary cell lines grown in special conditioned media was investigated [6].

5.3.6 Haemolysis assay

The ability of polymeric extract to destabilize cellular membrane was identified using pH dependent haemolysis assay describe elsewhere [7]**.** Briefly, human whole blood samples were collected on EDTA coated BD vacutainer tubes. Followed by the blood collection, the RBC cells were diluted at a concentration of 1:10 in 0.1M phosphate buffered in order to harvest final concentration of RBC at 10^8/200 µL solution (followed by washing). The pH of the RBC solutions was adjusted (5.8, 6.6 and 7.4) to acidic and normal microenvironment of cancer and normal cells respectively. The polymer extract was added to to eppendorf tubes at desired concentration containing 800 µL of PBS and 200 µL of RBC solution. The mixture was incubated at 37° C for 1h in water bath. Followed by the incubation, the eppendorf tubes were centrifuged at 13,500 g for 5 min and the supernatant containing haemoglobin was transferred to 96 well plate to take absorbance reading at 541 nm using 96-well plate reader. PBS and triton X-100 (non-ionic surfactant that has haemolytic property) was used as negative and positive control. All the experiments were done in triplicates [7].

5.3.7 Cellular morphological study

The primary rat uterus cell lines and cancer cell lines were fixed overnight in 4% formaldehyde prepared in phosphate-buffered saline after washing in cold Phosphate-Buffered Saline (PBS pH7.4) at their respective time points for fluorescent imaging. The morphology of cell lines were examined after by staining with Rhodamine-Phalloidin for cytoplasm and DAPI for nucleus. Morphology of the primary cell lines were visualized using Zeiss Observer.Z1 Microscope (Carl Zeiss, Germany).

5.4 Results

5.4.1 Viral cell culture and treatment

The drug AZT has not shown significant reduction in V% at any of the concentration used (Figure 5.2 a). SMA treated cells expressed significant reduction at the concentration of 1000 µg/ml. However the percentage of inhibition of plaque formation exhibited by SMA was more when compared with the AZT. The AI of SMA exerted towards the HIV was significantly more when compared with the standard drug AZT (Figure 5.2 b). Thus SMA may have the ability to reduce the viral load more effectively than that of AZT.

5.4.2 Haemolysis assay

The polymer extract provided favourable haemolytic activity (Figure 5.3 c) at pH 5.6 (90 - 95%), moderate haemolytic activity at pH 6.5 (30 - 35%) and very little haemolytic activity at pH 7.4 (< 10%). The highly favourable haemolytic activity provided by the polymer extract showed good evidence in order to establish contraceptive SMA polymer as an anti-cancer drug. The haemolytic activity at acidic pH may be due to the fact that that when the polymeric extract get exposed to microenvironment which is having pH value lower than pKa of carboxylic group present in the polymer extract, the polymer becomes protonated due to which the polymer becomes hydrophobic. This protonated polymer may have the ability to interact with biological membranes that ultimately results in membrane destabilizing activity of the polymer [7].
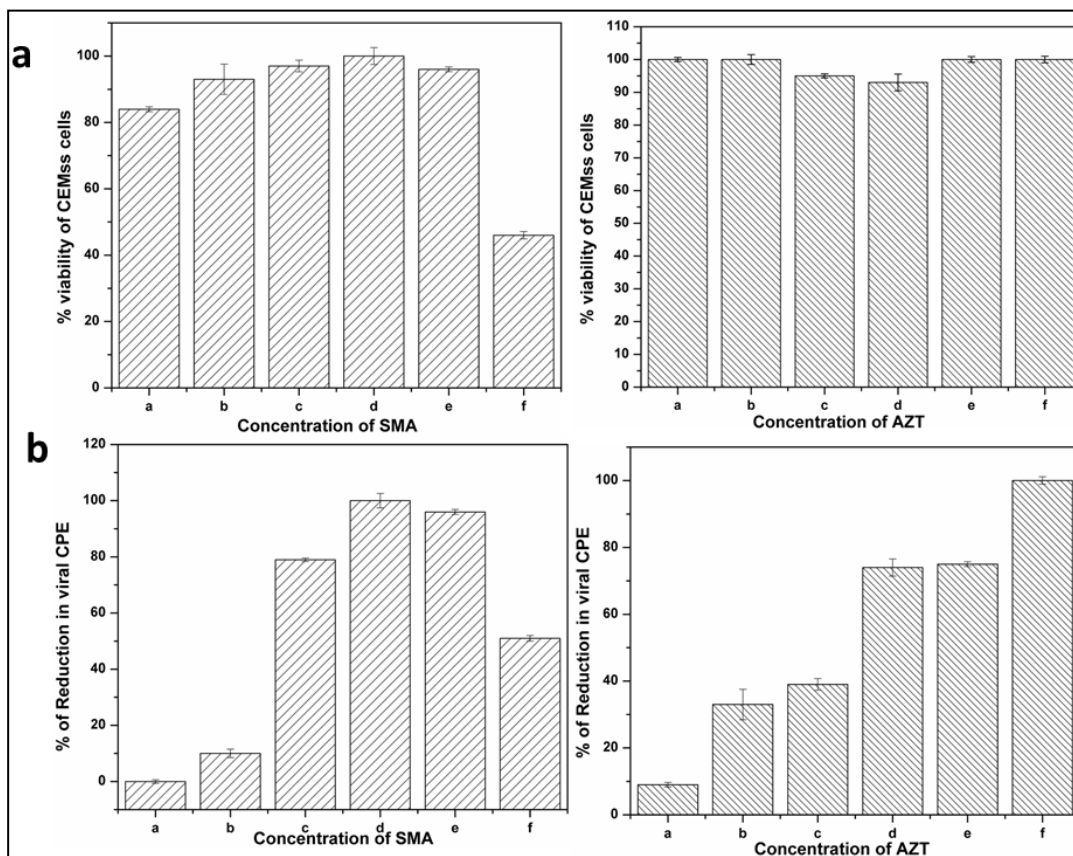
Figure 5.2. *In vitro* viral cell culture and drug treatment results. (a) Percentage viability of cells treated with SMA and AZT. (b) Percentage reduction of viaral load in cells after treating with SMA and AZT.

5.4.3 MTT assay

Cell growth inhibitory concentration 50 (IC50) value for the polymer extract was observed to be 20 µg/mL for SiHa and 30 µg/mL for ME180 (Figure 5.3 a and b). The IC50 value concentration of the polymeric extract has not shown any significant level of toxicity to the primary rat endometrial cell lines. Furthermore morphological changes of the cancer cell lines and primary rate endometrial cell lines were observed post treatment with polymeric extract (with IC50 concentration after 24 h). It was observed that no significant level of morphological changes to primary rat endometrial cell lines. Cell

death and morphological damage was observed in both the cancer cell lines (Figure 5.4). The observed results also provided evidences of anticancer activity of contraceptive SMA polymer.

5.5 Discussions

The FIR spectrum of SMA polymer explained about the property of hydration of the polymer after mixing with simulated uterine fluid. This property of hydration changes the electrochemistry of the polymer. Furthermore the anti HIV property established by HIV is significantly more than the drug molecule AZT. These results infer the hypothesis provided by Guha SK et al and Banergy S et al. The polymeric hydrogel RISUG® may effectively function as anti HIV implant after suitable *in vivo* characterization of the anti-viral efficacy. The SMA provided haemolysis only at acidic pH which clearly depicts that the anti-cancer activity is limited to the acidic cancerous cells and not to the normal cells however the mode of administration has to be validated for effective chemotherapeutic effect.
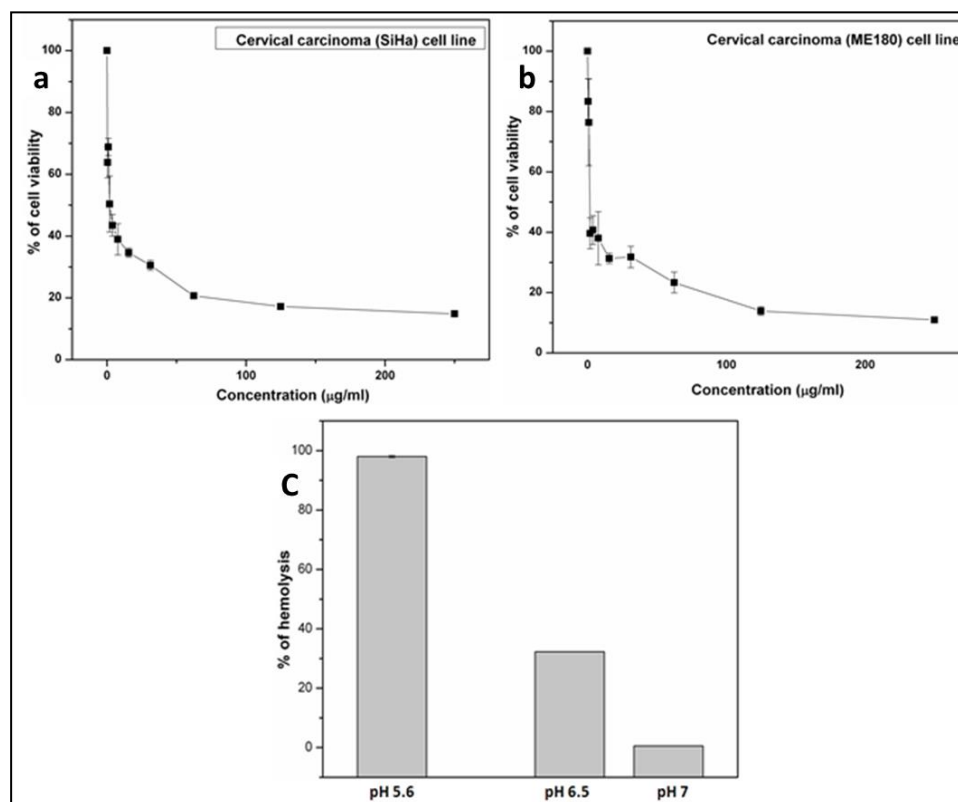
Figure5.3. (a) MTT assay for SiHa cell line, (b) MTT assay for ME180 cell line, (c) hemolysis % assay

The cell morphological and MTT assay evidenced the anti-cancer effect of SMA at various different concentrations. All the test results have supported the objective that SMA hydrogel RISUG® can be administered as anti-cancerous and anti-HIV establishing female contraceptive implant. Suitable *in vivo* model could provide additional validation for the results of *in vitro* characterization.
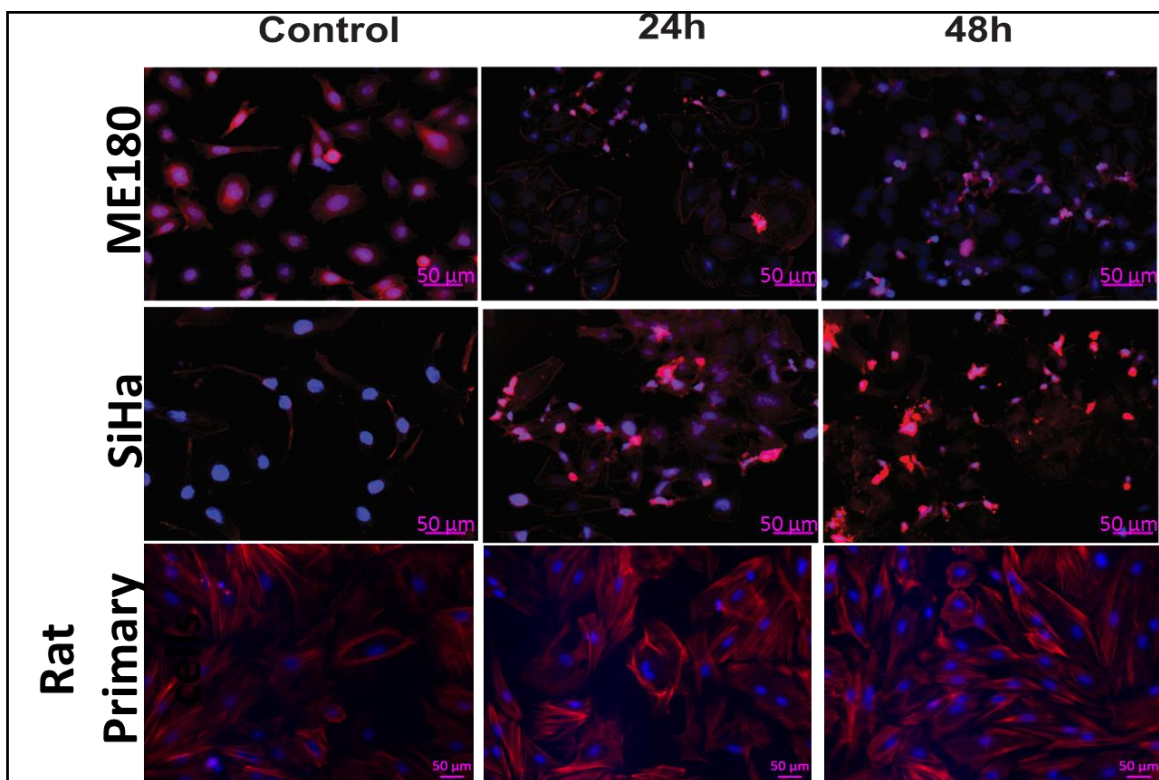
Figure 5.4 Microscopic cellular morphology of cancer cell line and primary rat uterine

cell lines

5.6 Conclusions

Observed evidences showed clear confirmation of anti-cancerous and anti-HIV activity of SMA hydrogel RISUG®. Upon implanting the polymer inside the female reproductive tract, the polymer not only function as contraceptive implant but may also act as anti-cancerous drug that may lower the risk of cancer induction and could establish entry inhibitory activity against HIV. This advantage will provide confidence of implanting IIUCD as s long term contraceptive device.

References

[1] Elchalal U, Abramov Y. Uterine biology and the intrauterine device. Adv Drug Deliv Rev 1995;17:151-164.

[2] Sturgeon SR, Brinton LA, Berman ML, Mortel R, Twiggs LB, Barrett RJ, Wilbanks GD, Lurain JR. Intrauterine device use and endometrial cancer risk. Int J Epidemiol 1997;26:496-500.

[3] Rowe PCJ. The intrauterine device: A review of recent advances and controversies. Oxford reviews of reproductive biology 1981;3:49-94.

[4] Castellsagué X, Thompson WD, Dubrow R. Intra-uterine contraception and the risk of endometrial cancer. Int J Cancer 1993;54:911-916.

[5] Corfman PA, Richart RM, Parenthood AP. Uterine epidermoid carcinoma induced in rats by plastic and stainless steel intra-uterine devices. Excerpta Medica Int Congr Ser 1968:pp. 89.

[6] Guha SK. An improved intra-uterine contraceptive device, Google Patents, 2013.

[7] Henry SM, El-Sayed ME, Pirie CM, Hoffman AS, Stayton PS. pH-responsive poly (styrene-alt-maleic anhydride) alkylamide copolymers for intracellular drug delivery. Biomacromolecules 2006;7:2407-2414.

[8] Guha SK. Biophysical mechanism-mediated time-dependent effect on sperm of human and monkey vas implanted polyelectrolyte contraceptive. Asian J Androl 2007;9:221-227.

[9] Kato Y, Ozawa S, Miyamoto C, Maehata Y, Suzuki A, Maeda T, Baba Y. Acidic extracellular microenvironment and cancer. Cancer Cell Int 2013;13:89.

[10] Griffiths J. Are cancer cells acidic?. Br. J. Cancer 1991;64:425.

[11] Kuo C-C, Wang S-P, Grayston JT. Effect of polycations, polyanions, and neuraminidase on the infectivity of trachoma-inclusion conjunctivitis and lymphogranuloma venereum organisms in HeLa cells: sialic acid residues as possible receptors for trachoma-inclusion conjunctivitis. Infect. Immun 1973;8:74-79.

[12] Koren E, Torchilin VP. Cell-penetrating peptides: breaking through to the other side, Trends Mol Med 2012;18:385-393.

[13] ATICI OG, Akar A, Rahimian R. Modification of poly (maleic anhydride-co-styrene) with hydroxyl containing compounds. Turk J Chem. 2001;25:259-266.

Chapter 6

Conclusions and Summary of the work

6.1 Conclusions and Summary

RISUG® polymer expresses significant rheological properties which could help in resisting expulsion in the upper reproductive tract for an extended duration after implantation which was evidenced in *In vitro* characterizations especially through rheological study results. In **chapter 2** it has been shown that water-mediated intermolecular H-bonding between maleic anhydride group of RISUG® and SUF is responsible for surface roughness and increase mechanical strength of RISUG®. Crystallite size estimated from broadening peaks by Scherer equation has proved that RISUG® after experiencing the dilution by SUF has not shown a structural change in its polymeric structure. The viscoelastic property of RISUG® and its dilutions increases with increase with the interaction with SUF. These results suggested that mechanical strength of RISUG® depends upon the intermolecular H-bonding interaction with SUF. RISUG® established selective antimicrobial activity against opportunistic pathogens while having limited consequence over the growth of *Lactobacillus spp*. RISUG® has not shown any significant damage to the rat uterine primary cell lines during the period of *in vitro* toxicological assessment. *In* vivo toxicity results inferred that RISUG® hydrogel implant has not exerted any implant associated toxicity post-implantation inside the uterus. RISUG® hydrogel has not inferred any change in the expression of ER-α, VEGF and cell cycle regulators (Cyclin D1 and CDK4) which are primarily responsible for estrogen signaling pathway. Organ tissue pathology studies post implantation of RISUG® have shown no significant damage observed in the organs and also in the blood biochemical parameters.

Interaction between PVOH and RISUG® via means of intermolecular hydrogen bonding was confirmed in **chapter 3**. Molecular interaction between PVOH and SMA hydrogels were studied by using Fowkes equation. *In-vitro* physiochemical characterization confirmed good miscibility between RISUG® (SMA) polymer and PVOH. ΔH_S values of the polymeric blends signify that the interaction between the polymers at different proportions happens at the thermodynamically favorable environment. The intensity of DSC curves of the polymeric blends showed continuous reduction upon increasing the concentration of RISUG®. This inference may be discussed as, the three-dimensional crystal growth of PVOH polymer is hindered by the increased concentration of RISUG® due to its amorphous nature. Increasing the concentrations of RISUG® increased hydrophobicity of the polymeric blends which affects the bidegradablity of the polymeric blends. *In-vitro* bio-compatibility of the polymeric blends was validated in cervical (female reproductive tract) cancer cell line (HeLa cell). *In-vivo* biocompatibility study revealed that RISUG® polymeric blend has not exerted any toxicological effect post exposure to the vaginal tissue. Microscopic anatomical observation depicted safety of the polymeric blends. Furthermore immunohistochemical study also confirmed the bio-comaptibility of the polymeric blend. Organ tissue pathology and blood biochemical parameters have not shown any evidence of toxicity in the vaginal tissues of the animal exposed to polymeric blend.

Polymeric formulation for the application of establishing biodegradable form of intra-uterine implantable contraceptive polymer was developed and characterized in **chapter 4**. RISUG® grafted with PCL-DA:PEG-DA polymeric mixture is proposed to have the property to degrade gradually post implantation inside the uterus by the

experimental results. These polymeric blends were evaluated for the application of biodegradable form of female contraceptive implant by grafting the polymeric blends with styrene maleic anhydride copolymer male contraceptive RISUG® for the development of nonhormonal female contraceptive implant. Physiochemical characterizations revealed the nature of interaction between RISUG® and PCL-DA: PEG-DA polymeric blend. Miscibility between the polymeric blends and RISUG® was clearly evidenced by the enthalpy of polymeric affinity (ΔH) between the polymeric mixtures. Weak hydrogen bond between the strong electronegative oxygen groups in maleic anhydride of RISUG® may interact with hydrogen molecules present in the PEG-DA: PCL-DA polymeric blends. The mechanical strength of the polymeric blends increased with increasing concentration of RISUG®. Thus the polymeric blend could withstand the structural integrity in the dynamic environment of uterus and could slowly degrade to establish the contraceptive effect. *In-vitro* toxicological effect of polymeric blend was evaluated in primary rat uterine cell lines. Histochemical and histopathological evaluation of control and treated uterine tissues of rats has not shown any significant levels of implant associated tissue irritation or tissue damage. Histological evaluation of organs like kidney, liver, spleen, heart and lungs has not shown any evidence of implant associated toxicity. The blood biochemical and haematological parameters of treated animals has not shown any significant change while compared with control animals.

Chapter 5 contains preliminary evaluation for the future scope of establishing RISUG® as anticancer/tumor and antiviral non-hormonal female contraceptive implant. The Antiviral Index (AI) of SMA exerted towards the HIV was significantly more when compared with the standard drug AZT in CEMss cells. Thus SMA may have the ability to

reduce the viral load more effectively than that of AZT. Furthermore percentage of inhibition of plaque formation exhibited by SMA was more when compared with the AZT. The polymer extract provided favourable haemolytic activity at pH 5.6 (90 - 95%), moderate haemolytic activity at pH 6.5 (30 - 35%) and very little haemolytic activity at pH 7.4 ($<$ 10%). Cell death and morphological damage was observed in both the cancer cell lines. The observed results also provided evidences of anticancer activity of contraceptive SMA polymer. Thus it was evidenced that SMA polymer not only could acts as a contraceptive polymer, it also provide antiviral and anticancer effect along with selective anti-microbial property only towards the opportunistic pathogens.

6.2 Future scope

RISUG® polymer can be fabricated as various forms of non-hormonal female contraceptive implants either as a virgin polymer or by grafting with other bio-polymeric mixtures. However detailed study on the mechanism of antimicrobial activity of the polymer has to be evaluated. Antimicrobial efficacy towards other pathogenic bacteria responsible for establishing female reproductive tract infections should also be evaluated. Sustained release of RISUG® breakdown products has to be evaluated and characterized in order to understand long duration contraceptive efficacy of the RISUG® and RISUG® grafted polymeric mixtures. The mode of action for establishing anti-cancerous activity of the SMA/RISUG® also has to be evaluated. Moreover, the bio-distribution of the degraded chemicals from the 3D polymeric structure and their accretion or excretory pathways also needs to be extensively evaluated. These detailed studies could aid in developing new form of female non-hormonal contraceptive implant which could eradicate the prevailing complications associated with known form of female

contraceptive modalities. This multiple advantage carrying contraceptive implants could decrease the fear of using contraceptives due to its side effects and increase the usage between sexually matured female practitioners with increased awareness that ultimately leads to the reduction in the burden of population explosion in developing countries.

Bhuvaneshwaran Subramanian

School of Bio-science and Engineering,   **Phone:** +91-8900355423
Jadavpur University, Kolkata,   +91-8348733022
West Bengal, India   **E-mail:** bhuvaneshmscbt@gmail.com
                                            bhuvaneswaran.sp@research.jdvu.ac.in

Passionate researcher having eight years of academic research experience in accomplishing various government projects. Learnt synthesis and characterization of synthetic and biological polymers for various applications during Ph.D research career. Genuinely interested for a postdoctoral position to invest my research experience and to learn research techniques to achieve innovative scientific solutions and to generate new research concepts.

EDUCATION

Jadavpur University   West Bengal, India
Ph.D in Bio-Science and Egineering   Expected March 2020

Barathidasan University   Tamil Nadu, India
Master of Philosophy (M.Phil) in Biotechnology   Awarded March 2012
Awarded with First class - Distinction

K. S. Rangasamy College of Technology   Tamil Nadu, India
Master of Science (M.Sc) in Biotechnology   Completed May 2010
Awarded with First class

 JJ college of Arts and Science   Tamil Nadu, India
Bachelor of Science (B.Sc) in Biotechnology   Completed April 2008
Awarded with First class – Distinction

RESEARCH POSITIONS HELD

Indian Institute of Technology, Kharagpur   **West Bengal, India**
Senior Project Assistant (SPA)   January 2014 – June 2016
In the project entitled National center of technology in family welfare; sponsored by Ministry of Health and Family Welfare (MHFW), Government of India.

Indian Institute of Technology, Kharagpur   **West Bengal, India**
Project Research Staff   November 2012 – November 2013
In the project entitled Concurrent exposure to pesticides in food, metals in health interactions and implications on control standards (CPF); sponsored by department of environment, Government of West Bengal, India.

AWARDS AND CERTIFICATES

- *Bhuvaneshwaran Subramanian*. awarded as **Senior Research Fellow (SRF)** In the project entitled Synergism and antagonism in concurrent exposure to microwave radiation (Mobile telephoning) and extra low frequency (50 Hz) electromagnetic fields (AEF);

sponsored by Science and Engineering Research Board (SERB), **Department of Science and Technology (DST), Government of India (October 2018 – present)**

- *Bhuvaneshwaran Subramanian*. **Selected as young scientist from India to participate in 68th Lindau Nobel Laureate Meeting** taking place from 24 to 29 June 2018, in Lindau, Germany, **dedicated to Physiology/Medicine** sponsored by (DST) Department of Science and Technology ,India

- *Bhuvaneshwaran Subramanian*. **Received Out sanding young scientist in Bio-materials award in RULA International Innovation and Betterment Awards 2018 ceremony** taken place on November 12th 2018 in Tiruchirappalli, Tamil Nadu, India.

- *Bhuvaneshwaran Subramanian*. Invited lecture on Evaluation of Physiochemical properties, anti-microbial activity, *In-vitro* and *In-vivo* toxicological effect of RISUG® hydrogel for promoting as improved intra-uterine contraceptive implant. Silver jubilee 25th Annual conference of SAI (Society of Andrology India (SAI) held on 28th and 29th October, 2017 at Counsil of Scientific and Industrial Research (CSIR)- Central Drug Research Institute (CDRI), Lucknow, India

- *Bhuvaneshwaran Subramanian*. Biodegradable IUCD. **Second prize in Idea pitch event "The Grill"** at the entrepreneurship summit held at Indian Institute of Management Calcutta on 5th February, 2017

- *Bhuvaneshwaran Subramanian.* **Selected as BRICS young scientist working in the area of Affordable Health care** and also selected to attend the BRICS young scientist conclave held at National Institute of Advanced Studies, Indian Institute of Science (IISC), Bangalore, India on 26-30 September 2016.

- *Bhuvaneshwaran Subramanian*. awarded as **Junior Research Fellow (JRF)** In the project entitled Synergism and antagonism in concurrent exposure to microwave radiation (Mobile telephoning) and extra low frequency (50 Hz) electromagnetic fields (AEF); **sponsored by Science and Engineering Research Board (SERB), Department of Science and Technology (DST), Government of India (July 2016 – September 2018)**

- *Bhuvaneshwaran Subramanian*, Arun Prabhu Rameshbabu, Kuntal Gosh, M Selvakumar, Piyali Basak, Santanu Dhara, Sujoy K Guha. Styrene Maleic Anhydride formulated polyelectrolyte hydrogel with selective antimicrobial property, potentially favorable for the application as female contraceptive implant. **World Biomaterial Congress 2016 Trainee award under the category of Merit awards held at Montreal, Canada** on May 17-22

- *Bhuvaneshwaran Subramanian*, Selvakumar M, Chattopadhyay Shantanu, Piayali Basak, Sujoy Kumar Guha. Flexible biodegradable anti-microbial new advanced form of Intra Uterine Contraceptive Device (IUCD). **Gandhian Young Technological Innovation (GYTI) Awards 2016**, Society for Research and Initiatives for Sustainable Technologies and Institutions under More or Less for Many (MLM) category (BIRAC-GYTI) at the hands of Dr. R.A.Mahelkar, FRS, National Innovative Foundation (NIF) of India

- *Bhuvaneshwaran Subramanian*, Selvakumar M, Chattopadhyay Shantanu, Piayali Basak, Sujoy Kumar Guha. Biodegradable advanced form of Intrauterine Contraceptive Device (IUCD) and Wound healing chocolate formulation. **Best Medical Device Innovation Award of the year 2016** from 13th National Conference and Technology Exhibition on "Indian Medical Devices & Plastics Disposables/ Implants Industry 2016" Ahmedabad Management Association (AMA), Ahmedabad, India

- **Best paper award** for the paper entitled "RISUG-polyelectrolytic charge generating polymer for tumor Immunotherapy" in National conference on ETEEE 2015 at Jamia Millia Islamia (A central University), New Delhi, India
- **Best Oral Presentation award** for the presentation on "Physiochemical and Rheological Characterization of RISUG for the application in Improved IntraUterine Contraceptive Device for female contraception" in International conference on Male Reproductive Health incorporating XIX Annual congress of Society of Andrology, India (ICMRH & ANDROCON 2014) at Amity University Utarpradesh, Noida (U.P) India
- **Best Project student certificate** for the project entitled "Seed extracts (Moringa oleifera and Phyllanthus emblica) with α- amylase and α-glucosidase inhibitory effects" for Master of Science Project at School of Medical Science and Technology, Indian Institute of Technology, Kharagpur, India

PATENT FILED

- **Bhuvaneshwaran Subramanian**, Sujoy Kumar Guha, Arun Prabhu Rameshbabu, Piyali basak, Shantanu Dhara. Indian Patent Ref. No./Application No. 201831011943. Title: Customized biodegradable flexible nano fabricated intra-uterine contraceptive device (IUCD)

RESEARCH PUBLICATIONS

1. Sanjoy Kumar Ghorai, Somnath Maji, **Bhuvaneshwaran Subramanian**, Tapas Kumar Maiti, Santanu Chattopadhyay. Promoted Osteoconduction of Polyurethane-Urea Based 3D Nanohybrid Scaffold through Nanohydroxyapatite Adorned Hierarchical Titanium Phosphate. ACS Applied Bio Materials (**Just accepted)**

2. Tarun Agarwal, **Bhuvaneshwaran Subramanian**, Tapas Kumar Maiti. Liver Tissue Engineering: Challenges and Opportunities. ACS Biomaterial Science and Engineering (Just accepted). **Impact factor 4.51**

3. **BhuvaneshwaranSubramanian**, Tarun Agarwal, Sanjoy Kumar Ghorai, Pijush Mandal, Santanu Chattopadhyay, Piyali Basak, Tapas Kumar Maiti, Sujoy K Guha. Biocompatible polyvinyl alcohol and RISUG® blend polymeric films with spermicidal potential. Journal of Biomedical Materials 14:1-12 **Impact factor 2.89**

4. **BhuvaneshwaranSubramanian**, Tarun Agarwal, Piyali Basak, Tapas Kumar Maiti, Sujoy K. Guha. RISUG® based improved intrauterine contraceptive device (IIUCD) could impart protective effects against development of endometrial cancer. Journal of Medical Hypothesis 124:64-71 **Impact factor 1.15**

5. **Bhuvaneshwaran Subramanian**, Arun Prabhu Rameshbabu, Kuntal Ghosh, Pradeep K. Jha, Rakhi Jha, Selvakumar Murugesan, Santanu Chattopadhyay, Santanu Dhara, Keshab C. Mondal, Piyali Basak, Sujoy K. Guha. Impact of styrene maleic anhydride (SMA) based hydrogel on rat fallopian tube as contraceptive implant with selective antimicrobial property. Journal of Materials Science and Engineering: C 94:94-107 **Impact factor 5.08**

6. Sanjoy Kumar Ghorai, Somnath Maji, **Bhuvaneshwaran Subramanian**, Tapas Kumar Maiti, Santanu Chattopadhyay. Coining attributes of ultra-low concentration graphene oxide and spermine: An approach for high strength, anti-microbial and osteoconductive

nanohybrid scaffold for bone tissue regeneration. Carbon 141:370-389 **Impact factor 7.08**

7. Paulomi Ghosh, ArunPrabhu Rameshbabu, Dipankar Das, **Bhuvaneshwaran Subramanian**, Sintu Kumar Samanta, Sabyasachi Roy, Sagar Pal, Sudip Kumar Ghosh, Santanu Dhara. Single-Pot Biofabrication of Living Fibers for Tissue Engineering Applications. Journal of Materials Research: Cambridge core 33:2019-2028 **Impact factor 1.49**

8. Elavarasan Subramani, Arun Prabhu Rameshbabu, Manivannan Jothiramajayam, **Bhuvaneshwaran Subramanian**, Debangana Chakravorty, Gunja Bose, Mamata joshi, Chaitali Datta Ray, Indrani Lodh, Ratna Chattopadhyay, Sudipto Saha, Anita Mukherjee, Santanu Dhara, Baidyanath Chakravarty and Koel Chaudhury. Mycobacterial heat shock protein 65 mediated metabolic shift in decidualization of human endometrial stromal cells. Nature Scientific reports 7:3942 **Impact factor 4.2**

9. Arun Prabhu Rameshbabu, Paulomi Ghosh, Elavarasan Subramani, Kamakshi Bankoti, Kausik Kapat, Sayanti Datta, Priti Prasana Maity, **Bhuvaneshwaran Subramanian**, Sabyasachi Roy, Koel Chaudhury and Santanu Dhara. Investigating the potential of human placenta-derived extracellular matrix sponges coupled with amniotic membrane-derived stem cells for osteochondral tissue engineering. Journal of Material Chemistry B 4:613-625 **Impact factor 4.7**

10. Rakhi Jha, Pradeep K. Jha, Santosh Gupta, **Bhuvaneshwaran S.P.**, Maidul Hossain, Sujoy K Guha. Probing suitable therapeutic nanoparticles for controlled drug delivery and diagnostic reproductive health biomarker development. Journal of Material Science and Engineering C 61:235-245 **Impact factor 5.08**

11. Paulomi Ghosh, Arun Prabhu Rameshbabu, Dipankar Das, Nimmy K. Francis, Harpreet Singh Pawar, **Bhuvaneshwaran Subramanian**, Sagar Pal, Santanu Dhara. 2014. Covalent Cross-links in Polyampholytic Chitosan Fibers Enhances Bone Regeneration in a Rabbit Model. Colloids and Surfaces B: Biointerphases 125:160-169 **Impact factor 4.4**

12. B.Dineshkumar, **SP.Bhuvaneshwaran**, P.Vigneshkumar, Analava Mitra, Manjunatha Mahadevappa. 2010. A brief description of diabetes in India. Journal of Pharmacy Research Solutions 3(8): 1719-1723

13. B Dineshkumar, P Vigneshkumar, **SP Bhuvaneshwaran**, Analava Mitra. 2010. Advanced drug designing softwares and their applications in medical research. International Journal of Pharmacy and Pharmaceutical Sciences 2(3): 16-18

14. B Dineshkumar, P Vigneshkumar, **SP Bhuvaneshwaran**, Analava Mitra. 2010. Phyto-pharmacology of Acalypha indica: A Review. International Journal of Bio Sciences, Alternative and Holistic Medicine 1(2): 27-32

15. B Dineshkumar, Rangadar Pradhan, P Vigneshkumar, **SP Bhuvaneshwaran**, Analava Mitra. 2010. A Brief Review of Edible oils and its Nutritional properties for a rural Indian. International Journal of Bio Sciences, Agriculture and Technology 2(1): 7-11

16. Sutapa Mukherjee, B Dineshkumar, **SP Bhuvaneshwaran**, P Vigneshkumar, Analava Mitra. 2010. *Ocimum sanctum* and its Therapeutic Effects - A Review. International Journal of BioSciences, Alternative and Holistic Medicine 1(1): 23-26

17. **SP Bhuvaneshwaran**, B Dineshkumar, Vigneshkumar P, Analava Mitra. 2010. Non-Conventional Approaches to In-vivo Drug Tracking and Targeting - A Review. International Journal of Biological Sciences and Technology 2(1): 1-10

18. P Vigneshkumar, B Dineshkumar, **SP Bhuvaneshwaran**, Analava Mitra. Green Technology and its Benefits – A Review. International Journal of Bio Engineering and Technology 1(1):23:29
19. B Dineshkumar, **SP Bhuvaneshwaran**, P Vigneshkumar, Analava Mitra, Manjunatha Mahadevappa. 2010. Diabetes: Techniques for Blood Glucose Measurement - A Review. International Journal of Bio Sciences, Healthcare Technology and Management 2(2): 5- 10
20. B Dineshkumar, P Vigneshkumar, **SP Bhuvaneshwaran**, Analava Mitra, Manjunatha Mahadevappa, Santanu Dhara, Jothirmoy Chatterjee. 2010. Nuts and Seeds Bioactive Compounds and Related Nutraceutical Properties - A Review. International Journal of Food Safety, Nutrition, Public Health and Technology 2(1): 1-8

CONFERENCE PUBLICATIONS

1. Bhuvaneshwaran Subramanian, Arun Prabhu Rameshbabu, Kuntal Gosh, M Selvakumar, Piyali Basak, Santanu Dhara, Sujoy K Guha. Styrene Maleic Anhydride formulated polyelectrolyte hydrogel with selective antimicrobial property, potentially favorable for the application as female contraceptive implant. Frontiers in Bioengineering and Biotechnology. Published Online: 30 Mar 2016. **Cite Score 4.36**
2. Satarupa Sarkar, Amrita Chaudhary, Swarnendu Bag, **Bhuvaneshwaran Subramanian**, Amit K. Das, Provas Banerjee, Jyotirmoy Chatterjee. Regenerative potential of characterised honey in wound healing. Published Online: 30 Mar 2016. **Cite Score 4.36**

LIST OF RESEARCH PROJECTS WRITTEN AND SANCTIONED

Sr.	Title of Research Project	Role	Sponsoring agency	Year of sanction	Duration	Amount
1	Artificial uterus generation using polymer biodrug	Student Innovator	Department of Biotechnology, Government of India, New Delhi	2019	3 Years	1.5 Crores
2	Flexible biodegradable anti-microbial new advanced form of Intra Uterine Contraceptive Device (IUCD)	PI	Biotechnology Industry Research Assistance Council (BIRAC) Gandhian Young Technological Innovation (GYTI)	2016	2 Years	15 Lakhs
3	Determination of fetal thymus involution by no image ultrasound sonography	Student Innovator	Ministry of Health and Family Welfare (MHFW) under the project "IUD"	2015	1 year	The project was selected as a sub-project under the main project entitled "National center for technology and Family welfare" and submitted

					as Compendium of scientific research and technology development performed at Indian Institute of Technology (IIT), Kharagpur, West Bengal

EXPERIMENTAL TECHNIQUES AND SKILLS

In vivo experiments

- Bone, Intestine, Fallopian tube, Skin tissue regeneration scaffold implantation live animal surgery in rat, mice and rabbit
- Subcutaneous, Oral toxicological experiment in rat and mice
- Cancer induction and anti-cancerous activity evaluation in rat and mice
- CAM (Chorioallantoic Membrane) assay to evaluate angiogenic and anti-angiogenic efficacy in chicken and duck eggs
- Immunohistochemistry (Chromogenic and Fluoresence) evaluation

In vitro experiments

- Fibroblast, Keratinocyte, Fallopian tube cell lines isolation and culturing from rat; culture and revival of immortalized cell lines
- Cell proliferation and live dead assay

Synthetic polymer scaffold fabrication

- Polycaprolactone (PCL), Polyurethane (PU), Polyethylene Glycol (PEG), Polyvinyl Alcohol (PVA), Styrene maleic Anhydride (SMA) hydrogel, porous and non-porous biocompatible scaffold fabrication
- Gamma radiation polymerization (Fricke dosimetry for dose rate calculation)
- Nano and Micro fiber fabrication using electrospinning
- Metal (Bismuth oxide, Bismuth Selanide, Iron, Gold, Silver) nanoparticle synthesis

Anti-microbial assay

- Aerobic pathogenic (*Escherichia coli*, *Staphylococcus aureus*, *Pseudomonas aeruginosa*) bacterial sample culture and revival
- Anaerobic bacterial (*Lactobacillus fermentum*, *Lactobacillus planatarum*) culture and revival
- Anti-microbial activity (zone of inhibition, direct and indirect contact assay)

Physiochemical characterization

- Spectroscopic (Nuclear Magnetic Resonance (NMR), Fourier Transform Infra-red (FTIR), X-ray Diffraction (XRD), Ultraviolet) characterization
- Differential Scanning Calorimetry
- Thermal Gravimetric Analysis (TGA)
- Tensile strength
- Rheology (soft matter)
- Micro computed Tomography (μ-CT)
- Contact angle measurement experiments

Molecular biology techniques
- Reverse Transcriptase and Real time Polymerase Chain Reaction (PCR)
- DNA RNA extraction from cell lines
- ELISA

Natural substance characterization
- Isolation and characterization of Indian medicinal plant extracts, characterization of plant secondary metabolites, natural honey, colostrum characterization

REFERENCES

NAME	ADDRESS	CONTACT
Prof. Dr. Sujoy K Guha	Professor of Biomedical Engineering, Indian Institute of Technology & All India Institute of Medical Sciences, New Delhi, India	skguhasmst@gmail.com
Dr. Piyali Basak	Assistant Professor & Director, Department of Bio-Science and Engineering, Jadavpur University, Kolkatta, West Bengal, India	piyali_basak@yahoo.com
Dr. Santanu Chattopadhyay	Professor, Rubber Technology Centre, Indian Insitute of Technology, Kharagpur, West Bengal, India	santanuchat71@yahoo.com santanu@rtc.iitkgp.ernet.in

DECLARATION

I hereby declare that the above furnished details are true to the best of my knowledge.

Place: Kharagpur
Date:03/12/2019   **Bhuvaneshwaran Subramanian**